Lígia Vanessa Rocha Fão

Amyloid-beta peptide-evoked Src signaling and redox changes in hippocampal cells

Dissertação de Mestrado em Engenharia Biomédica apresentada à Universidade de Coimbra
Orientador(es): Professora Doutora Ana Cristina Carvalho Rego e Doutora Sandra Mota

Setembro 2016

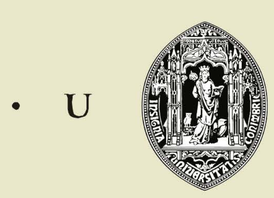

UNIVERSIDADE DE COIMBRA

FCTUC FACULDADE DE CIÊNCIAS
E TECNOLOGIA
UNIVERSIDADE DE COIMBRA

Lígia Vanessa Rocha Fão

Amyloid-beta peptide-evoked Src signaling and redox changes in hippocampal cells

Dissertação apresentada à Universidade de Coimbra para cumprimento dos requisitos necessários à obtenção do grau de Mestre em Engenharia Biomédica

Orientador(es):
Professora Doutora Ana Cristina Carvalho Rego (Faculdade de Medicina da Universidade de Coimbra, Centro de Neurociências e Biologia Celular de Coimbra)
Doutora Sandra Mota (Centro de Neurociências e Biologia Celular de Coimbra)

Coimbra, 2016

Este trabalho foi desenvolvido em colaboração com:

This work was supported by the Programa Operacional Temático Factores de Competitividade 2020 (COMPETE 2020), the European community fund FEDER and by the National Fundation for Science and Technology (FCT) UID/NEU/04539/2013 and Post-doctoral fellowship SFRH/BPD/99219/2013.

AGRADECIMENTOS

Cinco anos se passaram desde que cheguei a Coimbra, a cidade que me acolheu, me viu crescer, por vezes cair mas também evoluir. Ao longo desta caminhada conheci pessoas maravilhosas que contribuíram, de alguma forma, para o culminar deste objetivo. A todas elas, deixo os meus sinceros e humildes agradecimentos:

À Professora Doutora Ana Cristina Rego, primeiro por ter sido uma excelente professora, incutindo desde sempre o fascínio e entusiasmo pela investigação, e segundo pela oportunidade de integrar no grupo e de desenvolver este projeto, que contribuiu arduamente para o meu crescimento científico.

À Sandra, por toda a paciência, ajuda, experiência e conhecimento que me cedeu e por ter, desde cedo, confiado em mim permitindo a minha evolução. Este trabalho não teria sido possível sem ti, por isso aqui deixo o meu mais profundo obrigado.

A todo o grupo MDSN, pela prontidão na ajuda e contínua amizade cedida. À Catarina, uma amiga imprescindível ao longo deste último ano, que me ajudou a todos os níveis, profissionais e pessoais, pelos conselhos e pela constante preocupação, cooperação, companhia e amizade. À Carina, a minha alentejana, com quem partilho a bancada, mas muito mais do que isso, histórias, ensinamentos, nervosismos e ansiedades. Isto não teria sido a mesma coisa sem ti. À Luana, a minha inspiração como pessoa e como profissional, por toda a preocupação, boa disposição, companheirismo e exemplo. Continuo a pensar que, "quero ser como tu, quando for grande". À Filipa por partilhar este ano comigo, revelando-se ao longo do mesmo, uma pessoa querida e preocupada. À Carla, por ter ajudado sempre que necessário e pela preocupação. À Luísa, pelas suas ideias singulares e comentários exclusivos, que acabam por roubar um sorriso ou uma gargalhada a toda a gente.

A todos os amigos do curso, que ao longo destes cinco anos caminharam, trabalharam e cresceram comigo. Em especial, agradeço à Ana Tomé, a minha madrinha académica, que se tornou uma amiga fundamental nesta jornada, pela cooperação, dedicação,

carinho e amizade. Devo muito do que conquistei a ti. À Sá e à Joana Menoita, por terem sido as melhores companheiras de mestrado. Não poderia ter sido de outra forma, foram dois anos incríveis. À Ana Catarina, minha afilhada académica, pela fofura, constante preocupação e amizade. À Maria João que, apesar de termos seguido caminhos distintos, foi uma pessoa importantíssima durante este trajeto. E de uma forma geral, a todos que partilharam comigo esta experiência.

Aos meus melhores amigos de longa data, pessoas magníficas que me deram todo o apoio para que tudo isto fosse possível. À Sara, por todos estes anos de amizade, por me ter dado a conhecer Coimbra, por acreditar sempre em mim e nas minhas capacidades, mas acima de tudo, por nunca ter desistido de mim. À Eduarda, pela amizade, pelo crescimento, preocupação e por ter estado sempre presente nos momentos mais importantes. Ao Rui, peça chave neste percurso, que partilhou casa comigo desde os tempos mais remotos, mas muito mais do que isso, partilhou Coimbra, experiências, conhecimentos, momentos, companheirismo e amizade.

Ao Miguel, o namorado mais paciente da história, pelo carinho, amor e amizade, por me ter acompanhado desde sempre, por ter aturado as minhas birras, os meus choros, as minhas quedas, por me ter aplaudido sempre que conquistei uma etapa, mais ainda, por acreditar em mim mais do que eu própria.

À Diana, a irmã mais ansiosa de sempre, por toda a preocupação, por todos os telefonemas e vídeos que partilhamos, por animar os meus dias mais solitários e por estar sempre presente, mesmo de longe.

Por fim, às pessoas mais importantes da minha vida, os meus pais. Palavras nunca serão suficientes para expressar todo o meu sentimento por vocês. Fizeram sacrifícios indescritíveis para eu poder chegar até aqui. São um exemplo de dedicação, altruísmo e humildade. Em especial, à minha querida mãe que, mesmo de longe, esteve sempre presente, preocupada e atenciosa. A pessoa que dá tudo por mim (e eu por ela), que me incentiva a ser melhor, que me ensinou a ser quem sou, que é a minha maior fã e da qual eu mais me orgulho. O maior obrigado do mundo é para vocês.

"I had my ups and downs, but I always find the inner strength to pull myself up.
I was served lemons, but I made lemonade."

Hattie White

ABSTRACT

Alzheimer's disease (AD) is the major cause of dementia in the elderly population and is characterized by memory deficits and cognitive decline that arise from synaptic and neuronal loss, initially affecting the hippocampus. Neuropathologically, AD is characterized by extracellular accumulation of senile plaques composed by amyloid-beta peptides (Aβ) and intracellular neurofibrillary tangles formed by hyperphosphorylated tau. Aβ oligomers, namely of $A\beta_{1-42}$, are considered the most synaptotoxic forms, being responsible for early cognitive deficits in AD. Aβ induces Ca^{2+}_i dyshomeostasis and reactive oxygen species (ROS) formation, both largely associated with neuronal dysfunction in early stages of AD. Moreover, hydrogen peroxide (H_2O_2) can modulate the non-receptor tyrosine kinase protein Src activity and nuclear factor erythroid derived 2-related (Nrf2), the latter a transcription factor that regulates the antioxidant response. In this work, using mature rat hippocampal neurons cultures, we evaluated the effect of oligomeric $A\beta_{1-42}$ on H_2O_2-mediated Src and Nrf2 phosphorylation and feed-forward influence of Src activation on oxidative stress regulation. Moreover, using the hippocampal cell line HT22, we also evaluated the role of Src on mitochondrial dynamics as well as its relationship with Nrf2 subcellular localization.

We evidenced that, in hippocampal neurons, $A\beta_{1-42}$ oligomers trigger increased Ca^{2+}_i through the activation of *N*-methyl-D-aspartate receptors (NMDARs) and increased H_2O_2 levels, which can be generated by mitochondria. Moreover, these effects could be modulated by the inhibition of the tyrosine kinase Src, probably due to its effect on the regulation of NMDARs. Importantly, Aβ-associated ROS further led to increased Src activation. Concomitantly, Aβ induced Nrf2 phosphorylation in hippocampal neurons. Interestingly, in hippocampal neurons and in HT22 cells, exposure to H_2O_2 induced both Src and Nrf2 phosphorylation; additionally, Nrf2 phosphorylation at Ser40 occurred in a Src-dependent manner. In the nuclear extracts of HT22 cells exposed to H_2O_2, results evidenced unchanged levels of Nrf2, but decreased Src protein levels and increased phosphorylated Src, suggesting a possible novel role for Src in the nucleus, independently of Nrf2. Moreover, H_2O_2 treatment was also shown to induce Src and

Nrf2 phosphorylation in mitochondria obtained from HT22 cells. H_2O_2-mediated mitochondrial Src activation seemed to have a preventive effect on mitochondrial fission.

In hippocampal neurons, Aβ exposure evoked enhanced H_2O_2 production through mitochondria, and Src and Nrf2 activation occurring in a ROS and NMDAR-dependent manner, providing new insights into the characterization of cellular mechanisms potentially involved in AD pathogenesis. Furthermore, in HT22 cells, this study showed H_2O_2-mediated Src and Nrf2 phosphorylation in mitochondria, and Src phosphorylation in nucleus, suggesting modulation of alternative subcellular pathways that may help to regulate mild redox changes.

Keywords: Alzheimer's disease, amyloid-beta peptide, hydrogen peroxide, Src kinase; Nrf2 transcription factor.

RESUMO

A doença de Alzheimer (DA) é a principal causa de demência nos idosos e caracteriza-se por défices de memória e declínio cognitivo consequentes da perda sináptica e neuronal que afeta inicialmente o hipocampo. Histologicamente, a DA caracteriza-se pela acumulação extracelular de placas compostas pelo peptídeo beta-amilóide (Aβ) e a acumulação intracelular de tranças neurofibrilares compostas pela proteína tau hiperfosforilada. A forma oligomérica do peptídeo $A\beta_{1-42}$ é considerada como a mais tóxica a nível sináptico, sendo responsável pelas alterações cognitivas verificadas nas fases iniciais da DA. O peptídeo Aβ induz, entre outros, a formação de espécies reativas de oxigénio (ERO) e a desregulação da homeostasia do Ca^{2+}_i, efeitos comumente associados à disfunção neuronal nos estádios iniciais da DA. Além disso, o peróxido de hidrogénio (H_2O_2) pode modular a atividade da tirosina cinase Src e do fator de transcrição Nrf2 (do inglês "nuclear factor erythroid derived 2-related") que regula a resposta antioxidante. Assim, neste trabalho avaliámos o efeito de oligómeros de $A\beta_{1-42}$ na fosforilação/ativação de Src e Nrf2, através da produção de H_2O_2, e o retro-controlo da Src na regulação do stresse oxidativo utilizando culturas primárias de neurónios maduros de hipocampo. Estudámos também o papel da Src na dinâmica mitocondrial, assim como a sua relação com a localização subcelular de Nrf2, usando a linha celular de hipocampo HT22.

Os nossos resultados demonstraram que, em neurónios hipocampo, a exposição a oligómeros de $A\beta_{1-42}$ induziu um aumento do Ca^{2+}_i através da ativação dos recetores *N*-metil-D-aspartato (NMDA), e aumento da produção de H_2O_2 pela mitocôndria. Além disso, todos estes efeitos foram modulados após inibição da Src, provavelmente devido ao seu efeito na regulação dos receptores NMDA. É importante salientar que a produção de ERO associada ao Aβ levou, por si só, ao aumento da fosforilação da Src. Além disso, a produção de ERO associada ao Aβ induziu a fosforilação do Nrf2 em neurónios do hipocampo. Adicionalmente, tanto em neurónios primários de hipocampo como na linha HT22, observámos a fosforilação da Src e do Nrf2 após tratamento com H_2O_2; de forma interessante, a fosforilação do Nrf2 na Ser40 ocorreu de forma dependente da Src. Em extratos nucleares das células HT22 expostas a H_2O_2

não se verificaram alterações nos níveis totais de Nrf2, contudo observou-se uma diminuição dos níveis nucleares de Src e um aumento da sua fosforilação/ativação, sugerindo um possível papel da Src no núcleo, independente do Nrf2. Em extratos mitocondriais de células HT22, a exposição a H_2O_2 induziu um aumento dos níveis de fosforilação da Src e do Nrf2. Adicionalmente, a ativação da Src associada ao tratamento com H_2O_2 parece ter um efeito preventivo na fissão mitocondrial.

Estes resultados evidenciam, em neurónios primários maduros de hipocampo, a ativação da Src e do Nrf2 por Aβ de forma dependente dos recetores NMDA e dos ERO, fornecendo assim novas perspetivas sobre a caracterização de mecanismos celulares potencialmente envolvidos na DA. Além disso, nas células HT22, o nosso estudo evidencia a fosforilação da Src e do Nrf2 por H_2O_2 na mitocôndria, assim como a fosforilação da Src no núcleo, sugerindo a ocorrência de mecanismos subcelulares que poderão estar envolvidos na regulação de alterações redox.

Palavras-Chave: Doença de Alzheimer, peptídeo beta-amilóide, peróxido de hidrogénio, Src cinase, fator de transcrição Nrf2.

ABBREVIATIONS

α7nAChRs - Nicotinic Acetylcholine Receptors α 7 receptors

AD - Alzheimer's disease

ADP - Adenosine Diphosphate

AICD - Intracellular domain of APP

AKAP121 - A-Kinase Anchor Protein 121

AMPAR - 2-Amino-3-(5-Methyl-3-oxo-1,2- oxazol-4-yl)Propanoic Acid Receptors

ANT1 - Adenine Nucleotide Translocase 1

Aph-1 - Anterior-pharynx-defective-1

Apo E - Apolipoprotein E

APP - Amyloid Precursor Protein

ARE - Antioxidant Response Element

ATP - Adenosine Triphosphate

Aβ - Amyloid beta peptide

BACE - β-site APP-cleaving enzyme

BSA - Bovine Serum Albumin

bZIP - basic leucine zipper motif

CLU - Clusterin

CNS - Central Nervous System

CR1 - Complement Receptor 1

CSF - Cerebrospinal Fluid

CTF – Carboxyl Terminal fragment

DRP1 - Dynamin-Related Protein 1

DTT - Dithiothreitol

EOAD - Early Onset Alzheimer's Disease

ER - Endoplasmic Reticulum

ERK - Extracellular signal-Regulated Kinase

FBS - Fetal bovine serum

Fis1 - Mitochondria fission 1

G6PD - Glucose-6-Phosphate Dehydrogenase

GABA - γ-Aminobutyric Acid

GCL - ɣ-Glutamylcysteine ligase

GPX - Glutathione peroxidases

GR - Glutathione Reductase

GSH - reduced glutathione

GSK-3β - Glycogen Synthase kinase-3β

GSSG - oxidized glutathione

GSTs - Glutathione S-Transferase

$^{\bullet}$HO - Hydroxyl radical

HO-1 - Heme Oxygenase-1

H_2O_2 - Hydrogen peroxide

InsP3R - Inositol 1,4,5-trisphosphate Receptor

Keap1 - Kelch-like ECH-associated protein 1

LOAD - Late-Onset Alzheimer's Disease

LTD - Long-Term Depression

LTP - Long-Term Potentiation

MAM - Mitochondrial-associated endoplasmic reticulum membrane (

MCI - Mild Cognitive Impairment

MCU - Mitochondrial Ca^{2+} Uniport

MFN - Mitofusin

MIM - Mitochondrial Inner Membrane

MIS - Mitochondrial Intermembrane Space

MOM - Mitochondrial Outer Membrane

mPTP – Mitochondrial Permeability Transition Pore

MRC - Mitochondrial Respiratory Chain

MRI - Magnetic Resonance Imaging

NCX - NA^{+}/Ca^{2+} exchanger

NMDARs - *N*-Methyl-D-Aspartate Receptors

NF-κB - Nuclear Factor-kappaB

NFT - Neurofibrillary tangles

NQO1 - NAD(P)H:quinone dehydrogenase 1

Nrf2 - Nuclear factor erythroid derived 2-related factors

$O_2^{\bullet-}$ - Superoxide anion

OPA1 - Optic atrophy 1

PBMCs - Peripheral Blood Mononuclear Cells

PBS - Phosphate-buffered saline

PET - Positron Emission Tomography

Pen-2 - Presenilin enhancer 2

PERK - Protein kinase RNA (PKR)-like Endoplasmic Reticulum Kinase

PI3K - Phosphoinositide 3-Kinase

PICALM - Phosphatidylinositol Binding Clathrin Assembly Protein

PKA - Protein Kinase A

PKB - Protein Kinase B

PKC - Protein Kinase C

Prdx-1- Peroxiredoxin-1

PSD-95 - Post-Synaptic density protein 95

PSEN – Presenilins

PTP1B - Protein-Tyrosine Phosphatase 1B

PTPN – Protein Tyrosine Phosphatase Non-receptor

RAGE - Advanced Glycation End-products

ROS - Reactive Oxygen Species

RTKs - Receptor Tyrosine Kinases

sAPP - Soluble ectodomain of APP

SDS-PAGE – SDS polyacrylamide gel electrophoresis

SKF - Src Kinase Family

SOD - Superoxide Dismutases

SPECT - Single Photon Emission Computed Tomography

SULFs - Sulfotransferases

TR - Thioredoxin Reductase

TREM2 - Triggering Receptor Expressed on Myeloid cells 2

$\Delta\Psi_m$ – Mitochondrial membrane potential

TABLE OF CONTENTS

LIST OF FIGURES

LIST OF SUPPLEMENTARY FIGURES

LIST OF TABLES

CHAPTER I – INTRODUCTION

1.1 Alzheimer's Disease

Alzheimer's disease (AD) is the most common age-related neurodegenerative disorder and the most common cause of dementia worldwide, affecting 10% of the population over the age of 65 and 30-50% of the population over the age of 85 (Li et al., 2016, for review). AD is initially characterized by occasional minor lapses in recalling recent events of daily life, *i.e*. a loss of episodic memory, and lately by the impairment of other cognitive domains that interfere with mood, reasoning, judgment and language (LaFerla and Oddo, 2005). This episodic memory decline is related to pathological changes in entorhinal cortex and limbic brain regions, including the hippocampus that is early impaired in the disease process, and the amygdale (Pennanen et al., 2004). Amnesic symptoms are the turnover to mild cognitive impairment (MCI). Patients with MCI or mild AD have fully preserved alertness and no language, motor or sensory dysfunction. Some additional problems appear after the first couple of years. With increased deficits, the patients show disinterest in hobbies, apathy, as well as difficulties in language and mathematical problems. With the advancing of cognitive decline, motor function deficits begin, leading to marked dementia, full disorientation, memory impairment and global cognitive deficits (Selkoe and Schenk, 2003, for review).

The major histological hallmarks of AD are the accumulation of extracellular amyloid plaques and intracellular neurofibrillary tangles (NFT) both in cortex and hippocampus (**Fig. 1**). Amyloid plaques, also known as senile plaques, are aggregates of amyloid beta peptide (Aβ) that deposit outside neurons in dense formations. Neurofibrillary tangles (NFT) consist in the accumulation inside nerve cell bodies of abnormal hyperphosphorylated tau protein (Selkoe and Hardy, 2016). Both aggregates lead to a neurodegenerative cascade, including, among other, synaptic dysfunction, axonal transport impairment, excitotoxicity, mitochondrial dysfunction, triggering neuronal loss (Lambert and Amouyel, 2011; Li et al., 2016, for review).

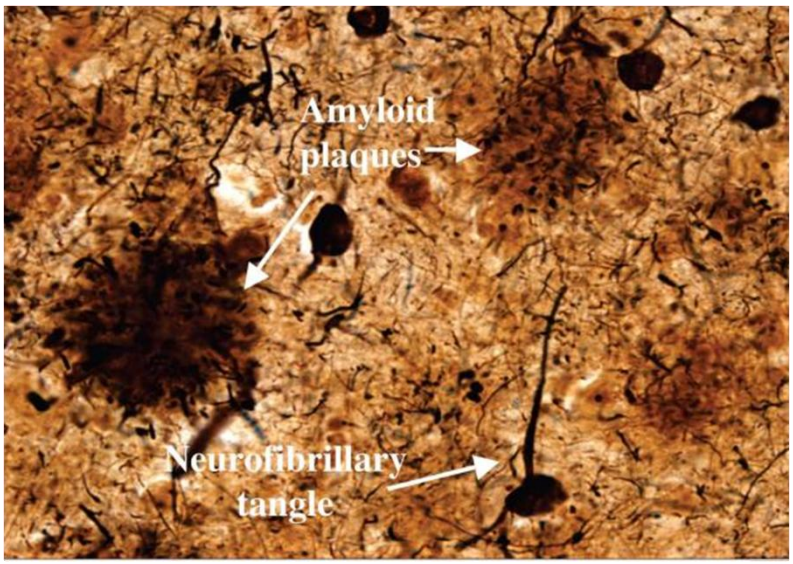

Fig. 1 | Neurofibrillary tangles and amyloid plaques in Alzheimer's disease brain patient. Neurofibrillary tangles are intraneuronal deposits of the hyperphosphorylated tau protein; amyloid plaques are extracellular accumulation of the Aβ peptide (round diffuse structures). Adapted from Irvine et al. (2008).

AD is a complex neurodegenerative disorder related with numerous pathogenic interactions between various factors, including genetic, epigenetic and environmental factors (Huang and Mucke, 2012). Age is the most prominent biological risk factor (Carr et al., 1997) The age of 65 years is often used to classify AD patients in early-onset (EOAD) and late-onset (LOAD) groups when the disease is detected before and after this age (Cacace et al., 2016). Only 10% of AD patients are diagnosed with EOAD, and an important part of them has a family history caused by rare autosomal dominant mutations in the genes encoding for Amyloid Precursor Protein (APP gene, at chromosome 21), presenilin-1 (PS-1 for PSEN1 gene, at chromosome 14), and presenilin-2 (PS-2 for PSEN2 gene, at chromosome 1) (Lambert and Amouyel, 2011). Late-onset forms are considered to be sporadic because they do not show any obvious genetic mutation. Since 1993, the apolipoprotein E (Apo E) ε4 gene polymorphism is considered as the major risk factor for the sporadic form of AD (Corder et al., 1993). ApoE is involved in the regulation of both intracellular and extracellular clearance of Aβ and the ε4 isoform is clearly associated with a lower efficient clearance, when compared to other isoforms (ε1, ε2 or ε3) (Laws et al., 2003). Due to genome-wide association studies, new other risk loci for LOAD have been discovered and studied,

such as the Complement Receptor 1 (CR1), the Clusterin (CLU) (Lambert et al., 2009), the Triggering Receptor Expressed on Myeloid cells 2 (TREM2) (Matarin et al., 2015) and the Phosphatidylinositol Binding Clathrin Assembly Protein (PICALM) (Lambert and Amouyel, 2011). These risk-associated genes have different possible functions: (i) CR1 probably favors the clearance of apoptotic cells and amyloid fibrils; (ii) CLU is one of the most abundant apolipoproteins in the central nervous system (CNS) and participates on Aβ clearance; (iii) TREM2 might be a determinant molecule of the CNS in response to Aβ accumulation; and (iv) PICALM seems to be implicated in the transport of Aβ across the blood brain barrier and into the bloodstream (Selkoe and Hardy, 2016).

Importantly, the definitive diagnosis of AD can only be confirmed after death. In fact, all pathological changes might not be measured *in vivo*. However, in the last years, development of molecular imaging techniques like magnetic resonance imaging (MRI), Positron Emission Tomography (PET) and Single Photon Emission Computed Tomography (SPECT), as well as the analysis of cerebrospinal fluid (CSF) biomarkers (Arora and Bhagat, 2016) were of great help in the diagnosis of AD. Core CSF biomarkers are: (i) decreased Aβ levels, which reflect cortical amyloid deposition (Bloudek et al., 2011); (ii) increased total tau protein (t-tau), which reflects the severity of neurodegeneration (Sunderland et al., 2003); and (iii) increased phosphorylated tau protein (P-tau), which correlates with neurofibrillary pathological changes (Sunderland et al., 2003). Therefore, it is possible to recognize a long pre-dementia stage, the MCI, which may evolve or not to AD (McKhann et al., 2011). AD can be divided into three stages, mild, moderate and severe, which may be difficult to differentiate (McKhann et al., 2011; Prestia et al., 2013). CSF tau changes have been shown to occur about 15 years before the onset of clinical AD and decreased Aβ in CSF is extrapolated up to 20 years before symptom onset. As the severity of the disease increases, Aβ levels in the CSF decrease, as a result of aggregation of the peptide in the brain, while t-tau and P-tau levels increase in the CSF (Dubois et al., 2016; Moghekar et al., 2013).

1.2 The Amyloid-beta peptide

1.2.1 APP Processing

Aβ peptide results from the processing of APP, a type I membrane glycoprotein of 87 kDa, consisting of a long N-terminal extracellular fragment (ectodomain, NTF), a transmembrane domain and a shorter intracellular C-terminal fragment (the cytoplasmic domain) (Vardy et al., 2005). APP has a half-life of about 45–60 minutes in most cell types (Weidemann et al., 1989) and can have multiple isoforms derived from alternative splicing, but its physiological functions are still not fully understood (Muller & Zheng, 2012). Full-length APP is synthesized in the endoplasmic reticulum (ER) and then transported to the Golgi apparatus and to membrane cell surface (Sisodia et al., 1993).

There are two proteolytic processing pathways of APP as shown in **Fig. 2**. In the non-amyloidogenic pathway, APP is initially cleaved by the α-secretase leading to the production of soluble form of APP (sAPPα) and α carboxyl terminal fragment with 83 amino-acid (C83). Subsequently, the C83 fragment is cleaved by ɣ-secretase, to produce the p3 peptide and the intracellular domain of APP (AICD) (Vardy et al., 2005). The sAPPα has several neuroprotective properties and AICD has nuclear signaling functions (Selkoe and Schenk, 2003). In the amyloidogenic pathway, APP is cleaved by β-secretase or β-site APP-cleaving enzyme (BACE), generating a membrane bound C-terminal fragment (C99). C99 is further cleaved by ɣ-secretase within the transmembrane domain to produce Aβ and the smaller AICD (CTFɣ) (Vardy et al., 2005). It was also shown that ɣ-secretase can cleave APP near to the boundary of the cytoplasmic membrane, named ε-cleavage, and in the middle of the membrane, also named as ɣ-cleavage (Weidemann et al., 2002). In this way, the total length of the Aβ peptide varies at C-terminal according to the cleavage pattern of APP, ranging 39 to 43 amino acid residue peptides.

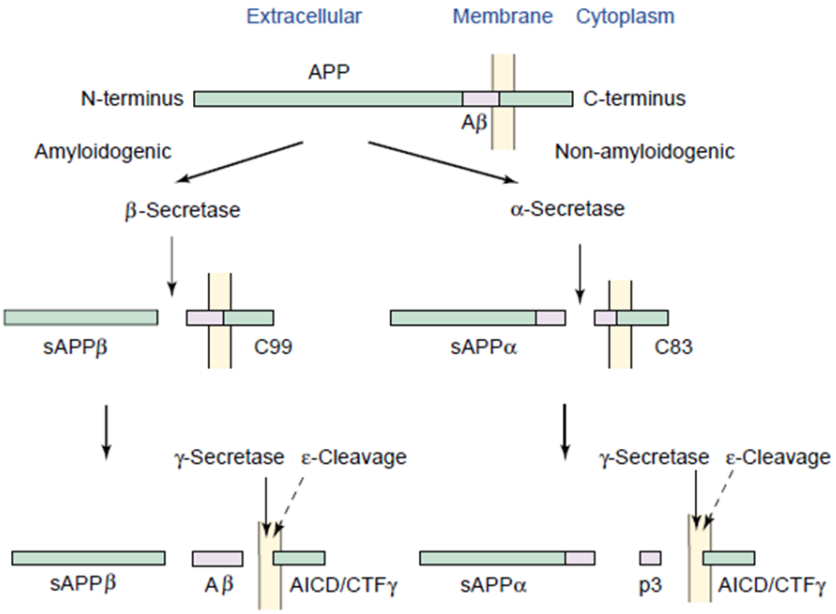

Fig. 2 | Structure and processing of APP in amyloidogenic and non-amyloidogenic pathways. Aβ (purple box) constitutes part of the transmembrane domain and an adjacent short fragment of the extracellular domain. α and ɣ secretases are responsible for the APP cleavage in the non-amyloidogenic pathway, originating sAPPα, p3 and AICD. In the amyloidogenic pathway β and ɣ secretases are involved, originating sAPPβ, Aβ and AICD (Vardy et al., 2005).

It is well established that mutations in APP and in PS-1 and PS-2 change the APP proteolytic processing, leading to increased levels of the Aβ peptides (Barage and Sonawane, 2015; Scheuner et al., 1996). The ɣ-secretase activity resides in a complex of four components, PS-1 or PS-2, nicastrin, anterior-pharynx-defective-1 (Aph-1) and presenilin enhancer 2 (Pen-2) (Haass and Selkoe, 2007), described in **Fig. 3**. PS-1 and PS-2 are homologous integral membrane proteins containing nine transmembrane domains (Guerreiro et al., 2012) that provide the active site aspartate residues required for the catalytic active site of ɣ-secretase (Wolfe, 2008). Mutations in *PSEN1* and *PSEN2* genes alter the cleavage pattern of ɣ-secretase, causing higher $A\beta_{1-42}$ production (Shen and Kelleher, 2007).

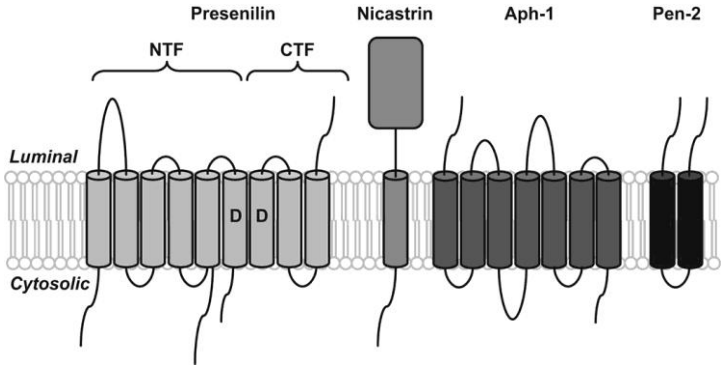

Fig. 3 | Components of the ɣ-secretase complex. γ-Secretase is composed by four different integral membrane proteins: presenilin, nicastrin, Aph-1, and Pen-2. Presenilins can modulate the transmembrane proteolysis carried out by γ-secretase, leading to increased proportion of Aβ peptides, being associated with familial forms of AD (Wolfe, 2008) authorized by "Neurotherapeutics".

The most common Aβ fragments have 40 and 42 amino-acids, with $A\beta_{1–40}$ isoform being the most prevalent, followed by the hydrophobic $A\beta_{1–42}$ that aggregates in a faster way and tends to form stable trimeric and/or tetrameric oligomers than $A\beta_{1–40}$ (Barage and Sonawane, 2015). Inherited missense mutations directly in the Aβ region of APP increase the propensity of the peptide to aggregate (Haass and Selkoe, 2007). In particular, the $A\beta_{1-42}/A\beta_{1-40}$ ratio can be increased by mutations in the three different genes referred above (Haass and Selkoe, 2007). Thus, it is possible to define two different forms of Aβ extracted in AD brains: aggregates that are termed oligomers or protofibrils (depending on their complexity) and mature amyloid fibrils based on their appearance by electron or atomic force microscopy or based on the separation of soluble and insoluble fractions (Thal et al., 2015). The major compound of amyloid plaques are mature amyloid fibrils (Masters et al., 1985) that have a width of ~10–20 nm and a length of usually more than 1 μm (Sachse et al., 2006). Aβ has been shown to adopt multiple fibril structures that can even be observed in the same sample (Schmidt et al., 2009).

1.2.2 The Amyloid Hypothesis

The amyloid hypothesis proposes that neurodegeneration in AD is caused by abnormal accumulation of Aβ plaques, acting as a pathological trigger for the cascade. Genetic, biochemical and pathological evidences support this hypothesis, suggesting that accumulation and aggregation of Aβ plaques are the primary causes of AD (Barage and

Sonawane, 2015). As depicted in **Fig. 4**, Aβ levels can be amplified through higher production or reduced clearance. Deficient Aβ clearance is considered to be involved in the majority of sporadic AD cases. The clearance can be reduced by several reasons, including increased aggregation, defective degradation and disturbed transport across the blood brain barrier or inefficient peripheral removal of the peptide (Sagare et al., 2012). Moreover, as referred above, $A\beta_{42}/A\beta_{40}$ ratio may be increased in FAD due to mutations in APP, PSEN 1 and/or PSEN 2 genes (Wolfe, 2008). The relative increase in $A\beta_{1\text{-}42}$ enhances oligomers formation and further diffuses plaques accumulation that evolves into fibrils responsible for microgliosis and astrocytosis (local inflammatory responses) (Haass and Selkoe, 2007). Over time, these events result in oxidative stress, altered ionic homeostasis and a host of additional biochemical changes (Palotas et al., 2002), leading to synaptic spine loss and neuritic dystrophy (Hartley et al., 1999). The cascade finish with cell death, leading to progressive dementia associated with extensive Aβ and tau pathology (Haass and Selkoe, 2007).

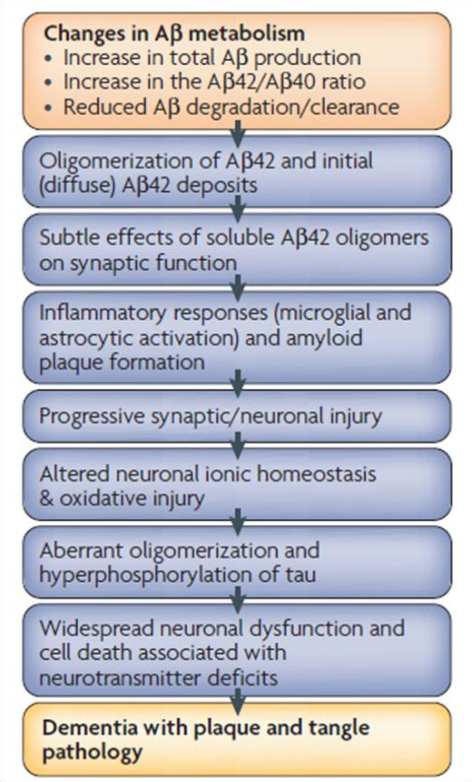

Fig. 4 | The amyloid cascade hypothesis. The hypothesis proposes that increased production or decreased clearance of Aβ peptides are initial pathological events in AD, resulting in accumulation of Aβ peptides and further hyperphosphorylated tau, which together trigger a cascade of deleterious changes, resulting in neuronal death and thus causing AD (Haass and Selkoe, 2007) authorized by "Nat Rev Mol Cell Biol".

In the early 2000s the amyloid hypothesis, in particular the importance of Aβ fibrils in AD pathogenesis, has begun to be questioned. In fact, amyloid fibrils levels were not always related to the severity of AD or to the cognitive defects verified in AD transgenic mice (Chui et al., 1999). Moreover, taking into account the toxicity of Aβ fibrils for most of cells (glial, retina and cerebellar granule cells) (Scorziello et al., 1997; Stix and Reiser, 1998), the fibrillar Aβ hypothesis did not explain the selective neurodegeneration affecting specifically the hippocampus and parietal lobes. Thus, researchers started to investigate the role of a prefibrillar and soluble stage of Aβ peptide, the Aβ oligomers. Aβ oligomers have rapidly been associated with potent neurotoxic activities (Walsh et al., 2002). Importantly, in contrast to the weak correlation of fibrillar density with AD severity, soluble Aβ concentrations in the brain are highly correlated with severity of disease (McLean et al, 1999), which is also consistent with familial AD mutations that lead to increased soluble Aβ.

Thus, in 2003, Kim and colleagues showed that both amyloid fibrils and soluble oligomeric species of Aβ exhibited neurotoxicity, contributing for neurodegeneration in AD. They showed that Aβ oligomers were toxic in NT-2 cells and in specific regions of organotypic slices from hippocampus and cerebellum, whereas Aβ fibrils were lethal to NIH-3T3, SH-SY5Y, HTB186 and M059K cells and also killed neurons in all regions of the cerebral slice cultures (Kim et al., 2003); these data suggested an initial selective regional neurodegeneration that characterizes AD.

Although Aβ is detected mainly in the extracellular space, there are several evidences that Aβ accumulates within neurons (Gimenez-Llort et al., 2007; Wirths et al., 2001) and this accumulation occurs early in AD (Gouras et al., 2000). Studies report the existence of intracellular Aβ in different regions of the brain, especially those presenting neurofibrillary tangles (D'Andrea et al., 2002; Oddo et al., 2003). Importantly, accumulation of oligomeric $A\beta_{1-42}$ has been shown to occur before neurofibrillary tangles and amyloid plaque deposition (Gouras et al., 2010). Aβ can also be internalized after its interaction with some membrane receptors like the *N*-methyl-D-aspartate receptors (NMDARs), Advanced Glycation End-products (AGE) Receptors (RAGE) and nicotinic Acetylcholine receptors α7 Receptors (α7nAChRs) (Nagele et al.,

2002; Sasaki et al., 2001; Snyder et al., 2005). In this way, interaction with Aβ may differ regarding cell type; it was demonstrated that $A\beta_{1-42}$ is internalized by CA1 hippocampal neurons in organotypic hippocampal slice cultures, whereas cells in other hippocampal subdivisions such as CA3 and dentate gyrus do not, leading to higher production of amyloidogenic APP fragments and enhanced deterioration of central synapses in a selective way (Bahr et al., 1998).

Indeed, $A\beta_{1-42}$ oligomers are the most toxic species of Aβ (Jan et al., 2011; Selkoe, 1996) namely due to their ability to promote excitotoxicity by interacting with different receptors (Nagele et al., 2002; Sasaki et al., 2001; Snyder et al., 2005), as well as to cause endoplasmic reticulum stress and Ca^{2+} levels depletion (Resende et al., 2008a), mitochondrial dysfunction (Wang et al., 2008), inhibition of bidirectional axonal transport (Pigino et al., 2009) and oxidative stress (De Felice et al., 2007) by interacting with several cellular structures (Benilova et al., 2012, for review). Interestingly, besides being present in AD patients brain, Aβ senile plaques can also exist in non-demented individuals with a similar composition, suggesting the existence of other important factors involved in AD (Fukumoto et al., 1996).

1.3 Synaptic Dysfunction in Alzheimer's Disease – Involvement of NMDARs

The idea that loss of synaptic function is a key characteristic of AD neuropathogenesis started in the 60s when Gonatas and colleagues first described abnormalities in synapses from AD brain tissues (Gonatas et al., 1967). Since then, several studies in brain samples from patients with symptoms between MCI and early-mild AD showed that synapse loss can be related with AD severity. Significant loss of synaptic elements such as proteins SV2 and p65, and about 45% of synaptic boutons in neocortex and hippocampus, have been found in MCI and AD brains when compared with cognitively normal controls (Masliah E, 1993; Masliah et al., 1989; Scheff and Price, 1993). Other studies confirmed a similar pattern of abnormalities related with dendrites, such as a significant reduction in the number of dendritic spines (Moolman et al., 2004) and reduced excitatory synaptic transmission (Shankar et al., 2008). These injurious effects may contribute to the cognitive deficit and memory loss verified in AD, demonstrating that synaptic fail could be one of the earliest events that occurs in the pathogenesis of AD prior to neuronal loss (Sheng et al., 2012).

Long-term potentiation (LTP), a basic mechanism underlying learning and memory (Malenka and Nicoll, 1999), is a process which inserts α-Amino-3-hydroxy-5-Methyl-4-isoxazolepropionic Acid Receptor AMPAR at the surface of the synapse in a Ca^{2+} and NMDAR-dependent manner to enhance the glutamatergic synaptic strength (Malenka and Bear, 2004). Structural remodeling of spine synapses, or synaptic plasticity, is implicated in memory formation (Gruart et al., 2006; Whitlock et al., 2006). Long-term depression (LTD), in opposite to the increase in synaptic transmission observed following induction of LTP, is a long-lasting decrease in synaptic efficacy followed by low frequency stimulation. Aβ oligomers accumulate around neurons in the very early stages of AD. They may be a direct trigger of synaptic dysfunction by blocking LTP and directly affecting the density and stability of dendritic spines or even targeting one or more receptors present on the surface of dendritic spines (Nimmrich and Ebert, 2009). Shankar and colleagues showed that Aβ oligomers extracted from AD patients inhibit

LTP and enhance LTD in rat organotypic hippocampal slices and lead to decreased spine density and memory impairments (Shankar et al., 2008). Importantly, induction of LTD or inhibition of LTP in AD seems to be directly related with changes in synaptic morphology, resulting in dendritic spine shrinkage or collapse by F-actin remodeling (Selkoe, 2008). Furthermore, Aβ can also significantly impair synaptic plasticity by directly decreasing the accessibility of AMPARs at excitatory synapses (Rui et al., 2010; Yan et al., 2016).

NMDARs are cationic channels gated by the neurotransmitter glutamate and the main source of synaptic Ca^{2+} involved in the rapid induction of synaptic plasticity. NMDARs are essential for excitatory transmission, synaptic integration, learning and memory in the CNS (Mota et al., 2014, for review). NMDARs are hetero-tetramer constituted by two required GluN1 subunits and two modulatory GluN2 or GluN3 subunits (Cull-Candy et al., 2001). The GluN2 subunit has different possible subtypes (GluN2A, B, C or D), which have diverse spatial and temporal patterns of expression (Zhang et al., 2016), being GluN2A and GluN2B the major subunits. NMDARs activation requires the binding of glutamate to the receptor and also a sufficient postsynaptic depolarization to remove the Mg^{2+} blocker ion from the channel, which results in intracellular Ca^{2+} (Ca^{2+}_i) increase (MacDermott et al., 1986) (**Fig. 5**). Downregulation of GluN2B subunits contributes to cognitive decline, exhibiting impaired LTP and memory (Brigman et al., 2010); contrariwise, upregulation of GluN2B significantly improves LTP and memory function in rodents, including in aged mice (Cao et al., 2007a).

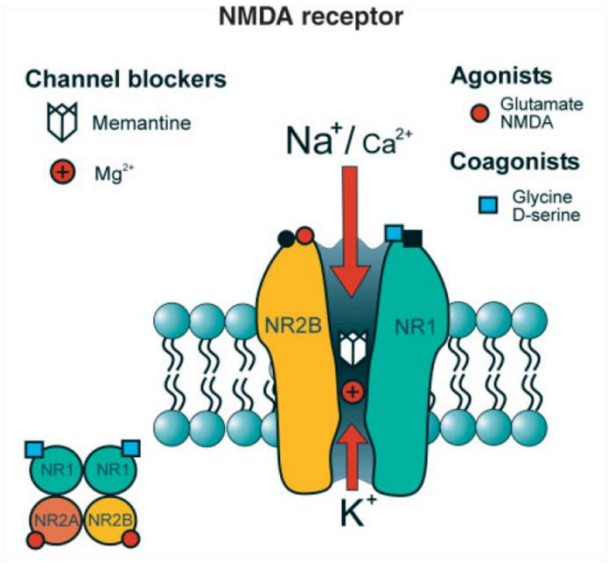

Fig. 5 | Scheme of the NMDA receptor. Activation of NMDA receptors, a glutamate receptor, results in the opening of the ion channel that is nonselective to cations, namely Na^+ and Ca^{2+}. NMDARs are constituted by two required GluN1 subunits and two modulatory GluN2 or GluN3 subunits (Danysz and Parsons, 2003) authorized by "Int J Geriatr Psychiatry". In current nomenclature of these receptors, NR stands for GluN.

Besides the differential temporal pattern of expression, NMDARs also present differential cellular localization pattern, namely synaptic or extrasynaptic localization. Extrasynaptic NMDARs require high glutamate concentrations and are located on dendrites or the sides of spines (Oliet and Papouin, 2014). Several reports propose that the function of synaptic and extrasynaptic NMDARs may depend on the receptor type (presence of different subunits) and associated proteins, as well as a preferential affinity of synaptic NMDARs for D-serine and extrasynaptic NMDARs for D-glycine (Mota et al., 2014, for review). Synaptic NMDARs are inhibited by D-serine degradation decreasing the LTP, while glycine degradation has no effect on LTP, suggesting that synaptic NMDARs play a key role on LTP, in contrast with extrasynaptic receptors (Papouin et al., 2012). Otherwise, both synaptic and extrasynaptic NMDARs are crucial for LTD (Newpher and Ehlers, 2009; Papouin et al., 2012). In this way synaptic NMDARs seem to be neuroprotective, whereas stimulation of extrasynaptic NMDARs cause loss of mitochondrial membrane potential and cell death (Zhang et al., 2016). Interestingly, it seems that extrasynaptic NMDARs are mainly composed by GluN2B subunits (Petralia, 2012). Moreover, injection of Aβ in rat brain impaired induction of LTP in a GluN2B subunit-dependent manner and not depending on GluN2A (Hu et al., 2009). Our group also showed that Aβ oligomers may cause microtubule disassembly in a

NMDARs-dependent manner associated to neurite retraction and DNA fragmentation in mature hippocampal cells, showing a relevant role of NMDARs on Aβ toxicity (Ferreira et al., 2012, 2015; Mota et al., 2012).

Aβ oligomers may interact with other cellular receptors, in γ-Aminobutyric Acid (GABA)ergic and dopaminergic synapses. First studies in AD postmortem patients revealed unchanged GABAergic synapses, resulting in less intensive studies; but more recently it was proven that reduction of GABA functions in AD patients is related to high levels of soluble Aβ, which can decrease bursting activity and impair inhibitory potentials of GABAergic neurons in the septohippocampal system (Nava-Mesa et al., 2014). Furthermore, NMDARS activation by endogenous glutamate seems to evoke a transient and reversible enhancement of postsynaptic $GABA_A$ receptor, being the crosstalk considered as a compensatory mechanism for the overexcitation frequently observed in pathological conditions (Potapenko et al., 2013).

1.4 Cellular dysfunction in Alzheimer's Disease

1.4.1 Oxidative Stress and Antioxidant defenses

Oxidative stress is a disturbance in the equilibrium status of pro-oxidant and antioxidant reactions in living organisms that happen due to metabolic reactions using oxygen. Reactive oxygen species (ROS) can be defined as a group of reactive molecules derived from oxygen with a short life time and extremely reactive because of their unpaired valence electron. Some examples of ROS are free radicals, such as superoxide anion ($O_2^{\bullet -}$) and the hydroxyl radical ($^{\bullet}OH$), or the non-radical hydrogen peroxide (H_2O_2) (Kim et al., 2015, for review). A large production of ROS can damage cellular lipids, proteins or DNA, but the delicate balance between beneficial and harmful effects of free radicals is a very important aspect of living organisms. The redox regulation protects living organisms from various oxidative stresses and maintains the homeostasis by controlling the redox status (Droge, 2002). In AD, increased oxidative stress induces cellular injuries, mitochondrial dysfunction and impair DNA repair system, which may play a critical role in the initiation and progression of the disease (Behl, 1994; Gandhi and Abramov, 2012; Patten et al., 2010).

The brain requires an elevated oxygen consumption rate to produce adenosine triphosphate (ATP) and it is known that oxygen metabolism in different organelles like mitochondria, ER, and peroxisomes generates oxidant free radicals (Gilgun-Sherki et al., 2001, for review). Cells have a complex mechanism of defense to fight oxidative stress. Indeed, cellular ROS levels may be reduced using a range of antioxidant enzymes and small-molecules, which prevent and repair damages caused by oxidative stress (Gandhi and Abramov, 2012). The key enzymes of antioxidant defense are: (i) superoxide dismutases (SOD) that play a significant role in catalyzing the breakdown of highly reactive $O_2^{\bullet -}$ to less reactive H_2O_2; (ii) Catalase that originate the conversion of H_2O_2 into water plus oxygen; (iii) Glutathione peroxidases (GPX) that catalyze the reduction of H_2O_2 and peroxides using reduced glutathione (GSH) as an electron donor, originating oxidized glutathione (GSSG), which can be reduced to GSH by glutathione reductase. Key antioxidant small molecules include: (I) GSH, a tripeptide synthesized from glutamate, cysteine and glycine; (II) Vitamin E that can attenuate the effects of

peroxide and protect against lipid peroxidation; or (III) Vitamin C that is involved in the removal of free radicals by electron transfer and also acts as a cofactor for antioxidant enzymes (Dasuri et al., 2013; Kim et al., 2015, for review).

Interestingly, high levels of ROS damage most biomolecules, serving as oxidation markers. These include lipid peroxidation (e.g. 4-hydroxynonenal), protein oxidation (e.g. carbonyl) and DNA/RNA oxidation (e.g. 8-hydroxyldeoxyguanosine and 8-hydroxylguanosine), which have been observed in the cortex and hippocampus from AD patients (Butterfield et al., 2002). Interestingly, Baldeiras and colleagues demonstrated that the oxidative changes found in mild AD patients are already present in the MCI group; the plasma levels of mild AD patients revealed decreased vitamin E levels and both MCI and mild AD patients showed increased levels of oxidized glutathione (Baldeiras et al., 2008). Moreover, we previously demonstrated a decrease in the levels of SOD1 protein in MCI PBMCs (Mota et al., 2015). The 3xTg-AD mouse model of AD also showed reduced glutathione and vitamin E, and increased activity of the antioxidant enzymes GPX and both SOD (Resende et al., 2008b). Furthermore, decreased levels of other antioxidant defenses, namely SOD1 and heme oxygenase-1 (HO-1) were also seen in this AD mouse model (Mota et al., 2015). These observations support the concept of the importance of oxidative stress in AD pathogenesis. Importantly, Aβ seems to increase oxidative stress and lead to mitochondrial dysfunction even in early stages since AD transgenic mouse models expressing mutant APP and PS-1 showed high levels of H_2O_2 and oxidation of proteins and lipid (Apelt et al., 2004; Manczak et al., 2006; Mohmmad Abdul et al., 2006).

On the other hand, oxidative stress may increase the production and aggregation of Aβ and sustain the polymerization and phosphorylation of tau protein (Dumont et al., 2011; Li et al., 2004). Moreover, high levels of ROS stimulate pro-inflammatory gene transcription and release of cytokines, such as IL-1β, IL-6, and TNF-alpha, which in turn activate microglia and astrocytes to generate large amounts of ROS; this interaction between oxidative stress and neuroinflammation promotes increased Aβ production (Chakrabarty et al., 2010; Motta et al., 2007; Sokolova et al., 2009). NMDARs may also be a target of oxidative stress since they contain three pairs of extracellular cysteine

residues which can interact and form disulfide bonds, leading to an altered receptor conformation and decreased function (Aizenman et al., 1990; Lipton et al., 2002).

1.4.2 Mitochondrial dysfunction

Mitochondria represent the main source and one of the main targets of ROS, being implicated in neuronal death. These organelles, present in all aerobic cells, are able to use O_2 as final acceptor of electrons to form ATP as well as perform other functions, namely maintenance of Ca^{2+} homeostasis, ROS generation, heme synthesis, amino acids, fatty acids and steroids metabolism, and apoptosis regulation. Mitochondria are divided into the following membrane compartments: the mitochondrial outer membrane (MOM), the mitochondrial intermembrane space (MIS), the mitochondrial inner membrane (MIM) and the mitochondrial matrix. The matrix contains mitochondrial DNA that encodes proteins needed for replication and energy transduction, although most of the mitochondrial proteins are encoded by the nuclear DNA (Mattson et al., 2008). The MIM contains the mitochondrial respiratory chain (MRC), which is one of the main functional and structural parts of mitochondria. The MRC is composed by five complexes (I, II, III, IV, V) responsible for the final phosphorylation of ADP to ATP by transferring electrons between these integrated complexes (Ghezzi and Zeviani, 2012) (**Fig. 6**). Neurons are highly dependent on mitochondria to execute numerous cellular processes, such as neurotransmitter vesicle transport and release, axonal transport of organelles and macromolecules and maintenance of transmembrane ionic gradients; interestingly, in contrast to astrocytes, neurons do not use glycolysis when mitochondria are dysfunctional or damaged (Almeida et al., 2004; Bolaños et al., 2009).

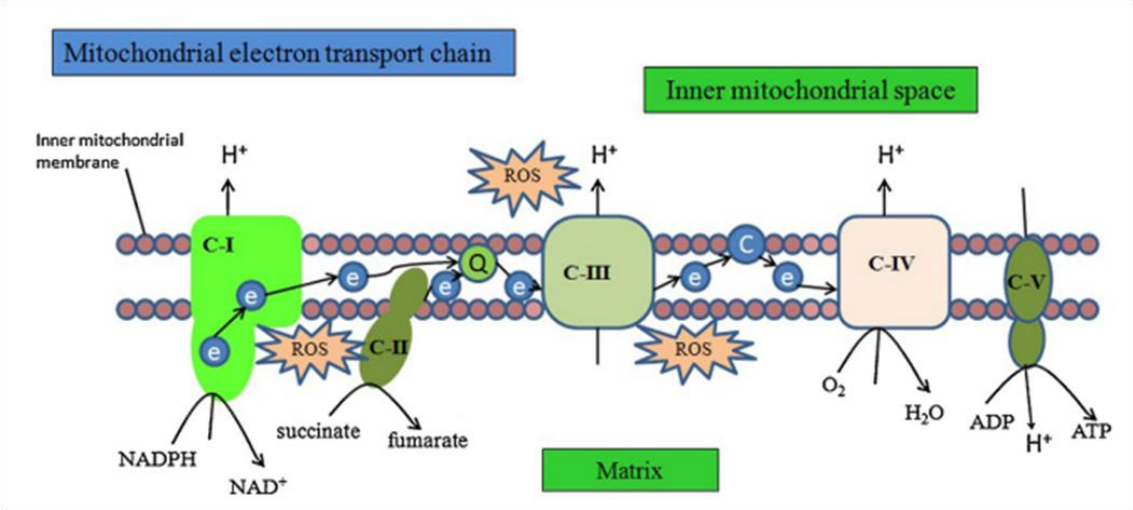

Fig. 6 | ATP and ROS formation in mitochondria. Mitochondrial electron transport is composed by five multimeric complexes that shuttles electrons from NADH and $FADH_2$ to molecular oxygen. During electron transfer, proton pumping to the intermembrane space (complexes I, III and IV) generates an electrochemical gradient (Δψm) across the mitochondrial inner membrane. Complex V (ATP synthase) utilizes the proton motive force to synthesize ATP from ADP (Bhat et al., 2015).

Mitochondria are dynamic structures, continuously subjected to cycles of fission and fusion depending on the needs of the cell. Thus, mitochondria are able to communicate between them and with other organelles in order to assemble the energetic needs of the cell, as well as to prevent cellular damage. Mitochondrial fission is an important mechanism that allows the renewal and proliferation of the organelle, facilitating their autophagic clearance, while mitochondrial fusion contributes to communication with each other, as well as to their distribution across long distances and to the synapses, preventing the expansion of oxidative damage (Hoppins et al., 2007). The energy required for these events are obtained from a family of GTPase proteins: (i) Dynamin-Related Protein 1 (DRP1) is present in the cytosol and recruited to the MOM, acquiring an active conformation state to promote fission; Mitochondrial Fission 1 protein (FIS1) is also situated in MOM and required in fission process; (ii) Mitofusin 1 (MFN1) and Mitofusin 2 (MFN2), both in MOM, and Optic Atrophy 1 (OPA1) in MIM promote fusion (Bolaños et al., 2009, for review).

Mitochondrial dysfunction has been suggested to be an early event in AD; in fact, patients display early metabolic changes that precede the appearance of any histopathological or clinical abnormalities (Gibson and Shi, 2010). Additionally, increased oxidative damage on mitochondrial DNA, promoting mutations, has been

reported in patients with AD (Gandhi and Abramov, 2012; Wang et al., 2014). Several reports suggest that accumulation of APP and Aβ mediates mitochondrial toxicity, since they were found in purified mitochondria from AD patient and AD mouse model brains (Caspersen, 2005). Aβ peptide seems to interact with mitochondria inducing cytotoxic effects, affect mitochondrial fusion and fission and alter mitochondrial motility (Manczak et al., 2011). Furthermore, disruption of MRC function and increased ROS production were also verified in the presence of Aβ (Caspersen, 2005; Rui et al., 2006). Interestingly, an atypical accumulation of Aβ within synaptic mitochondria was observed, possibly contributing for early AD synaptic dysfunction (Du et al., 2010). Different studies described possible routes for Aβ entry into mitochondria, which may involve the mitochondrial-associated endoplasmic reticulum membrane (MAM) (Hedskog et al., 2013; Pinho et al., 2014) or the translocase of MOM complex (Hansson Petersen et al., 2008).

Regarding Aβ-mediated changes on mitochondria dynamic, neurons exposed to Aβ oligomers and primary neurons cultured from APP mice showed mitochondrial fragmentation and reduced mitochondrial density (Du et al., 2010). Furthermore, AD patient brains present increased levels of Drp1 and Fis1 and reduced expression of Mfn1, Mfn2 and OPA1, suggesting that increased production of Aβ and interaction of Aβ with Drp1 are crucial factors in mitochondrial fragmentation, causing abnormal mitochondrial dynamics and synaptic damage (Manczak et al., 2011). Exposure to Aβ leads to mitochondrial Ca^{2+} accumulation that seems to be related with increased ROS production and opening of the permeability transition pore (PTP) (Moreira et al., 2001). Aβ-induced mitochondrial dysfunction may also contribute to an impairment in Ca^{2+} homeostasis, resulting in increased Ca^{2+} overload and decreased organelle reuptake (Abramov et al., 2003). Indeed, we previously demonstrated in primary cortical neurons, that Aβ and NMDA largely induced immediate mitochondrial depolarization, when compared with Aβ or NMDA alone, and also that mitochondria control Ca^{2+} entry through NMDARs in Aβ presence, suggesting that mitochondrial Ca^{2+} dyshomeostasis and subsequent dysfunction are relevant mechanisms for early neuronal dysfunction in AD linked to Aβ-mediated GluN2B-composed NMDARs activation (Ferreira et al., 2015).

1.4.3 Intracellular Calcium Dyshomeostasis

Ca^{2+} is an essential intracellular messenger, governing the activity of neuronal cells and relevant in multiple physiological functions. This divalent cation binds different proteins, receptors or ion channels. Several studies showed a connection between disruption of Ca^{2+} homeostasis and the development of AD (Berridge, 2013).

Ca^{2+} buffering is secure by two organelles: the endoplasmic reticulum and the mitochondria, while ATPase Ca^{2+} pump and NA^{+}/Ca^{2+} exchanger (NCX) are the two main systems involved in Ca^{2+} efflux through the plasma membrane (Magi et al., 2016). When Ca^{2+} is highly concentrated in microdomains close to mitochondria, its uptake occurs via the mitochondrial Ca^{2+} uniport (MCU) at the MIM due to the negative mitochondrial transmembrane potential ($\Delta_{\psi m}$) and it is rapidly accumulated within this organelle (Naia et al., 2016, for review). It is well established that Aβ leads to upregulation of neuronal Ca^{2+} signaling, which has been associated with age-related deficits in learning or memory and apoptosis (Berridge, 2013; Thibault et al., 2007). The Increase in cytosolic Ca^{2+} levels mediated by Aβ can occur through the Ca^{2+}-permeable channels in membranes formed by Aβ oligomers (Fernández-Morales et al., 2012), the activation of ionotropic receptors (Ferreira et al., 2012) such as the NMDARs, or Aβ-mediated activation of metabotropic receptors coupled to Ca^{2+} release from internal stores (Naia et al., 2016, for review). ER Ca^{2+} release through inositol 1,4,5-trisphosphate receptor (InsP3R) was further shown to cause mitochondrial dysfunction induced by Aβ, particularly a loss of $\Delta\psi_m$ and cytochrome c release (Ferreiro et al., 2006). We previously demonstrated that $A\beta_{1-42}$ oligomers bind to NMDARs through the GluN2B subunit (Costa et al., 2012), thus leading to an increase in cytosolic Ca^{2+} (Ferreira et al., 2012; Ferreira et al., 2015). Activation of NMDARs in the presence of Aβ was also shown to potentiate the neurodegenerative process in AD through mitochondrial depolarization and mitochondrial Ca^{2+} retention (Ferreira et al., 2015). However, mitochondrial Ca^{2+} overload involving the ER, observed in AD, seems to be not exclusively due to Aβ-mediated NMDARs activation (Thathiah and De Strooper, 2011). Importantly, Jensen and coworkers showed that intracellular Ca^{2+} rise

stimulated by Aβ does not seem to be necessarily sustained by extracellular Ca^{2+} influx, suggesting an important role for Ca^{2+} release from the ER (Jensen et al., 2013).

1.5 Nuclear factor erythroid 2 related factor 2 - Nrf2

Nuclear factor erythroid 2 related factor 2 (Nrf2) is generally considered an adaptive cell response and inducible cell defense component to endogenous and environmental oxidative stress. Nrf2 mediates the expression of more than 100 oxidative stress-related genes, including antioxidant proteins, detoxifying enzymes, transport proteins, proteasome subunits, chaperones, growth factors and their receptors, and some transcription factors. All of these cytoprotective genes contain, in their promoter, a cis-regulatory element sequence named as the antioxidant response element (ARE), which constitutes a binding target for Nrf2 (Stępkowski and Kruszewski, 2011, for review). Nrf2 contains six conserved NRF2-ECH (Neh) domains: (i) Neh1 domain, which contains a basic leucine zipper motif (bZIP) and allows binding to the ARE; (ii) Neh2 domain, located in the most N-terminal region, which possesses the Keap1 binding domain and acts as a negative regulatory domain; (iii) Neh3 domain, located in the most C-terminal region and that has a role in Nrf2 transactivation; (iv) Neh4 domain along with (v) Neh5 domain, which seem to be also essential for Nrf2 transactivation; and (vi) Neh6 domain, required for Nrf2 protein degradation (Taguchi et al., 2011) (**Fig. 7**).

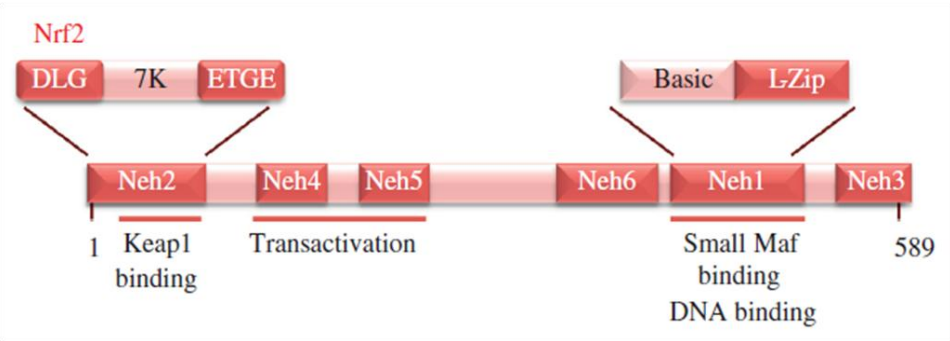

Fig. 7 | Domains structure of Nrf2 protein. Nrf2 protein consists of 589 aminoacids and has six homology domains, Neh1–6. The domains of interest in Nrf2 are: the Neh1 domain, that contains a bZip motif, a basic region – leucine zipper (L-Zip) structure, where the basic region is responsible for DNA recognition and the L-Zip mediates dimerization with small Maf proteins; and the Neh2 domain that contains ETGE and DLG motifs, which are required for the interaction with Keap1, and a hydrophilic region of lysine residues, which are indispensable for the Keap1-dependent polyubiquitination and degradation of Nrf2. Adapted from (Kansanen et al., 2013) authorized by "Redox Biol".

Nrf2 is ubiquitously expressed in most eukaryotic cells and under normal conditions is maintained in the cytosol at low levels due its constant polyubiquitination. Indeed, in

the cytosol, Nrf2 binds to Kelch-like ECH-associated protein 1 (Keap1) through the N-terminal Neh2 domain, inhibiting its activity by acting as an adaptor for Cullin-3-based E3 ubiquitin ligase complex. Under physiological conditions, Keap1 constitutively targets Nrf2 for poly-ubiquitination via the Cul3 E3 ligase, which lead to consequently degradation of Nrf2 by the 26S proteasome (Nguyen et al., 2003). Komatsu and colleagues have demonstrated that p62, a polyubiquitination binding protein that targets substrates for autophagy, interacts with Keap1 in its Nrf2 binding site leading to its degradation , which in consequent inhibits polyubiquitination of Nrf2 (Komatsu et al., 2010; Lau et al., 2010).

Keap1 has a large number of cysteine residues working as a sensor molecule for oxidative stress through thiol oxidation, altering its activity. In this way, under oxidative stress conditions, Keap1 alters its conformation, inhibits the E3 ubiquitin ligase and release Nrf2, resulting in the stabilization and accumulation in cytosol; this allows Nrf2 to translocate to the nucleus to transcribe several cytoprotective genes codified in the ARE (**Table 1**). In this way, dimerization of transcriptional co-activator Mafs with Nrf2 facilitates stable Nrf2-ARE interaction and enhances the transcription of the genes (Hirotsu et al., 2012). This type of Nrf2 regulation is considered to be Keap1-dependent (reviewed by Obuobi et al., 2016) (**Fig. 8)**.

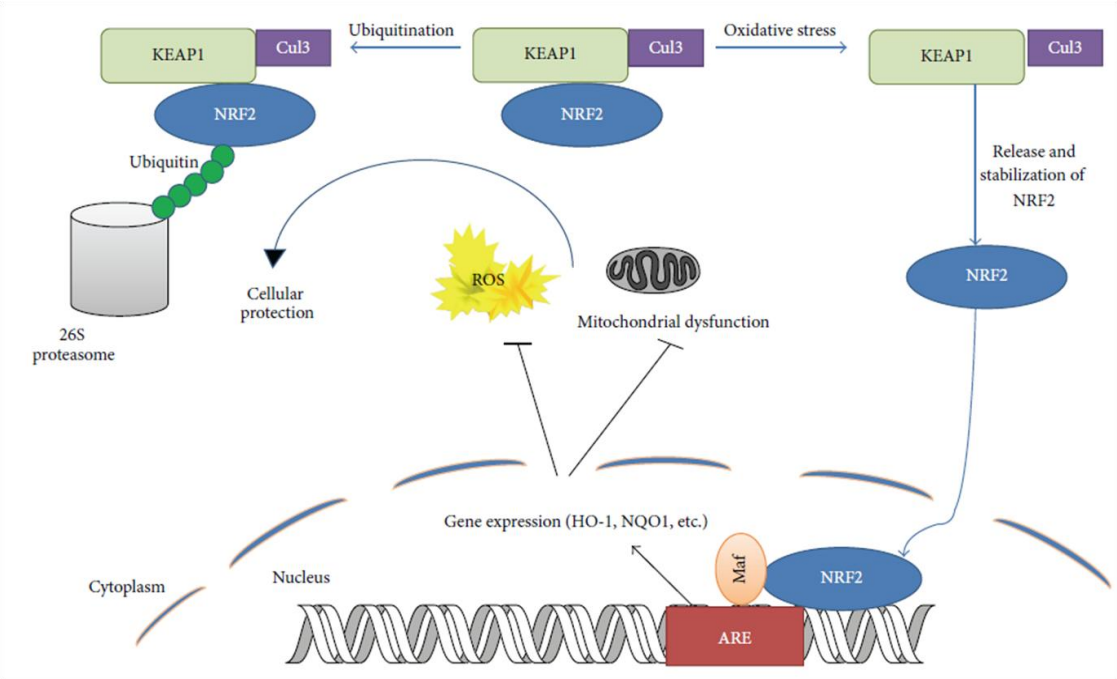

Fig. 8 | Keap1-dependent mechanisms Nrf2 activation. Under unstressed conditions Nrf2 is constantly recruited for ubiquitination by Keap1–Cul3 complex resulting in low constitutive level of activity. Electrophilic compounds or ROS covalently bind to reactive cysteines interfering with the normal function of the complex and resulting in accumulation of Nrf2. Nrf2 then translocates into nucleus and promote the transcription of antioxidant enzymes binding to ARE (Kim et al., 2016).

On the other hand, some authors suggest that phosphorylation of Nrf2 which contribute to its nuclear migration can be also regulated independently of Keap1 (reviewed by Obuobi et al., 2016). Thus, Nrf2 contains many serine, threonine and tyrosine residues, which may provide sites for phosphorylation by different kinases (Rojo et al., 2012). The phosphorylation of Nrf2 by Protein kinase RNA (PKR)-like endoplasmic reticulum kinase (PERK) (Cullinan et al., 2003) or specifically on Nrf2 Ser-40 residue, mediated by protein kinase C (PKC) (Huang et al., 2002), and also its phosphorylation in the transcription activation domain (Neh4 and Neh5), mediated by protein kinase CK2 (Apopa et al., 2008), seems to disrupt the association between Nrf2 and Keap1 thus promoting the translocation of Nrf2 into the nucleus. Furthermore, acetylation and deacetylation of Nrf2 can regulate the nuclear-cytoplasmic movement and its transcriptional activity. For instance, Nrf2 acetylation of lysine residues enhances Nrf2-DNA binding and transcription of target genes (Kawai et al., 2011). Additionally, glycogen synthase kinase-3β (GSK-3β) was shown to negatively regulate Nrf2 by reducing its nuclear localization. This protein can also phosphorylate members

of the Src family kinases, which translocate into the nucleus and phosphorylate Nrf2 in Tyr568 residue, leading to its nuclear export (Niture et al., 2011).

Concluding, under basal intracellular conditions, Keap1 continuously regulates Nrf2 degradation, maintaining low cellular levels of the protein, however, under conditions of oxidative stress, the regulation of Nrf2 becomes complex, involving both Keap1-dependent and -independent mechanisms.

Table 1 | Cytoprotective genes regulated by Nrf2 transcription factor

Gene	Protein	Principal Function
Glucose-6-phosphate dehydrogenase	G6PD	Provides NADPH to glutathione reductase
Glutathione peroxidase	GPx	Detoxifies peroxides and hydroperoxides
Glutathione S-transferase	GSTs	Catalyzes the conjugation of the reduced form of glutathione (GSH) to xenobiotic substrates
Glutathione reductase	GR	Catalyzes the reduction of glutathione disulfide (GSSG) to the sulfhydryl form of glutathione or reduced glutathione (GSH)
Heme oxygenase-1	HO-1	Degrades heme and generates the antioxidant molecules, biliverdin and CO
NAD(P)H:quinone dehydrogenase 1	NQO1	FAD-binding protein, reduces quinones to hydroquinones
Superoxide dismutases	SOD1 SOD2	Catalyzes the dismutation of the superoxide radical ($O_2^{\bullet-}$) into hydrogen peroxide (H_2O_2) or molecular oxygen (O_2)
Thioredoxin reductase	TR	Reduces thioredoxin
ɣ-Glutamylcysteine ligase (Catalytic subunit or modulatory subunits)	GCLc GCL_M	Catalyzes the rate limiting step in the biosynthesis pathway of cellular glutathione (GSH)
Sulfotransferases	SULFs	Catalyze sulfation of many xenobiotics
Peroxiredoxin-1	Prdx-1	Reduces hydrogen peroxide and alkyl hydroperoxides

(Adapted from Loboda et al., 2016)

1.5.1 Nrf2 in AD

It has been described that different potential sources of oxidative stress might be present in early stages of AD. Interestingly, *in vitro* studies showed that Nrf2 activity is essential to neutralize oxidative damage and neuronal death induced by Aβ (Kärkkäinen et al., 2014). In postmortem AD human brains, there are evidences for decreased nuclear Nrf2 levels (Ramsey et al., 2007), suggesting decreased Nrf2 activity. In contrast, studies demonstrated that different target genes of Nrf2 are increased in AD compared to control brain tissues, namely NQO1, GR, GPx, HO-1, p62 and GCL (Raina et al., 1999; Schipper et al., 1995; SantaCruz et al., 2004) suggesting a higher activity of the transcription factor as the result of higher oxidative stress. However, these contradictory findings may be explained by the stage of the disease and the type of tissue collected for the study. In a mouse model of AD (APP/PS1 mouse), mRNA levels of GCL_M, GCLc and NQO1 were decreased at 6 months of age and Nrf2 at 16 months of age (Kanninen et al., 2008). Furthermore, studies in hippocampus and cortex, using 3xTg-AD mouse also showed a significant increase in NQO1 protein at 2 months of age, but a decrement at later stages in hippocampus at 6 months of age (Torres-Lista et al., 2014). Finally, also in 3xTg-AD mice, we previously showed increased Nrf2 phosphorylation at Ser40 and increased nuclear Nrf2 levels in 3 month-old male mouse peripheral blood mononuclear cells (PBMCs) and brain cortex, respectively (Mota et al., 2015). Accordingly, an increase in oxidative stress and Nrf2 phosphorylation was found in human PBMCs isolated from individuals with mild cognitive impairment (MCI) (Mota et al., 2015). Despite this, SOD1 protein levels were decreased in human MCI PBMCs and in 3xTg-AD mouse brain cortex, suggesting that Nrf2 failed to regulate some of its targets in these AD models, as demonstrated by reduced mRNA levels of SOD1, HO-1 and Prdx-1 (Mota et al., 2015).

1.6 Src family tyrosine kinase

Src kinase family (SKF) is a family of non-receptor tyrosine kinases composed by eleven members: Src, Yes, Fyn, Fgr, Frk, Srm, Lyn, Hck, Lck, Brk and Blk, wherein only Src, Yes and Fyn are expressed ubiquitously (Roskoski, 2004). Several reports refer that Src kinase family is involved in numerous processes, namely cell growth, differentiation, metabolism, signal transduction and neuronal ion channel and receptor regulation (Cao et al., 2007b). All Src family members share the same structure, composed of six functional regions: (i) N−terminal Src homology domain (SH) 4 (SH4) containing a myristic acid that is essential for its localization at the inner surface of the cell membrane; (ii) a unique domain that is characteristic of each element of the Src family, located between the SH4 and SH3 domains; (iii) a SH3 domain, linked to a sequence rich in proline to mediate intra- and intermolecular interactions; (iv) a SH2 domain, that binds phosphorylated tyrosine residues on Src and other proteins; (v) a SH1 domain, known for its catalytic capacity; and (vi) C‑terminal tail containing a negative regulatory Tyr530, in humans (**Fig. 9**).

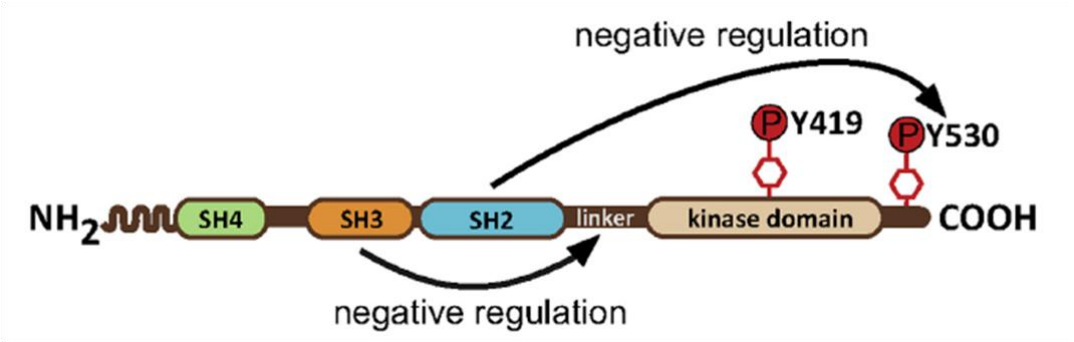

Fig. 9 | The structural domains of human Src. Src is composed to an N-terminal group attached to an Src homology (SH) 4 domain (SH4), a unique region following the SH4 domain, an SH3 domain, an SH2 domain, a kinase domain (also known as the SH1 domain), and a C-terminal domain (Chojnacka and Mruk, 2015) authorized by "Mol Cell Endocrinol".

Src tyrosine kinase has been intensively investigated for more than three decades due to its association with malignant transformation and oncogenesis (Levinson et al., 1972). Brain, osteoclasts, and platelets express higher levels of Src than other cells; in neurons, this expression suggest that Src is involved in different processes besides cell division, since neurons are post-mitotic cells (Brown and Cooper, 1996). Src can be located at different cellular compartments, such as the cytosol, plasma membrane,

nucleus, rough endoplasmic reticulum, mitochondria, endosomes, lysosomes, phagosomes and the Golgi apparatus (Sandilands and Frame, 2008). The activity of Src is regulated by phosphorylation and dephosphorylation of its tyrosine residues, mainly at Tyr530 and Tyr419 (in humans) or Tyr527 and Tyr416 (in mice and rats) by kinase and phosphatase proteins, which cause structural changes by intramolecular interactions (Roskoski, 2015). Thus, phosphorylation of Tyr530 closes Src conformation by approaching the SH2 domain, preventing this way the autophosphorylation of Tyr419 and keeping Src unable to bind substrates. This closed conformation is supported by an interaction between the SH3 domain and the region rich in prolines. Conversely, Tyr530 dephosphorylation opens the conformation of Src, allowing Tyr419 autophosphorylation and consequently activating Src, permitting the phosphorylation of substrates and the interaction with SH3 and SH2 with downstream proteins. Under normal conditions, Src is maintained in an inactive state but can be activated by intra- and intermolecular interactions, a reduction in the C-terminal Src kinase activity, the action of tyrosine phosphatases and a mutation at Tyr530 residue (Chojnacka and Mruk, 2015) (**Fig. 10**).

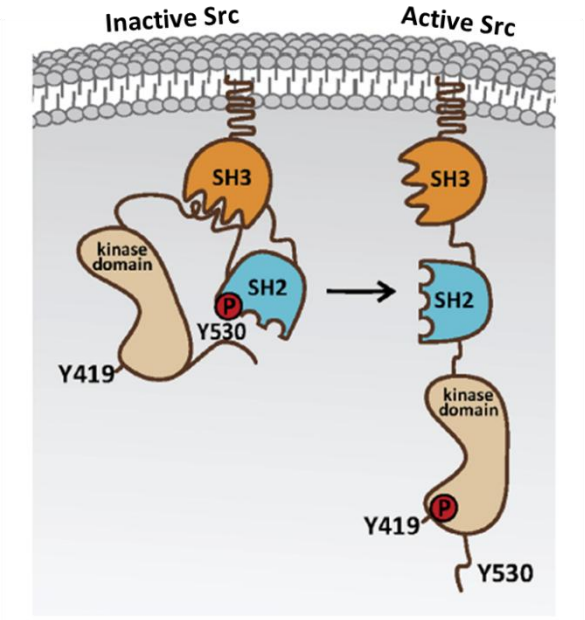

Fig. 10 | The inactivation and activation forms of Src. Src is maintained in an inactive state under normal conditions, in a closed conformation that is strengthened by an interaction between the SH3 domain and the proline-rich region, flanked by the SH2 domain and the kinase domain. In contrast, Src can be activated by several interactions leading to Tyr530 dephosphorylation, opening the conformation and Tyr419 autophosphorylation, thereby creating a fully activated Src kinase. (Chojnacka and Mruk, 2015) authorized by "Mol Cell Endocrinol".

Csk or Csk-homologous kinase are proteins that can phosphorylate the Tyr530 and inactivate Src protein, whereas tyrosine phosphatase non-receptor type 1, 2, 6, 11 (PTPN1, PTPN2, PTPN6, and PTPN11) and receptor-like protein tyrosine phosphatases (alpha, gamma and type C) activate Src through dephosphorylation of Tyr530. Furthermore, Src can also be activated by extracellular signals resulting from the activation of integrin receptors, growth factor receptors, steroid receptors, and G-protein coupled receptors, controlling Src (reviewed in Hebert-Chatelain, 2013). Moreover, a crosstalk between Src and several tumor-associated pathways such as phosphoinositide 3-kinase (PI3K), protein kinase B (PKB) or Akt, and extracellular signal-regulated kinase (ERK) signaling cascades lead to Src activation. Interestingly, Src kinase family members are redox-sensitive and can be activated by H_2O_2 and peroxynitrite. At the same time, tyrosine phosphatases are also sensitive to ROS and oxidation of their SH groups, inhibiting their activities and favoring Src activation (Akhand et al., 1999). Sato and colleagues showed that hypoxia-dependent increase in mitochondrial ROS production activates Src protein in vascular smooth muscle cells (Sato et al., 2005).

1.6.1 Src Kinases and NMDARs

An essential function of Src family kinases in the adult CNS is to regulate the activity of different channels and receptors: (i) ion channels namely, NMDARs (Wang and Salter, 1994); (ii) voltage-gated ion channels, including K^+ channels (Fadool et al., 1997) and Ca^{2+} channels (Cataldi et al., 1996); (iii) ionotropic neurotransmitter receptors, including $GABA_A$ receptors and NMDARs (Moss et al., 1995); and (iv) nicotinic acetylcholine receptors (Wang et al., 2004). By transducing signals from these pathways, Src family members might be involved in learning and memory, pain, epilepsy and neurodegeneration (Salter and Kalia, 2004). Of relevance, Src protein can regulate the activity of NMDARs channels at the synaptic level. Src co-immunoprecipitated as part of the NMDAR complex of proteins and was found within the postsynaptic density (Yu et al., 1997). Several evidences linking Src protein and NMDARs have also emerged since electrophysiological studies showed that NMDARs currents in neurons are regulated by a balance between tyrosine phosphorylation and

dephosphorylation. In HEK293 cells transiently expressing NMDARs, addition of exogenous Src or Fyn potentiated NMDARs currents (Köhr and Seeburg, 1996) and this upregulation of the ion channel activity occurred through GluN2A and GluN2B phosphorylation (Ali and Salter, 2001; Lau and Huganir, 1995). Furthermore, in hippocampal mouse neurons, potentiation of NMDARs currents stimulated by PKC is prevented by Src inhibitors, whereas PKC inhibitors do not prevent the effects of stimulating Src (Lu et al., 1999), reinforcing the direct interaction between NMDARs and Src. Additionally, phosphorylation of GluN2B at Tyr1472 residue, by Src or Fyn, was associated with enrichment of synaptic NMDARs (Goebel-Goody et al., 2009). Furthermore, postsynaptic density 95 protein (PSD-95), an adaptor protein that binds to NMDARs at GluN2A and GluR2B subunits, is phosphorylated by Src and Fyn at Tyr523 residue, *in vitro* and *in vivo* (Du et al., 2009). Interestingly, the interaction between Src and mitochondrial complex I allows the anchoring of Src to the NMDARs and the regulation of this receptor activity (Gingrich et al., 2004).

1.6.2 Src family and Mitochondria

Over the years, it became increasingly clear that protein phosphorylation has an major influence on mitochondrial function (Hebert-Chatelain, 2013). Different Src family members were observed in rat brain mitochondria, namely Fgr, Fyn, Lyn and Src (Salvi et al., 2002). It was shown that Src-mediated phosphorylation of complex IV or cytochrome c oxidase (subunit II) increases the activity of this enzyme and appears crucial for the normal function of osteoclasts (Miyazaki et al., 2006). Furthermore, both Src Homology 2 domain-containing tyrosine Phosphatase-2 (SHP-2) and PTPN1, also known as protein-tyrosine phosphatase 1B (PTP1B), which are important regulators of Src kinases activity (Liu et al., 2015), as well as Csk that phosphorylates Src at Tyr530, are found in rat brain mitochondria, suggesting that Src activity can be directly regulated in mitochondria (Augereau et al., 2005; Salvi et al., 2002, 2004). Interestingly, previous studies reported that addition of ATP increases phosphorylation of Src at Tyr419 (Arachiche et al., 2008). Moreover, a specific inhibitor of PTP1B leads to the deactivation of Src in mitochondria (Hébert Chatelain et al., 2011).

While previous studies suggested that Src, Fyn, Lyn, Fgr and Csk could be resident proteins in mitochondria (Salvi et al., 2004), Boerner and colleagues suggest that the intramitochondrial localization of Src could result from continuous mitochondrial import and export (Boerner et al., 2004). Since Src family kinases do not have a mitochondrial localization signal, these enzymes need an adaptor protein to be translocated to mitochondria. In the past few years, different proteins were shown to import Src to mitochondria. This includes A-kinase anchor protein 121 (AKAP121), an anchoring protein that targets protein kinase A (PKA) to the MOM through interaction with β-tubulin; AKAP121 was shown to be able of bind PTP1B as well as Src (Livigni et al., 2006). It has been shown that AKAP121 binds to mitochondria, increasing complex IV activity in a Src-dependent manner (Livigni et al., 2006). Moreover, overexpression of AKAP121 in HEK293 cells increased mitochondrial production of ATP and mitochondrial membrane potential in a process dependent on Src and PKA (Livigni et al., 2006). Other proteins seem to be involved on Src translocation within mitochondria, such as Dok-4, a member of the downstream of kinase family (Itoh et al., 2005). When Dok-4 is overexpressed in endothelial cells, mitochondrial Src localization is increased, while its downregulation of Dok-4 leads to increased cytosolic localization of Src (Itoh et al., 2005). Furthermore, Dok-4 increases the association of Src with complex IV without altering the activity of this enzyme and decreases the expression of the complex I subunit of 39 kDa (Itoh et al., 2005). Interestingly, if mitochondrial localization of Src kinases results from its translocation from the cytosol, mechanisms responsible for the export of Src kinases out of the mitochondria have not been unraveled. It is important to mention that active Src kinases seem to be rapidly degraded by the ubiquitin–proteasome system (Hebert-Chatelain, 2013).

It has been previously reported that Src can have different targets in mitochondria. As referred above, complex IV can be phosphorylated by Src, resulting in increased enzymatic activity of this enzyme complex in osteoclasts (Miyazaki et al., 2006). Other authors suggested that adenine nucleotide translocase 1 (ANT1), which transports ADP from cytosol to mitochondria in exchange of ATP, is another mitochondrial Src substrate (Feng et al., 2010). Moreover, treatments that are known to increase Src tyrosine phosphorylation, such as ATP, H_2O_2 or orthovanadate increased the enzymatic

activity of complex IV and decreased the activity of complexes I, III and V, suggesting a regulatory effect of Src on these complexes (Hébert Chatelain et al., 2011). In human T98G glioblastoma cells and primary neocortex mouse neurons it was also suggested that Src is essential for regulating the oxidative phosphorylation system and consequently for maintaining cell viability (Ogura et al., 2012, 2014). Src can also bind to mitochondrial complex I (NADH dehydrogenase) subunit 2 (ND2), as observed in excitatory synapses in the brain (Gingrich et al., 2004). Finally, Src kinases are also considered key players in different mitochondrial-dependent apoptotic pathways. Moreover, although Lyn and Lck members seem to have a pro-apoptotic role in mitochondria, Src has anti-apoptotic properties, since activated Src can phosphorylate the nuclear factor-kappaB (NF-κB), contributing to cell survival during hypoxia (Lluis et al., 2007).

1.6.3 Src Kinases in AD

The hypothesis that Src kinase family could be related to AD started to be investigated few years ago. In 2007, Zou and colleagues demonstrated in HEK293 cells and mouse hippocampus that BACE activity could be regulated by receptor tyrosine kinases (RTKs), consequently leading to changes in Aβ production (Zou et al., 2007). Interestingly, enhancement in BACE activity and Aβ production were abrogated by Src family kinase inhibitors and by depletion of endogenous Src with RNAi (Zou et al., 2007). In agreement, Chaufty and colleagues showed that Src is responsible for the phosphorylation of Mint2, a member of the Mint adaptor proteins, which is involved in the regulation of APP endocytic sorting pathway, increasing intracellular Aβ accumulation (Chaufty et al., 2012).

In previous studies, our group showed that hippocampus and cortex of 3 month-old 3xTg-AD male mice exhibited reduced Src phosphorylation, which in the case of hippocampus was related with decreased GluN2B Tyr1472 phosphorylation (Mota et al., 2014). On the other hand, Wu and Hou, showed that treatment with $A\beta_{25–35}$ resulted in higher tyrosine phosphorylation of GluN2A-contaning NMDARs in rat hippocampal CA1 region, facilitating the interactions of GluN2A and PSD-95 with Src (Wu and Hou, 2010). Importantly, the effects of $A\beta_{25–35}$ could be impaired by 4-Amino-

3-(4-chlorophenyl)-1-(t-butyl)-1H-pyrazolo[3,4-d]pyrimidine (PP2), a Src kinase family inhibitor, protecting against neuronal loss in the CA1 region (Wu and Hou, 2010). Additionally, $A\beta_{25–35}$ leads to Src and Fyn-induced PSD-95 phosphorylation at Tyr523, which may be responsible for Aβ neurotoxicity neurotoxicity in SH-SY5Y cells (Du et al., 2012). Furthermore, in primary murine microglia cultures, Src also seems to be related with microglial activation induced by $A\beta_{1–42}$ fibrils (Dhawan and Combs, 2012). Finally, pharmacological activation (using the agonist SKF38393) of dopamine D1/D5 receptors (D1R/D5R), known to increase surface expression of synaptic NMDARs and facilitate LTP, was shown to protect LTP of hippocampal CA1 synapses from the negative effect of Aβ oligomers in a Src-dependent manner; in contrast, the use of Src family kinase inhibitor completely eliminated the protective effects of D1R/D5R stimulation (Yuan Xiang et al., 2016).

1.7 Objectives

It has been recognized that Aβ can interact with NMDARs, leading to increased H_2O_2 production, intracellular Ca^{2+} dyshomeostasis (Ferreira et al., 2012) and mitochondrial dysfunction (Ferreira et al., 2015), which are largely associated with neuronal dysfunction in AD (Ferreira et al., 2015). Oxidative stress is an important feature in AD pathogenesis, present in several models of AD (Butterfield, 2002), and it is also known to be able to activate Src protein (Akhand et al., 1999). Src can regulate the activity of NMDARs, by phosphorylating GluN2B-containing NMDARs at Tyr1472, which leads to increasing NMDARs targeting in the synaptic membrane (Goebel-Goody et al., 2009). Moreover, low levels of ROS can activate the transcription factor Nrf2, described to be altered in AD (Ramsey et al., 2007). In the present study, we aimed to define the impact of H_2O_2 produced following $A\beta_{1-42}$ oligomers exposure as a regulator of Src and Nrf2 proteins phosphorylation, as well as the feed-forward influence of Src activation on oxidative stress regulation. For this purpose, the following specific objectives have been pursued:

I. **Evaluate H_2O_2 generation after $A\beta_{1-42}$ oligomers exposure in hippocampal neurons, whether it occurs by mitochondria, and the involvement of Src protein and NMDARs in this process.**

   Taking into account that Aβ increase NMDAR-mediated Ca^{2+}_i levels (Ferreira et al., 2012) and that Src is involved in NMDARs regulation (Mota et al., 2014b), we hypothesized that Aβ could increase oxidative stress in a Src and NMDARs dependent manner. We aimed to determine cellular and mitochondrial production of H_2O_2 in mature rat hippocampal neurons and HT22 cells (mouse hippocampal cell line) exposed to $A\beta_{1-42}$ oligomers. Moreover, we further evaluated the role of NMDARs and Src in this effect.

II. **Determine the effect of Aβ-induced H_2O_2 on Src activation and Nrf2 phosphorylation as well as the feed-forward role of Src on Nrf2 activation.**

   In this part of the study we aimed to evaluate Aβ-mediated Src and Nrf2 activation and determine whether this occurs through ROS formation, or NMDARs interaction;

for this purpose we measured total and phosphorylated levels of these proteins in mature primary hippocampal neurons exposed to $A\beta_{1-42}$ oligomers in the presence of antioxidants or NMDARs antagonist. The relationship between Src activation and Nrf2 phosphorylation under oxidant stimulus was also evaluated in total and nuclear extracts from primary hippocampal neurons and HT22 cells.

III. Elucidate the role of Src on mitochondrial dynamics and the involvement of Nrf2.

Since Src protein can be located in mitochondria (Salvi et al., 2002), where it mediates different pathways and is directly regulated in this organelle, and Nrf2 was also found in mitochondria (Strom et al., 2016), we hypothesized that Src might have a role on mitochondrial dynamics, with a possible relation with Nrf2. To answer this question, we measured, in mitochondrial extracts derived from HT22 cells treated with H_2O_2, total and phosphorylated levels of Src and Nrf2, as well as the levels of dynamic mitochondrial proteins.

CHAPTER II – MATERIAL AND METHODS

2.1 Materials

Neurobasal medium, B27 supplement, fetal bovine serum (FBS) and all antibiotics were purchased from GIBCO (Paisley, UK). Dulbecco's Modified Eagle's Medium (DMEM) culture medium (SIGMA D5648), protease cocktail inhibitors, Fura-2/AM, Amplex® Red, Hoechst 33342 nucleic acid stain were purchased from Invitrogen/Molecular Probes (Life Technologies Corporation, Carlsbad, CA, USA). Trypsin, trypsin inhibitor, fatty acid free bovine serum albumin (BSA), SU 6656, L-Buthionine-Sulfoximine (BSO), L-Glutathione reduced (GSH-EE), N-Acetyl-L-Cysteine (NAC), Hydrogen peroxide (H_2O_2), 5-Fluoro-2'-deoxyuridine (5-FDU), horseradish peroxidase, Mito PY1 and other analytical grade reagents were purchased from Sigma Chemical and Co. (St.Louis, MO, USA). The compound MK-801 [(+)-5-methyl-10,11-dihydro-5H-dibenzo[a,d] cyclohepten-5,10-imine maleate)], were obtained from Calbiochem (Merck Millipore, Darmstadt, Germany). BioRad Protein Assay and Western Blot PVDF membrane were purchased from BioRad Laboratories, Inc. (Munich, Germany). BSA used in Western blotting was purchased from Santa Cruz Biotechnology (Santa Cruz Biotechnology, Inc., TX, USA). ECF substrate was purchased from GE Healthcare (GE Healthcare Bio-Sciences, PA, USA) and Lennox L Broth (LB) from Invitrogen (Eugene, OR, USA). All the primary and secondary antibodies used for Western Blotting and immunocytochemistry are described in **Table 2.**

Table 2 | Antibody information used in this data

Primary Antibodies	Host	Dilution	Reference/Supplier
β Actin	Mouse	1:5000 (WB)	Sigma A5316 (Sigma)
Complex II (70kDa subunit)	Mouse	1:1000 (WB)	Molecular Probes A11142 (Molecular Probes—Invitrogen)
Drp1	Mouse	1:500 (WB)	BD biosciences 611112 (BD Biosciences)
GAPDH	Mouse	1:2500 (WB)	Chemicon MAB374
GFAP (H50)	Rabbit	1:200 (ICC)	Santa Cruz sc-9065 (Santa Cruz)
HSP60	Mouse	1:1000 (WB) 1:200 (ICC)	Millipore MAB3514 (Merck Millipore)
Lamini B1	Rabbit	1:1000 (WB)	Abcam # 16048 (Abcam)
MAP-2	Rabbit	1:200 (ICC)	Chemicon AB5622
Mfn2	Rabbit	1:1 000 (WB)	Sigma M6319 (Sigma)
Nrf2	Rabbit	1:500 (WB)	Abcam #31163-500 (Abcam)
OPA1	Mouse	1:500 (WB)	BD Biosciences 612606 (BD Biosciences)
Phospho-Nrf2 (S40)	Rabbit	1:500 (WB)	Abcam ab76026 (Abcam)
Phospho-Src (Tyr 416)	Rabbit	1:1000 (WB)	Cell Signalling 6943 (Cell Signalling)
Src	Mouse	1:1000 (WB) 1:200 (ICC)	Cell Signalling 2110 (Cell Signalling)
TFAM	Rabbit	1:2000 (WB)	Abcam ab131607
Tom20	Rabbit	1:200 (WB)	Santa Cruz sc-11415
Secondary Antibodies			
Alexa Fluor-647	Donkey (Anti-Mouse)	1:300(ICC)	#A31571 (Molecular Probes-Invitrogen)
Alexa Fluor-594	Goat (Anti-Rabbit)	1:300 (ICC)	#R37117 (Molecular Probes-Invitrogen)
Alexa Fluor-488	Donkey (Anti-Rabbit)	1:300(ICC)	#R37118 (Molecular Probes-Invitrogen)
Alexa Fluor-488	Donkey (Anti-Mouse)	1:300 (ICC)	#R37114 (Molecular Probes-Invitrogen)
Anti-Rabbit (H+L), Alkaline Phosphatase Conjugated	Goat (Anti-Rabbit)	1:10000 (WB)	Thermo Scientific Pierce #31340 (Pierce Thermo Fisher Scientific)
Anti-Mouse (H+L), Alkaline Phosphatase Conjugated	Goat (Anti-Mouse)	1:10000 (WB)	Thermo Scientific Pierce #31320 (Pierce Thermo Fisher Scientific)

2.2 Primary hippocampal cultures

Primary hippocampal neurons were prepared as described previously (Ambrósio et al., 2000), with some minor modifications. Female Wistar rats with 17-18 days of gestation were sacrificed by cervical dislocation following anesthesia with 2-bromo-2-chloro-1,1,1-trifluoroethane. Hippocampus were dissected out from fetal rats and then digested with 0.6 mg/mL trypsin for 5 min at 37°C in Ca^{2+}- and Mg^{2+}-free Hank's balanced salt solution, containing 137 mM NaCl, 5.36 mM KCl, 0.44 mM KH2PO4, 0.34 mM $Na_2HPO_4.2H_2O$, 5 mM glucose, 1 mM sodium pyruvate and 10 mM HEPES, pH 7.2. Trypsin was inhibited using 1.5mg/ml of trypsin inhibitor in Ca^{2+}- and Mg^{2+}-free Hank's balanced salt solution. Cells were separate by mechanical digestion using a pipette. Cells were plated at a density of $8.4x10^4$ cells/cm^2 in poly-D-lysine coated 6-well or 96-well plates for total extracts preparation and H_2O_2 and Ca^{2+} monitoring respectively, and at a density of $4.2x10^4$ cells/cm^2 in poly-D-lysine coated glass coverslips for immunocytochemistry. Cells were cultured for 17 days in vitro (DIV) in 95% air and 5% CO_2, in serum-free Neurobasal medium supplemented with 2% B27, 25 µM glutamate, 0.5 mM glutamine and 0.12 mg/mL gentamicin. In order to reduce glia growth, 10 µM of the mitotic inhibitor 5-FDU was added to the culture at 72 hours in culture. One half of the medium was changed with fresh medium without added glutamate or 5-FDU each 7 DIV. Immunofluorescence to detect the presence of glial cells revealed 1,7% of astrocytes (Supplementary **Fig. S1**). All animal experiments were carried accordingly to the care and use of laboratory animals and guidance of CNC, University of Coimbra, with care to minimizing the number of animals and their suffering.

2.3 HT22 cell line culture

Mouse clonal hippocampal HT22 cells, a glutamate-sensitive cell line and a subclone of the HT4 hippocampal cell line (Morimoto and Koshland, 1990), were obtained from Dr. Dave Schubert from The Salk Institute, La Jolla. Cells were cultivated in 95% air and 5% CO2 at 37°C, in high glucose DMEM containing 10% FBS, 12mM $NaHCO_3$, 5 mM HEPES pH 7.3 supplemented with 100 µg/mL streptomycin and penicillin. Sub-cultures were

made using dissociation medium containing 140 mM NaCl, 8.1 mM Na_2HPO_4, 1.47 mM KH_2PO_4, 1.47 mM KCl, 0.55 mM EDTA, Fenol Red, pH 7.3, when confluence was about 80%.

2.4 $A\beta_{1-42}$ and $A\beta_{42-1}$ oligomers preparation

Aβ peptide preparation, previously described as ADDLs (Aβ-derived diffusible ligands), was made from synthetic $A\beta_{1–42}$ or $A\beta_{42-1}$ peptide, as previously described [W.L. Klein, 2002]. Briefly, synthetic Aβ peptide was dissolved in 1,1,1,3,3,3-hexafluoro-2-propanol (HFIP) to a final concentration of 1 mM. The peptide—HFIP solutions were incubated at room temperature for 60 min, with the vial closed and then was back on ice for 5-10min. HFIP was first evaporated overnight in the hood at room temperature and then removed in a Speed Vac (Ilshin Lab. Co. Ltd., Ede, The Netherlands), and dried HFIP film was stored at −20 ◦C. The peptide film was resuspended to make a 5 mM solution in anhydrous dimethyl sulfoxide. Aβ peptides were further prepared by diluting the solution in phenol red-free Ham's F-12 medium without glutamine to a final concentration of 100 μM and incubated overnight at 4°C. The preparation was centrifuged at 14,000 × g for 10 min at 4°C to remove insoluble aggregates, and the supernatant containing soluble oligomers and monomers was transferred to pre-lubrificated clean tubes (Costar) and stored at -20°C. Protein content was determined by using the BioRad protein assay and quantified by using a microplate reader Spectra Max Plus 384 (Molecular Devices, USA). The presence of different assembly peptide forms (monomers, oligomers and/or fibrils) in the preparation was evaluated by 4–16% Tris–Tricine SDS-PAGE gel electrophoresis and further staining with Coomassie blue. The $A\beta_{1-42}$ and $A\beta_{42-1}$ preparation contained about 65% and 50% of oligomers and about 35% and 50% of monomers, respectively (**Fig. 11**).

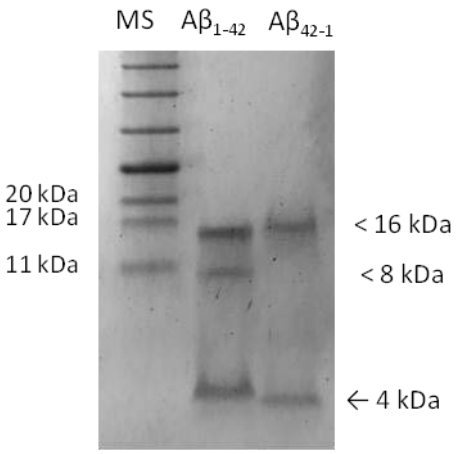

Fig. 11 | Representative gel of electrophoretic separation of $A\beta_{1-42}$ and $A\beta_{42-1}$ peptides prepared from synthetic forms. Oligomeric forms of $A\beta_{1-42}$ and $A\beta_{42-1}$ are represented by the arrow heads and monomeric form is represented by the arrow. MS – molecular weight standard

2.5 Cells treatments

Hippocampal and HT22 cells were exposed to 1 µM of soluble $A\beta_{1-42}$ and $A\beta_{42-1}$ or to 1mM of H_2O_2 for 5, 10 and 30 min (or 1, 2 or 6 h when indicated) in conditioned culture medium. In some conditions, cells were also exposed to GSH (0.1mM) and Mitotempo (1µM) for 24 h, BSO (0.5mM) for 6 h, SU6656 (5µM), and NAC (1mM) for 1 h or MK-801 (10 µM) for 10 min.

2.6 Proteins extraction

2.6.1 Total extract preparation

Cells were washed 3 times in ice-cold PBS and then scrapped in RIPA extraction buffer (containing 150 mM NaCl, 50 mM Tris HCl, 5 mM EGTA, 1% Triton X-100, 0.1% SDS, 0.5% deoxycholate, pH 7.5) supplemented with 100 nM okadaic acid, 1 mM PMSF, 25 mM NaF, 1 mM Na3VO4, 1 mM DTT and 1 µg/ml protease inhibitor cocktail (chymostatin, pepstatin A, leupeptin and antipain). Homogenates were then lysed in a ultrasonic bath (UCS 300 – THD; at heater power 200 W and frequency 45 kHz) during 10 sec and centrifuged for 10 minutes at 20 800×g (4^{o}C) to remove cell debris and the supernatant was collected.

2.6.2 Nuclear fractions

Nuclear fractions from primary hippocampal cell cultures and HT22 cells were obtained using the Nuclear/Cytosolic fractionation kit (Biovision, CA, USA). The characterization of the nuclear fractions is expressed in Fig.2.

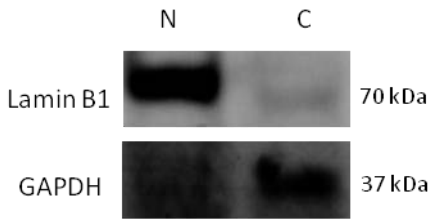

Fig. 12 | Characterization the nuclear fractions. The purity of the fractions was evaluated by Western Blotting. N – Nuclear fractions, C – Cytosolic fraction

2.6.3 Mitochondrial fractions

HT22 cells were washed twice with PBS 1x. Cells were scratched in ice-cold sucrose buffer (250 mM sucrose, 20 mM HEPES, 10 mM KCl, 1.5 mM MgCl2, 1 mM EDTA, 1 mM EGTA – pH 7.4), supplemented with 100 nM okadaic acid, 1 mM PMSF, 25 mM NaF, 1 mM Na3VO4, 1 mM DTT and 1 µg/ml protease inhibitor cocktail (chymostatin, pepstatin A, leupeptin and antipain). Lysates were homogenized using a potter with 40 strokes, at 280 rpm, and later centrifuged at 1300×g for 12 minutes (4^{o}C). The nuclear/cell debris pellet was discarded, and the supernatant was centrifuged again at 11 900×g for 20 minutes (4^{o}C). The mitochondrial pellet was resuspended in ice-cold supplemented sucrose buffer. Trichloroacetic acid (TCA) at 15% was used to precipitate cytosolic proteins from the cytosolic supernatant and centrifuged at 16 300×g for 10 minutes (4^{o}C). Cytosolic pellet was resuspended in ice-cold supplemented sucrose buffer, and brought to pH 7 with 10 M KOH. The characterization of the mitochondrial fractions is expressed in **Fig. 13**.

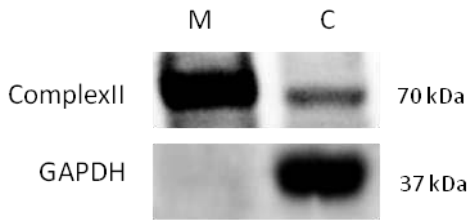

Fig. 13 | Characterization of the mitochondrial fractions. The purity of the fractions was evaluated by Western Blotting. M – Mitochondrial fractions, C – Cytosolic fraction

2.7 Western blotting

Protein content of cellular fractions was determined using the BioRad protein assay reagent based on the Bradford dye-binding procedure. Then, proteins extracts were denaturated with 6x concentrated loading buffer (containing 300 mM Tris-HCl pH 6.8, 12% SDS, 30% glycerol, 600 mM DTT, 0.06% bromophenol blue) at 95°C for 5 min. Equivalent amounts of protein samples (15µg-30µg) were separated by 8-12% SDS-PAGE gel electrophoresis and electroblotted onto polyvinylidene difluoride (PVDF) membranes. The membranes were further blocked with 5% (w/v) BSA in Tris Buffered Saline (containing Tris-HCl 25 mM pH 7.6 and NaCl 150 mM) with 0.1% Tween-20 (TBS-T), for 1h at room temperature and then incubated overnight at 4°C with primary antibodies. Furthermore, Actin, GAPDH, ComplexII and TBP were used as control loading, for the total, cytosolic, mitochondrial and nuclear extracts, respectively. Anti-mouse or anti-rabbit IgG secondary antibody conjugated to the alkaline phosphatase prepared in 1% (w/v) BSA in TBS-T were used for 1 hour, at room temperature. Immunoreactive bands were visualized by alkaline phosphatase activity after incubation with ECF reagent and visualized by using a BioRad ChemiDoc Touch Imaging System (BioRad, Hercules, USA) and quantified using Image Lab analysis software (BioRad). All the primary and secondary antibodies used are described in **Table 2.**

2.8 Immunocytochemistry

Mature hippocampal and HT22 cells cultured in glass coverslips were washed 3 times with warm PBS, fixed with 4% paraformaldehyde (pre-warmed at 37^{o}C) for 20 minutes and permeabilized in 0.1% Triton X-100 in PBS for 2 minutes. Then, cells were blocked for 1h at room temperature with 3% (w/v) BSA in PBS (blocking solution) and further incubated with the primary antibody prepared in blocking solution, overnight, at 4°C. Cells were washed with PBS and incubated with the secondary antibody in blocking solution for 1 hour at room temperature. Nuclei were stained using Hoechst 33342 in PBS (1 µg/mL) for 10 minutes and coverslips were mounted using Mowiol 40-88 (Sigma Chemical and Co., St.Louis, MO, USA). Confocal images were obtained using a Plan-

Apochromat/1.4NA 63x lens on an Axio Observer.Z1 confocal microscope (Zeiss Microscopy, Germany) with Zeiss LSM 710 software.

2.9 H_2O_2 levels determination

H_2O_2 levels were determined by following Amplex® Red fluorescence. Amplex® Red reagent (10-acetyl-3,7-dihydroxyphenoxazine) is a colorness substrate that reacts with H_2O_2 in a 1:1 stoichiometry to produce the red-fluorescent oxidation product, the resorufin (excitation 550 nm; emission 580 nm) allowing the monitoring of H_2O_2 production/release. After a washing step with Na^+ medium (containing 140 mM NaCl, 5 mM KCl, 1 mM CaCl2, 1 mM MgCl2, 10 mM Glucose, 10 mM Hepes, pH 7.4/NaOH), H_2O_2 were measured in 10 µM Amplex® Red plus 0.5 units/mL of horseradish peroxidase in Mg^{2+}-free Na^+ medium during 3 min (basal) and further 30 min after stimuli using a microplate reader Spectrofluorometer Gemini EM (Molecular Devices, USA).

2.10 Mitochondrial H_2O_2 levels determination

MitoPY1 was used to evaluate mitochondrial-derived H_2O_2 in primary hippocampal neurons. Cells were incubated with 10 µM MitoPY1 in Na^+ medium at 37°C for 30 min to allowed entry into mitochondria. Then, cells were washed to remove not internalized probe and changes in mitochondrial H_2O_2 levels were evaluated in Mg^{2+}-free Na^+ medium supplemented with glycine (20 µM) and serine (30 µM) using confocal images obtained with a 20x objective, on a Cell Observer SD microscope. Basal Mitochondrial H_2O_2 production was recorded for 15 min basal followed by 30 min after stimuli.

2.11 Intracellular Ca^{2+} recording

Primary hippocampal neurons were incubated with the Fura-2/AM ratiometric fluorescent probe (10 µM) for 40 min at 37 °C in Mg^{2+}-free Na^+ medium supplemented with glycine (20 µM) and serine (30 µM). When added to cells, Fura-2/AM crosses cell membrane and once inside the cell, the acetoxymethyl groups are removed by cellular esterases, which generate "Fura-2", the pentacarboxylate calcium indicator. After a

washing step, Fura-2 fluorescence was analyzed using a Spectrofluorometer Gemini EM (Molecular Devices, USA) microplate reader at a 340/380 nm excitation and 510 nm emission wavelengths. Fura-2 fluorescence was recorded for 2 min (basal values) and for further 5 min after stimuli. Fluorescence values (ratio 340/380) were normalized to the baseline.

2.12 Constructs and Transfection

2.12.1 Constructs

Plasmids used for transfection were**:** pLNCX chick src Y527F (Addgene plasmid #13660) and pLNCX chick src K295R (Addgene plasmid #13659) obtained from Addgene (UK) in the form of already transformed bacteria. For the empty vector, in order to separate Src amino acids sequence from the vector plasmid, we firstly used restriction enzyme digestion ClaI (BioLabs #Ro197L, New England), according to the manufacturer's protocol. Then, we visualize the results of digestion in a 1% Agarose Gel. The DNA band corresponding to the empty vector was cropped and DNA was extracted using the NucleoSpin® Gel and PCR Clean-up (Macherey-Nagel #740609, Germany) accordingly to the manufacturer's protocol. Finally, the blunt end and cohesive end termini of the resulting empty vector were join using T4 DNA Ligase enzyme.

2.12.2 Bacteria transformation and Plasmid DNA extraction

The pLNCX (empty vector) plasmid expressing bacteria were obtained adding 1 µg of plasmid DNA to competent DH5α Escherichia coli bacteria and mixed by tapping. Bacteria were incubated for 25 minutes on ice, suffered a heat shock of 30 seconds at 42ºC and returned to ice for 3 more minutes.

Transformed E. coli were incubated in LB at 37ºC for 5 hours under 220 rpm agitation and then plated overnight at 37ºC in LB-Agar plates, prepared with the respective antibiotic (100 µg/mL Ampicillin for SrcY527F, SrcK295R). Isolated colony from each culture was picked from the LB-Agar plates and was grown overnight, at 37^{o}C, under 220 rpm agitation, in LB with the respective antibiotic. Cells were centrifuged at 4000×g for 10 minutes and growth medium was discarded. PureLink® HiPure Plasmid

Filter DNA Purification kit (Invitrogen, Eugene, OR, USA) was used for plasmid DNA extraction. Plasmid DNA quantification was done using NanoDrop® 2000 (Pierce Thermo Fisher Scientific, Rockford, IL, USA).

2.12.3 Transfection of Hippocampal neurons and HT22 cells

HT22 cells were co-transfected with SrcY527F, SrcK295R or empty plasmid, by calcium phosphate co-precipitation, 48 hours before experiments. HT22 cells were plated and maintained in culture until reach 50% of confluence. A solution 1 was prepared adding sequentially H_2O, 3 µg of DNA plasmid and 250 mM CaCl2 (2M stock in H_2O). Then, solution 1 was mix dropwise with an equal volume of a 2x HBS (HEPES buffered saline) pH 7.5 to obtained a transfection solution. Transfection solution was incubated at room temperature for 30 min, with vortex every 5 minutes, to allow the formation of precipitates and latter added dropwise to the cells. Cells were maintained 4-6h in the incubator (37ºC, 5% CO_2) and finally transfection medium was replaced by culture medium. Plasmids expression was enabled for 48 hours.

2.13 Statistical analysis

Statistical significance was determined by one-way or two-way ANOVA followed by the Bonferroni post-hoc test for multiple groups or by the Student's t-test for comparison between two Gaussian populations, as described in figure legends. Data were analyzed by using Excel (Microsoft, Seattle, WA, USA) and GraphPad Prism 5 (GraphPad Software, San Diego, CA, USA) softwares Data were expressed as the mean ± S.E.M. of the number of experiments indicated in figure legends. $P<0.05$ was considered significant.

CHAPTER III – RESULTS

3.1 Aβ induces increased mitochondrial H_2O_2 production related with Src protein and NMDA receptors in mature hippocampal neurons

In this study, we first investigated the effect of $A\beta_{1-42}$ oligomers (prepared and characterized as described in Materials and Methods) on H_2O_2 production and Ca^{2+}_i levels, exploring the possible role of Src and NMDARs, in primary mature hippocampal neurons. Aβ has been largely recognized to increase ROS levels, as described by Behl (1994) in rat cortical neurons, leading this way to oxidative stress and mitochondrial dysfunction (Zhao and Zhao, 2013). In this context, we evaluated the specific production of H_2O_2 in mature hippocampal neurons after $A\beta_{1-42}$ oligomers immediate exposure. By following the fluorescence of resorufin (see Material and methods section) we were able to evaluate the production of H_2O_2 in our cell culture. We observed a significant increase in H_2O_2 production along 30 minutes of $A\beta_{1-42}$ exposure, which was prevented, as expected, by pre-treatment with antioxidants namely, GSH-EE and NAC (**Fig. 14A**). We also observed a tendency for a decrease in the H_2O_2 production following pre-treatment with Mitotempo, a mitochondrial antioxidant, although this is very preliminary data (**Fig. 14A**). Moreover, in order to identify some possible pathways that could participate in increased H_2O_2 production, we also used a Src protein inhibitor, SU6656, and an antagonist of NMDARs, MK-801. Interestingly, we observed that the effect induced by Aβ oligomeric species could be prevented in the presence of SU6656 and MK-801 (**Fig. 14B**), suggesting the involvement of Src and NMDARs activation on Aβ-mediated H_2O_2 levels in mature hippocampal neurons. Moreover, to prove the specific effect of $A\beta_{1-42}$ and discard the hypothesis of non-specific effect due to the addition of a peptide, we also exposed the cells to $A\beta_{42-1}$, the reverse peptide. Results depicted in **Fig. 14C** show no significant differences in H_2O_2 levels in hippocampal neurons treated with the $A\beta_{42-1}$ peptide, in comparison to the control (untreated conditions), validating the selective effects of $A\beta_{1-42}$. Of note, SU6656, MK-801 and GSH-EE treatments *per se* did not affect H_2O_2 levels under control conditions (data not shown) and further studies should be performed with NAC and Mitotempo treatments. In HT22 cell line, no differences were verified with $A\beta_{1-42}$ oligomers on H_2O_2 production (supplementary **Fig. S2**).

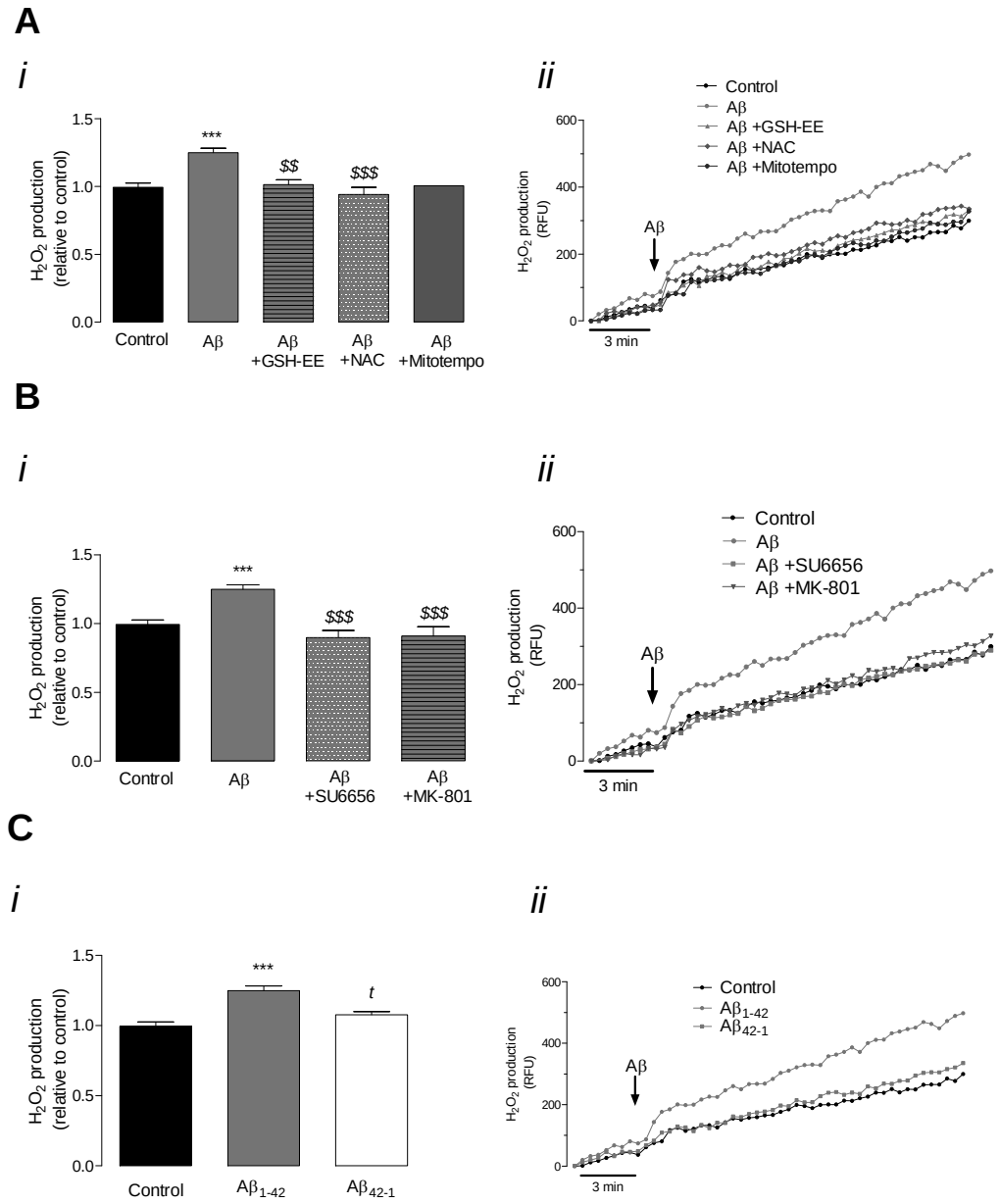

Fig. 14 | H_2O_2 production under $A\beta_{1-42}$ stimulus in mature hippocampal neurons. H_2O_2 production was evaluated by monitoring the fluorescence of resorufin using a microplate reader Spectrofluorometer Gemini EM (excitation 550 nm; emission 580 nm). Basal fluorescence was recorded for 3 min, while the effect of Aβ oligomers (1 µM) was recorded for 30 min. The influence of NAC (1 mM), a precursor of GSH, GSH-EE (0.1 mM), Mitotempo (1 µM), a mitochondrial antioxidant (**A**) and the effect of Src inhibitor (SU6656, 5 µM) and MK-801 (10 µM), an NMDARs antagonist (**B**), were evaluated. The influence of the reverse peptide, $A\beta_{42-1}$ (1 µM), was also evaluated (**C**). In graphics (i), results were plotted as the difference between the last value achieved and the basal value before Aβ addition. Graphics (ii) are the representative line charts. Data are expressed as the mean ± SEM of n=1 to 7 experiments in quadruplicates. Statistical analysis: (**A** and **B**) $^{***}p < 0.001$ *versus* control, $^{\$\$}p < 0.01$ and $^{\$\$\$}p < 0.001$ *versus* Aβ (two-way ANOVA followed by Bonferroni *post-hoc* test); (**C**) $^{***}p < 0.001$ versus Control (one-way ANOVA followed by Bonferroni *post-hoc* test) and $^{t}p < 0.05$ versus $A\beta_{1-42}$ (Student's t-test).

Oxidative stress and mitochondrial dysfunction are closely related in AD. Furthermore, AmplexRed allows the measurement of extracellular H_2O_2, thus leaving uncertainty as to the origin of H_2O_2 in the cell. Taking this into account, we evaluated the specific mitochondrial H_2O_2 production in the presence of $A\beta_{1-42}$ oligomers by monitoring the fluorescence of MitoPY1, a specifically mitochondrial probe, in the same conditions described before. Our results showed increased mitochondrial H_2O_2 production after $A\beta_{1-42}$ treatment that was prevented in the presence of antioxidants like NAC or Mitotempo, the latter a mitochondrial antioxidant (**Fig. 15A**). Additionally, Aβ-induced mitochondrial H_2O_2 was precluded following exposure to SU6656 and MK-801 (**Fig. 15B**). These results suggest that H_2O_2 production induced by Aβ may occur in mitochondria, further confirming the involvement of Src and NMDARs in Aβ-mediated mitochondrial H_2O_2 production. Of note, all treatments largely reduced mitochondrial H_2O_2 levels under control/untreated conditions (**Fig. 15A,B**).

∇ **Fig. 15 | Mitochondrial H_2O_2 production under $A\beta_{1-42}$ stimulus in mature hippocampal neurons.** Levels of mitochondrial H_2O_2 production were evaluated by monitoring the fluorescence of MitoPY1 (10 μM) in confocal images obtained with a 20x objective, on a Cell Observer SD microscope. Basal mitochondrial H_2O_2 production was recorded for 15 min and the effect of Aβ oligomers (1 μM) was recorded for 30 min; fluorescence intensity was quantified in Image J. The effect of Mitotempo (1 μM) and NAC (1 mM) (**A**) or SU6656 (5 μM) and MK-801 (10 μM) (**B**), were also evaluated. In graphics (i), slope was calculated using values of RFU before and after Aβ addition. (ii) Representative line charts. (iii) Fluorescence image of representative cells before and after the treatment. Scale bar: 10 μm. Data are presented as the mean ± SEM of 20 to 100 single cell lecture analysis obtained from 2 to 5 independent experiments. Statistical analysis: $^{****}p < 0.0001$ *versus* control "no treatment", $^{\$\$\$\$}p < 0.0001$ *versus* Aβ "no treatment" (two-way ANOVA followed by Bonferroni *post-hoc* test).

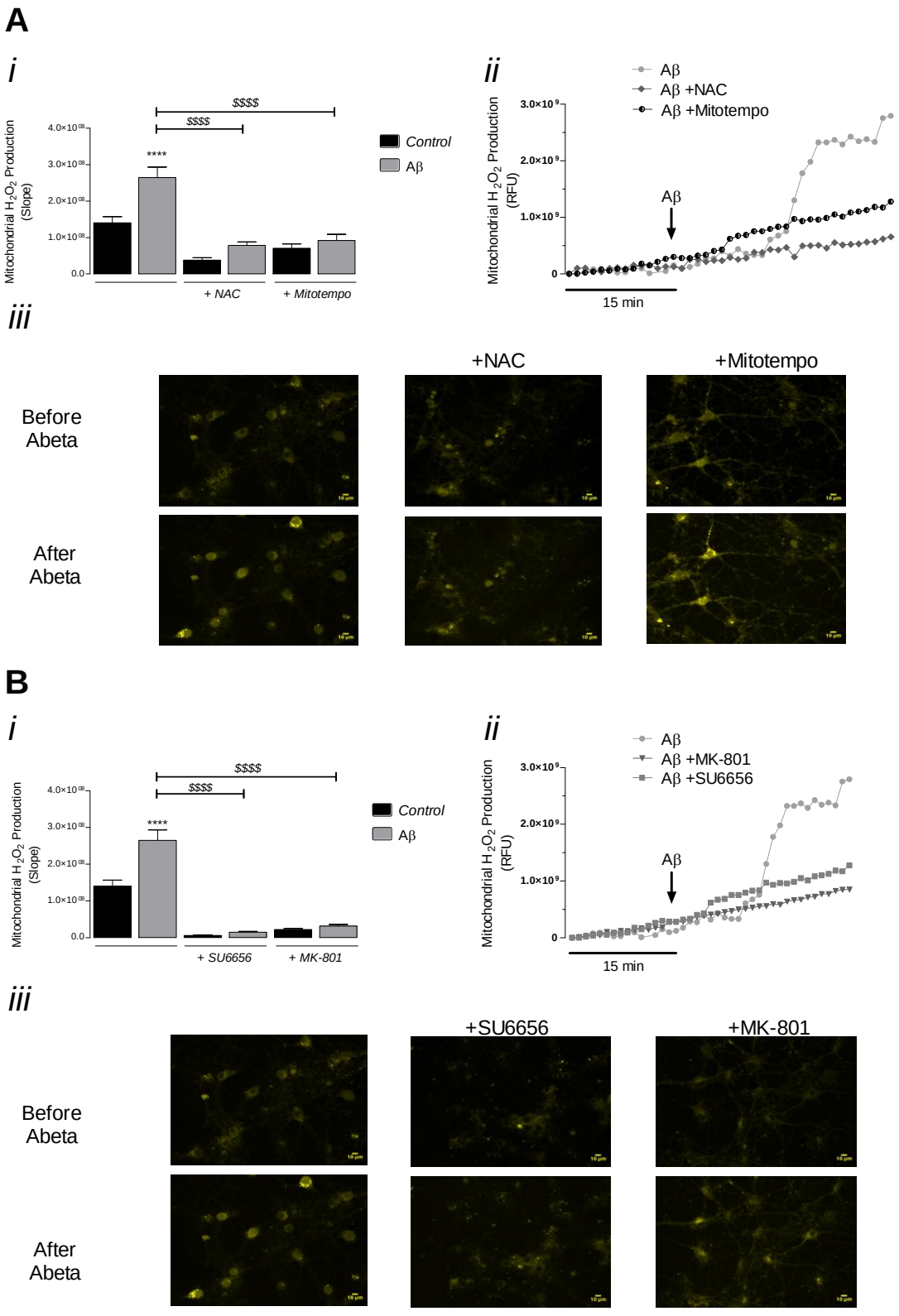
A
i
Mitochondrial H2O2 Production (Slope)
$$$$
$$$$
****
Control
Aβ
+ NAC
+ Mitotempo
ii
Mitochondrial H2O2 Production (RFU)
Aβ
Aβ +NAC
Aβ +Mitotempo
Aβ
15 min
iii
+NAC
+Mitotempo
Before Abeta
After Abeta
B
i
Mitochondrial H2O2 Production (Slope)
$$$$
$$$$
****
Control
Aβ
+ SU6656
+ MK-801
ii
Mitochondrial H2O2 Production (RFU)
Aβ
Aβ +MK-801
Aβ +SU6656
Aβ
15 min
iii
+SU6656
+MK-801
Before Abeta
After Abeta

3.2 Increased Ca^{2+}_i levels after $A\beta_{1-42}$ acute treatment depends on Src protein

Taking into account the close relationship between Ca^{2+}_i homeostasis, mitochondrial dysfunction and oxidative stress, and considering that Aβ can lead to Ca^{2+} entry through NMDARs (reviewed in Naia et al., 2016), we examined whether Src or ROS influence Aβ-mediated Ca^{2+}_i levels changes in mature hippocampal neurons. Using the fluorescence probe Fura-2, we confirmed the significant increase in Ca^{2+}_i after $A\beta_{1-42}$ acute treatment (**Fig. 16**), observed by Ferreira and co-authors (2012). Interestingly, this Ca^{2+} rise was notably decreased in the presence of SU6656 or MK-801 (**Fig. 16A**), confirming the involvement of NMDARs and supporting an important role Src kinase in Ca^{2+}_i levels mediated by Aβ exposure. Results depicted in **Fig. 16B** show no differences in Ca^{2+}_i levels in hippocampal neurons control or treated with $A\beta_{42-1}$ reverse peptide, validating once again the specificity of $A\beta_{1-42}$ effect. In **Fig. 16A**, the absence of preventive effect of the antioxidant NAC suggests that $A\beta_{1-42}$-mediated Ca^{2+}_i rise is not regulated by ROS levels.

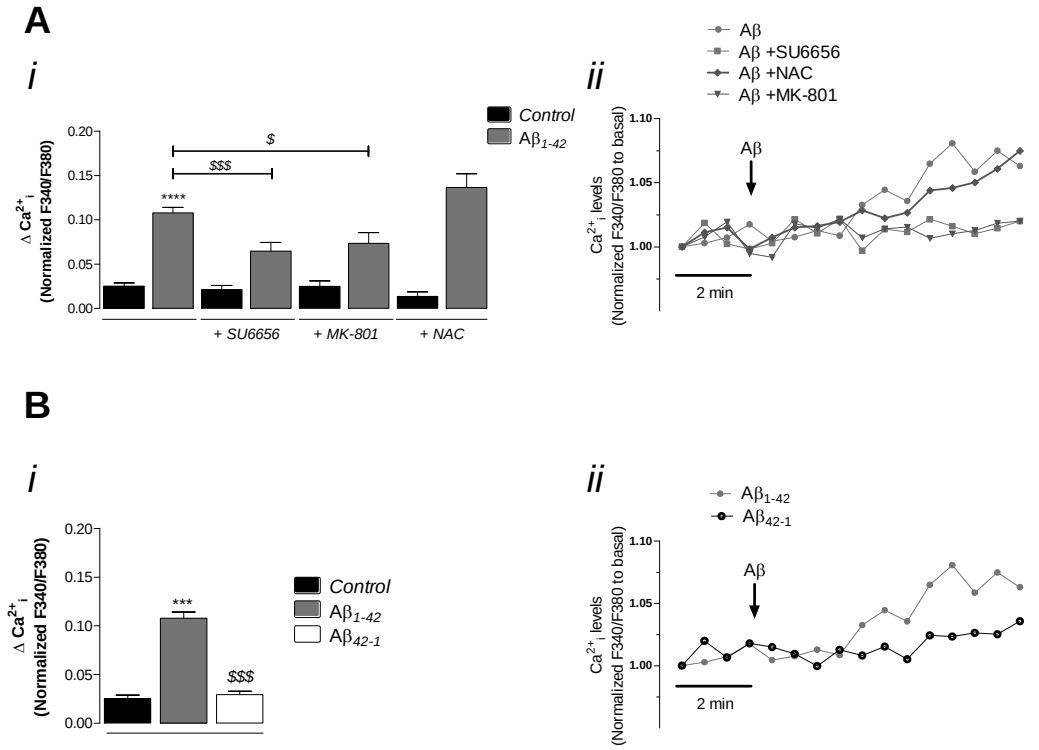

Fig. 16 | Ca^{2+}_i levels after Aβ acute treatment in mature hippocampal neurons. Levels of Ca^{2+}_i were evaluated by monitoring the fluorescence of Fura-2. Basal Ca^{2+}_i levels were recorded for 2 min and the effect of Aβ oligomers (1 μM) were recorded for 5 min. The effect of Aβ was calculated by analyzing the Fura-2 fluorescence ratio at 340/380 nm. SU6656 (5 μM), MK-801 (10 μM) and NAC (1 mM) were evaluated in (**A**). The influence of the reverse peptide, $Aβ_{42-1}$ (1 μM), was also evaluated in (**B**). In graphics (i) results were plotted as the difference between the last and the first value achieved before and after Aβ addition. Graphics (ii) are the representative line charts. Data are expressed as the mean ± SEM of n=2 to 9 experiments, run in quadruplicates. Statistical analysis: (**A**) $^{****}p < 0.0001$ *versus* control "no treatment", $^{\$}p < 0.05$ and $^{\$\$\$}p < 0.001$ *versus* $Aβ_{1-42}$ with "no treatment" (two-way ANOVA followed by Bonferroni *post-hoc* test) and (**B**) $^{***}p < 0.001$ *versus* control and $^{\$\$\$}p < 0.001$ *versus* $Aβ_{1-42}$ (one-way ANOVA followed by Bonferroni *post-hoc* test).

3.3 $A\beta_{1-42}$ mediates Src activation in an oxidant-dependent manner in hippocampal neurons

It is known that H_2O_2 may directly or indirectly induce the activation of Src protein (Hebert-Chatelain, 2013) and we demonstrated that $A\beta_{1-42}$ oligomers lead to increased H_2O_2 production in mature hippocampal neurons. Thus, in this part of the study, we evaluated the activation of Src protein through its phosphorylation on residue Tyr416 by Western Blotting in hippocampal neurons after H_2O_2 or $A\beta_{1-42}$ exposure for 10 and 30 min. Moreover, a similar analysis was evaluated in a mouse clonal hippocampal cell line, the HT22 cells, described as a glutamate-sensitive cell line.

Results depicted in **Fig. 17** show the effect of 1 mM of H_2O_2 on Src phosphorylation in mature hippocampal cells (**A-C**) and HT22 cells (**D-E**). We observed a large tendency for an increase in the ratio P(Tyr416)Src/Src after H_2O_2 treatment in mature hippocampal neurons at 30 min, indicating an enhanced phosphorylation/activation of the protein (**Fig. 17B,C**). HT22 cells also presented higher levels (although still not significant) phosphorylated Src after 30 min of exposure to 1 mM H_2O_2 when compared to the control (**Fig. 17F**); this effect was also observed after longer exposure times, such as 2, 4 or 6 hours treatment with 1 mM H_2O_2 (preliminary data, not shown). Importantly, in both cell types, the levels of total Src remained unaffected by the treatment (**Fig. 17A, D**). These results confirmed the positive effect of H_2O_2 in Src regulation in both cell models.

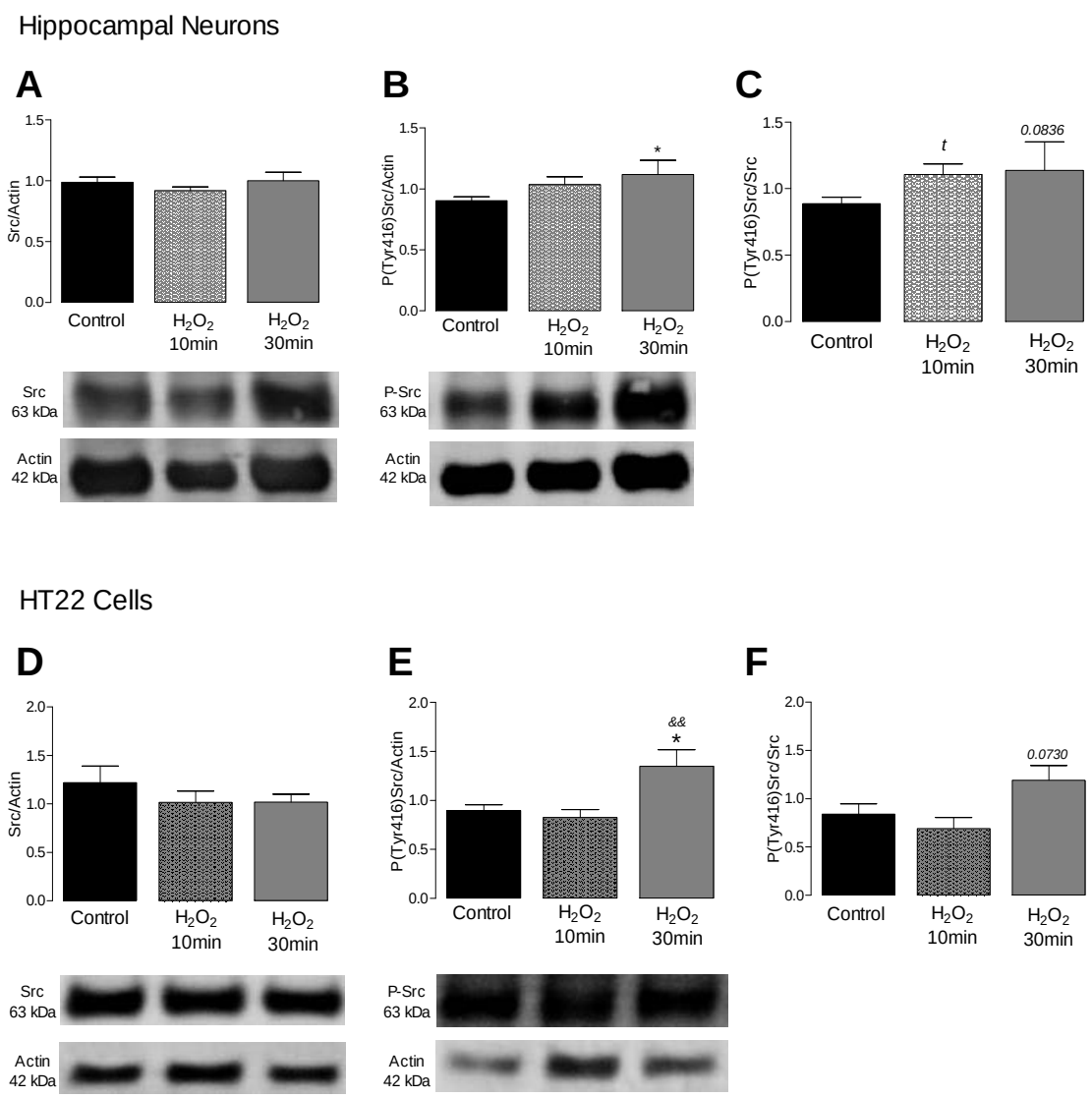

Fig. 17 | Src protein total and phosphorylated levels in mature hippocampal neurons and HT22 cell line after H_2O_2 exposure. (**A**, **B** and **C**) Hippocampal mature cells and (**D**, **E** and **F**) HT22 cells were incubated for 10 min and 30 min with H_2O_2 (1 mM). Levels of Src/Actin (**A** and **D**), P(Tyr416)Src/Actin (**B** and **E**) and P(Tyr416)Src/Src (**C** and **F**) were analyzed by Western blotting. Data are expressed in arbitrary units relative to actin as the mean ± SEM of n=4 to 10 experiments in (A, B and C) and n=6 to 10 experiments in (D, E and F). Statistical analysis:*$p < 0.05$ *versus* control and $^{\&\&}p < 0.01$ *vs* H_2O_2 10 min (one way ANOVA followed by Bonferroni post-hoc test); $^{t}p < 0.05$, p=0.0836 and p=0.0730 *versus* Control (Student's t-test).

In order to evaluate the effect of Aβ on Src activation and whether this effect was mediated by oxidative stress, we measured Src phosphorylated levels in mature hippocampal neurons incubated with $A\beta_{1-42}$ oligomers. Our experiments evidenced a significant increase in the levels of phosphorylated Src protein at 10 and 30 min of $A\beta_{1-42}$ treatment, being more robust at 30 min (**Fig. 18C**). Interestingly, the use of MK-801 showed a strong trend for a decrease in Src activation induced by $A\beta_{1-42}$ (**Fig. 18F**), suggesting a possible involvement of NMDARs in regulating Src activation pathway in the presence of $A\beta_{1-42}$. Furthermore, to evaluate if $A\beta_{1-42}$-mediated Src activation was primarily dependent on $A\beta_{1-42}$-induced H_2O_2 production, we pre-treated hippocampal neurons with antioxidants, namely NAC and GSH-EE (**Fig. 18G-I**). Results showed that GSH-EE and NAC were able to prevent the increase in Src phosphorylation induced by $A\beta_{1-42}$ oligomers, strongly suggesting that the effect of $A\beta_{1-42}$ on Src may not be a direct effect, but is dependent on a prior increase in ROS production. In these experiments, BSO, a sulfoximine that reduces glutathione levels (Griffith, 1982), was used as a positive control to indirectly increase the levels of H_2O_2, as described by Harlan et al. (1984), and further activate Src protein (**Fig. 18G-I**). No significant changes in total levels of Src protein were observed in any of the applied treatments. Importantly, no effect of $A\beta_{1-42}$ oligomers was observed in HT22 cell line (supplementary **Fig. S3A**), suggesting the absence of sensibility to Aβ of this cell line, at least in the conditions tested.

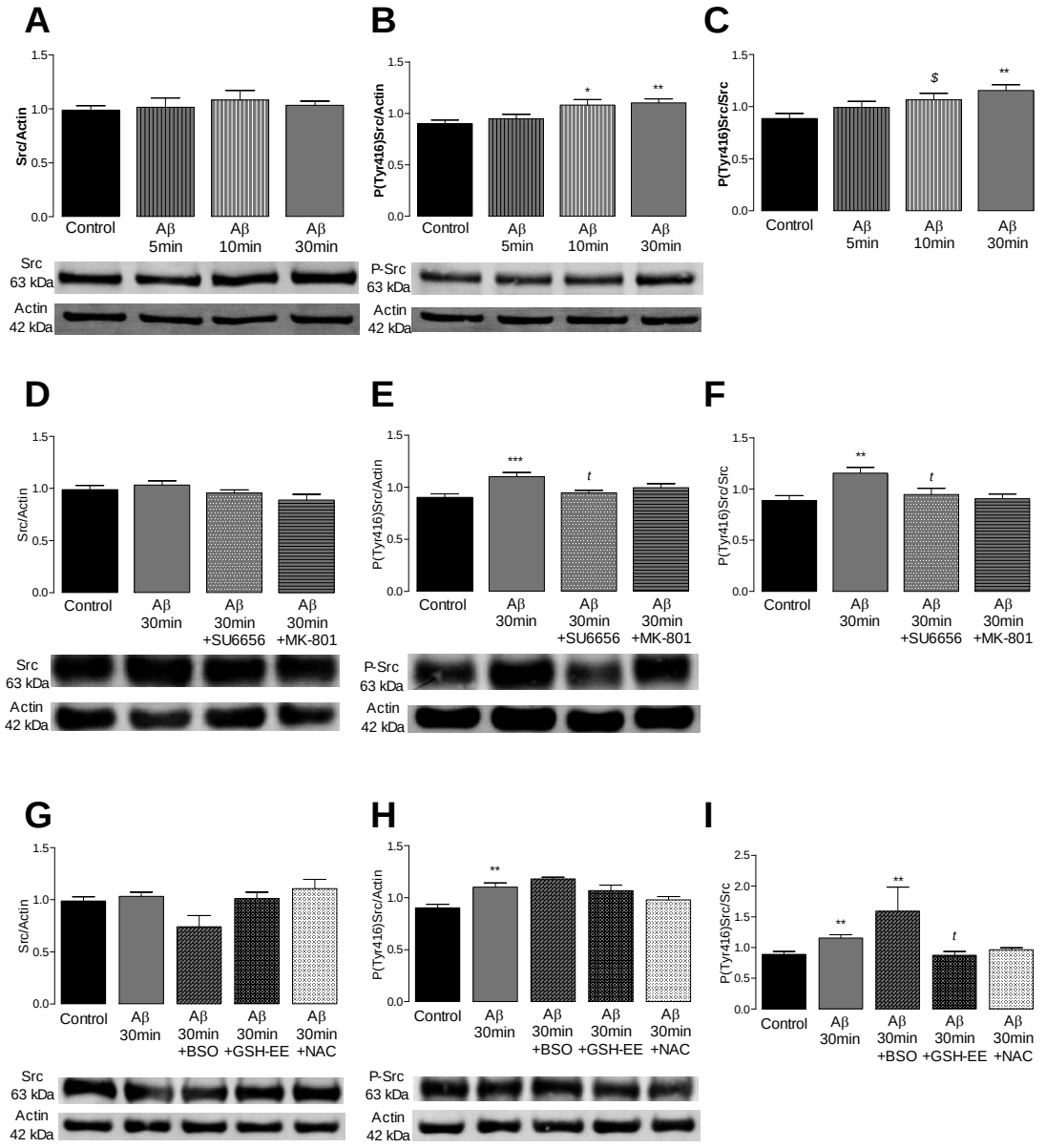

Fig. 18 | Src protein levels in mature hippocampal neurons after $A\beta_{1-42}$ exposure. Hippocampal mature cells were incubated with 1 µM $A\beta_{1-42}$ for 5, 10 and 30 min and the levels of Src/actin (**A**, **D** and **G**), P(Tyr416)Src/actin (**B**, **E** and **H**) and P(Tyr416)Src/Src (**C**, **F** and **I**) were evaluated by Western blotting. The effect of SU6656 (5 µM) and MK-801 (10 µM), (**D**, **E** and **F**) as well as NAC (1 mM), GSH-EE (0.1 mM) and BSO (0.5mM) (**G**, **H** and **I**) were evaluated in cells exposed to $A\beta_{1-42}$, for 30 min. Data are expressed in arbitrary units relative to actin as the mean ± SEM of n=3 to 10 experiments. Statistical analysis: $^{*}p < 0.05$, $^{**}p < 0.01$ and $^{***}p < 0.001$ *versus* Control (one-way ANOVA, followed by Bonferroni post-hoc test); $^{\$}p < 0.05$ *versus* Control and $^{t}p < 0.05$ *versus* Aβ 30 min, (Student's *t-test*);

3.4 $A\beta_{1-42}$ and H_2O_2 induce Nrf2 phosphorylation in a Src-dependent manner in hippocampal neurons and in HT22 cells

We have demonstrated above that $A\beta_{1-42}$ oligomers lead to increased $Ca^{2+}{}_i$ and H_2O_2 production, which is further involved in Src phosphorylation/activation. Mild oxidative stress conditions have been shown to induce the activation of the transcription factor Nrf2, which once phosphorylate at Ser40 in the presence of ROS, translocate to the nucleus and induce ARE-dependent gene expression (Niture et al., 2009). In this regard, we first evaluated Nrf2 phosphorylation in mature hippocampal neurons and in HT22 cells after H_2O_2 treatment. We observed a significant increase in P(Ser40)Nrf2/Nrf2 ratio after 30 min of H_2O_2 exposure in hippocampal neurons (**Fig. 19A-C**). In HT22 cells, which we have demonstrated to be slightly sensitive to 1 mM H_2O_2, we observed a strong tendency for increased Nrf2 phosphorylation (**Fig. 19D-F**). Interestingly, this increase was prevented by the Src inhibitor SU6656, suggesting that phosphorylation of Nrf2 at Ser40 may occur in a Src-dependent manner. No alterations in Nrf2 total levels were observed in these conditions (**Fig. 19A, D**).

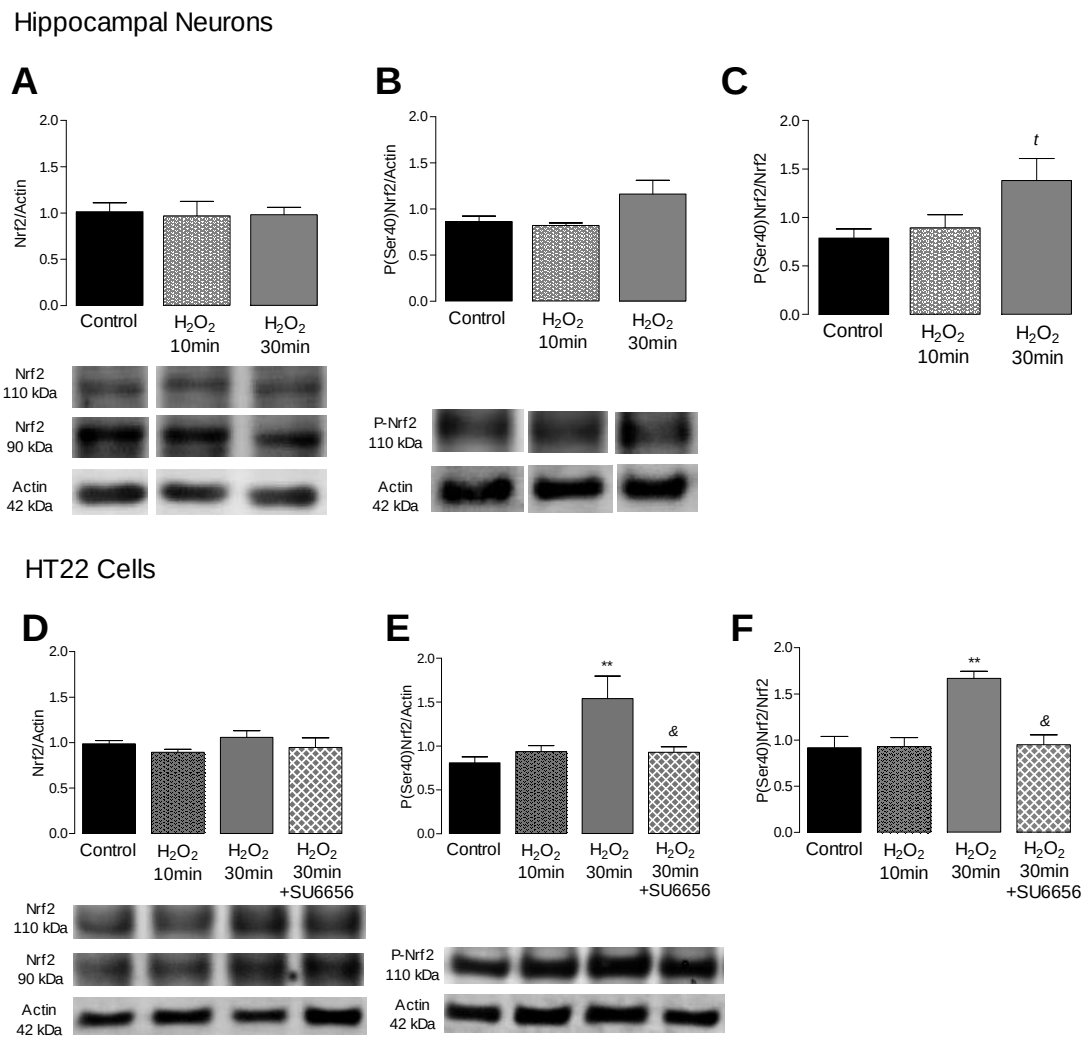

Fig. 19 | Nrf2 protein levels in mature hippocampal neurons and HT22 cell line after H_2O_2 exposure. (**A**, **B** and **C**) Hippocampal mature cells and (**D**, **E** and **F**) HT22 cells were incubated for 10 min and 30 min with H_2O_2 (1 mM) in the absence or presence of SU6656 (5 μM). Levels of Nrf2/Actin (**A** and **D**), P(Ser40)Nrf2/Actin (**B** and **E**) and P(Ser40)Nrf2/Nrf2 (**C** and **F**) were analyzed by Western blotting. Data are expressed in arbitrary units relative to actin as the mean ± SEM of n=3 to 6 experiments in (A, B and C) and n=4 to 6 experiments in (D, E and F). Nrf2 total levels were considered both at 90 and 110 kDa. Statistical analysis: $^{**}p < 0.01$ *versus* control, $^{\&}p < 0.05$ *versus* H_2O_2 30 min (one-way ANOVA, followed by Bonferroni post-hoc test); and $^{t}p < 0.05$ *versus* Control (Student's *t-test*)

To examine the effect of $A\beta_{1-42}$ treatment on Nrf2 phosphorylation in mature hippocampal neurons, total and phosphorylated Nrf2 levels were evaluated after incubation with $A\beta_{1-42}$ oligomers. Our results showed a significant increase in Nrf2 phosphorylation levels after 30 min of $A\beta_{1-42}$ exposure (**Fig. 20B, C**), which was prevented by the antioxidants GSH-EE and NAC (**Fig. 20D-F**). Interestingly, $A\beta_{1-42}$ oligomers-induced Nrf2 phosphorylation was also prevent by SU6656 and tendentiously prevent by MK-801 (**Fig. 20G-I**), suggesting once again the dependence on Src for Nrf2 phosphorylation and a possible indirect role of NMDARs. No differences were observed in Nrf2 phosphorylation after $A\beta_{1-42}$ oligomers exposure in HT22 cells (supplementary **Fig. S3B**), which is in accordance with the absence of Aβ effects in regard to Src protein.

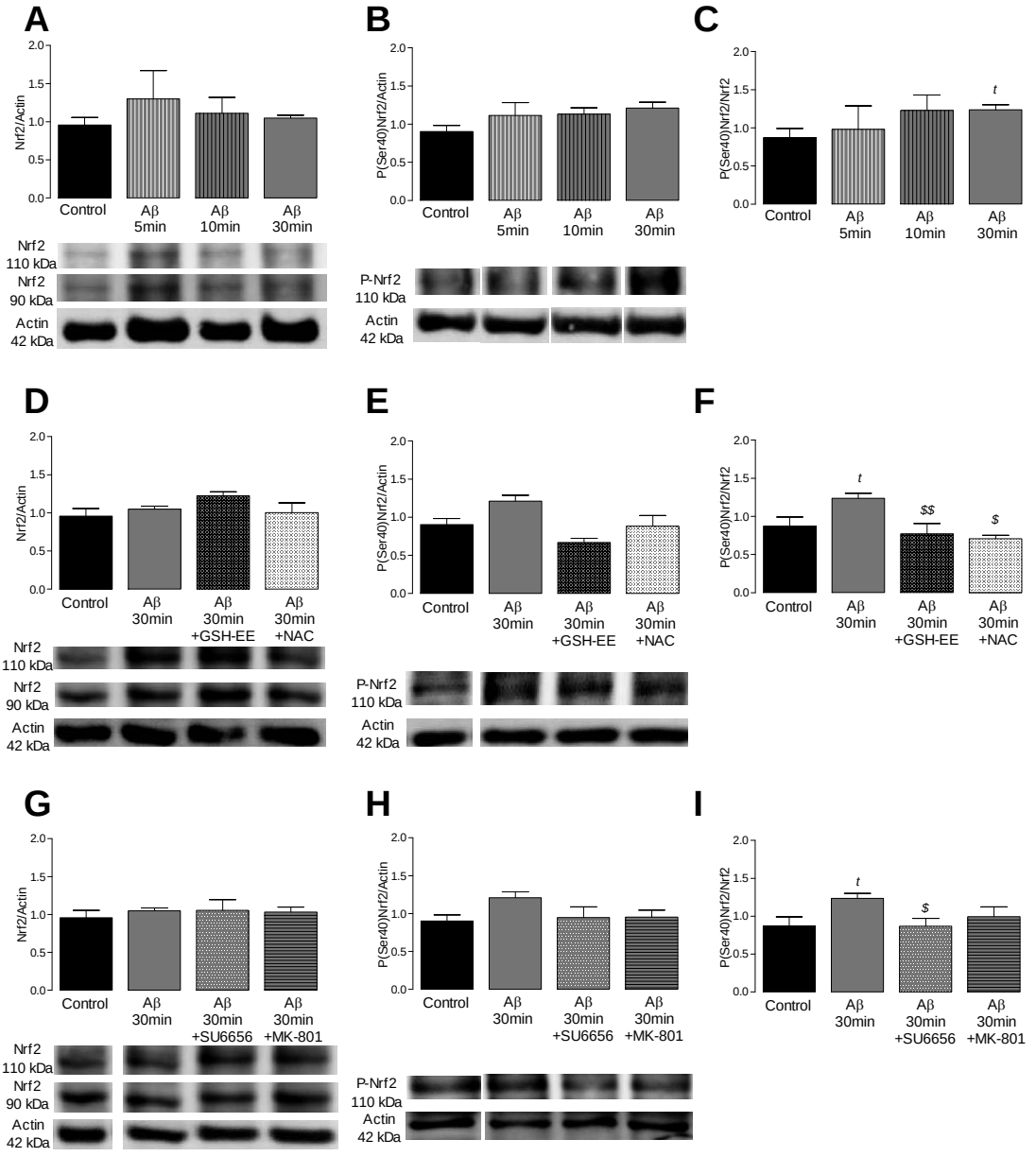

Fig. 20 | Nrf2 protein total and phosphorylated levels in mature hippocampal neurons after $A\beta_{1-42}$ exposure. Hippocampal mature cells were incubated with 1 μM $A\beta_{1-42}$ for 5, 10 and 30 min and the levels of Nrf2/Actin (**A**,**D** and **G**), P(Ser40)Nrf2/Actin (**B**, **D** and **H**) and P(Ser40)Nrf2/Nrf2 (**C**,**F** and **I**) were evaluated by Western blotting. The effect of NAC (1 mM) and GSH-EE (0.1 mM) (**D**, **E**, **F**) were also evaluated on the condition $A\beta_{1-42}$ 30 min, as well as the effect of SU6656 (5 μM) and MK801 (10 μM) (**G**, **H**, **I**). Data are expressed in arbitrary units relative to actin as the mean ± SEM of n=3 to 9 experiments. Nrf2 total levels were considered both at 90 and 110 kDa. Statistical anamysis: $^{t}p < 0.05$ *versus* Control, $^{\$}p < 0.05$ and $^{\$\$}p < 0.01$ *versus* Aβ 30 min (Student's *t-test*)

3.5 Constitutive activation of Src protein leads to increased Nrf2 phosphorylation in HT22 cell line

Taking into account the results obtained in **Fig. 19** and **Fig. 20** regarding the dependence of Src for H_2O_2–induced Nrf2 activation, we further evaluate Nrf2 phosphorylation in transfected HT22 cells with a constitutively active form of Src protein. Thus, cells were transfected with constitutively active form of Src (Y527F-Src), negative form (K295R-Src) and empty vector (empty) and, after 48h of plasmid expression, levels of total and phosphorylated Src and Nrf2 protein were measured. No differences were observed in total levels of Src protein (**Fig. 21A**); however, we detected significantly higher levels of P(Tyr416)Src in HT22 cells transfected with the active form (Y527F-Src) when compared to control and more importantly when compared to the negative form (K295R-Src) and the empty vector (**Fig. 21B, C**). Interestingly, cells transfected with the active form (Y527-Src) also revealed significant increased levels of phosphorylated Nrf2 (**Fig. 21E,F**), while no differences were verified in total levels of Nrf2 protein (**Fig. 21D**), strengthening the hypothesis of a Src-dependent phosphorylation of Nrf2.

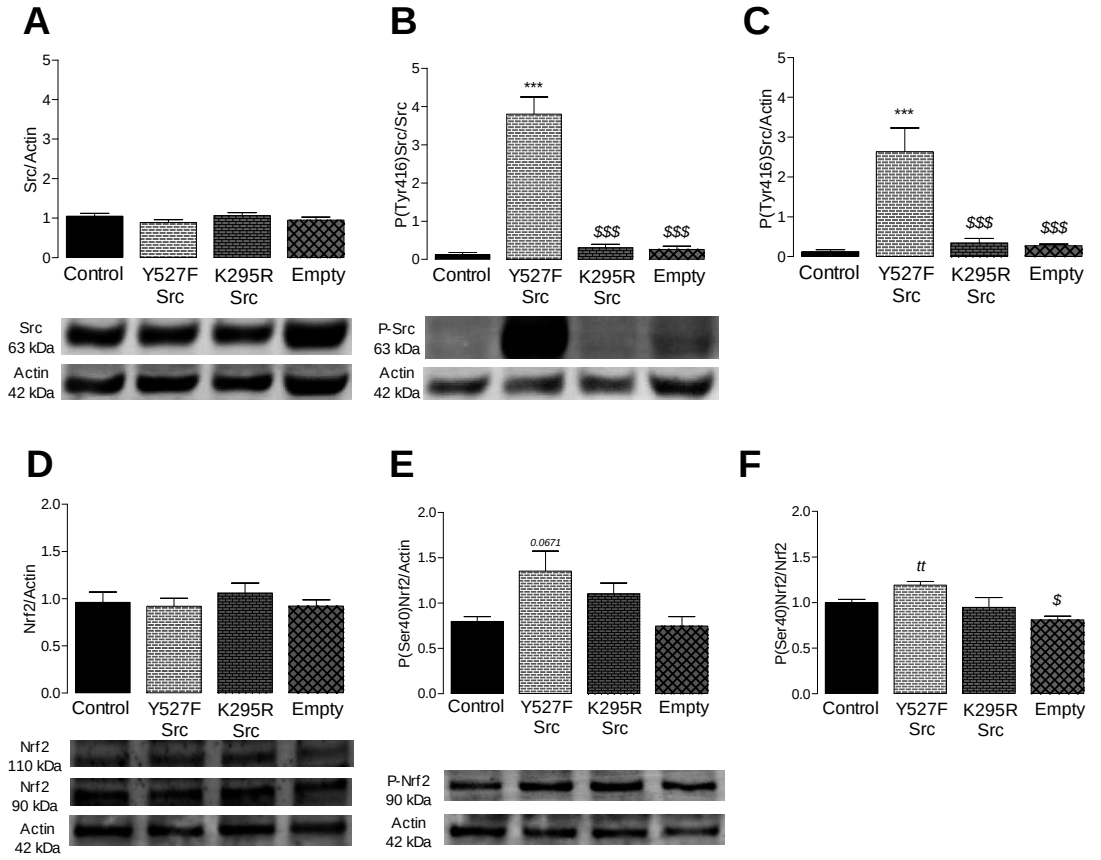

Fig. 21 | Src and Nrf2 protein levels and phosphorylation in transfected HT22 cells following expression of constitutively active form of Src protein. HT22 cells were transfected with plasmid constructs codifying for the constitutively active form of Src (Y527F-Src), the negative form (K295R-Src) and the empty vector (empty). Expression of plasmids was allowed for 48 hours and levels of Src/Actin (**A**), P(Tyr461)Src/Actin (**B**) and P(Tyr461)Src/Src (**C**), Nrf2/Actin (**D**), P(Ser40)Nrf2/Actin (**E**) and P(Ser40)Nrf2/Nrf2 (**F**) were analyzed by Western blotting. Data are expressed in arbitrary units relative to actin as the mean ± SEM of n=4 experiments. Nrf2 total levels were considered both at 90 and 110 kDa. Statistical analysis: $^{***}p < 0.001$ *versus* control, $^{\$}p < 0.05$ and $^{\$\$\$}p < 0.001$ *versus* Y527F Src (one-way ANOVA, followed by Bonferroni post-hoc test), $^{tt}p < 0.01$ and p=0.0671 *versus* control (Student's *t-test*).

3.6 Altered Src kinase in the nucleus is apparently independent of Nrf2

It has been shown that Src protein can localize in the nucleus and interact with Nrf2 (Niture et al., 2011). In order to further understand the relationship between Src and Nrf2, we analyzed total and phosphorylated levels of these proteins in nuclear fractions of HT22 cells and hippocampal neurons. We firstly validated the presence of Src in the nucleus of HT22 cells using immunocytochemistry (**Fig. 22-Inset**). Fluorescence images in **Fig. 22** show the co-labeling for Src, HSP60 (to label mitochondria) and Hoechst (nuclear labeling).

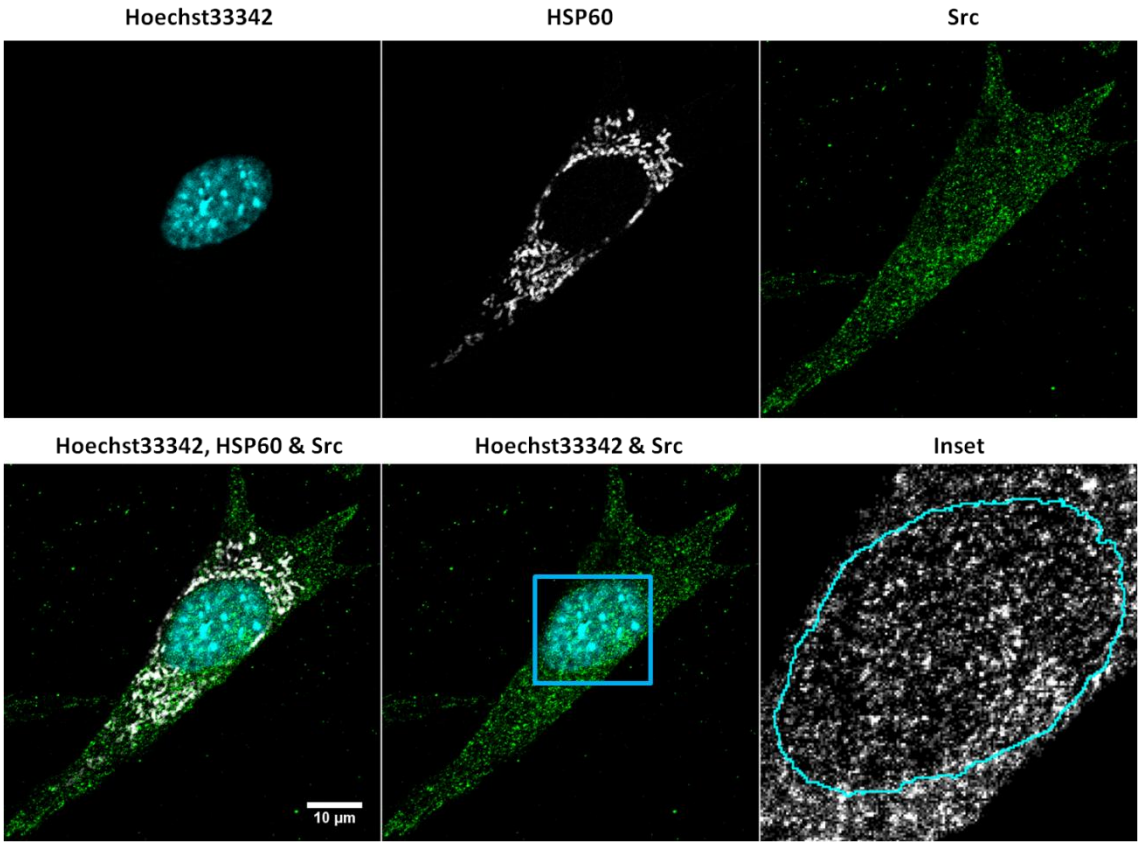

Fig. 22 | Src protein in nucleus of HT22 cells. Nucleus was visualized by Hoechst staining (blue), mitochondria were labeled with an antibody against HSP60 (white) and Src was immunostained with a specific antibody (green), Images were treated using Fiji program. In inset image, the perimeter delimited by a blue selection is the nucleus and white labeling represents Src. Confocal images were obtained using a 63x objective, NA=1.4 on a Zeiss LSM 710 inverted microscope. Scale bar: 10 µm.

Results depicted in **Fig. 23A** showed that treatment with 1 mM H_2O_2 induced a decrease in total Src levels in the nucleus, while inhibition of Src with SU6656 did not cause a significant effect. In contrast, increased Src phosphorylation was observed in the nucleus following treatment with H_2O_2 for 30 min, which was not affected by the Src inhibitor (**Fig. 23B and C**). These data suggest another role of Src in the nucleus independent of Nrf2. No significant differences were found in Nrf2 protein levels in HT22 cell nucleus after 30 min of H_2O_2 exposure, although there was a tendency for decrease after SU6656 addition (**Fig. 23D**). Although H_2O_2 incubation for 30 min caused an increase in Nrf2 phosphorylation, the same time point may not be sufficient to observe its nuclear accumulation. An apparent effect of Src inhibition on nuclear Nrf2 levels might be in accordance with a possible (indirect) role of Src on Nrf2 phosphorylation, at a Ser residue commonly associated to its translocation to the nucleus.

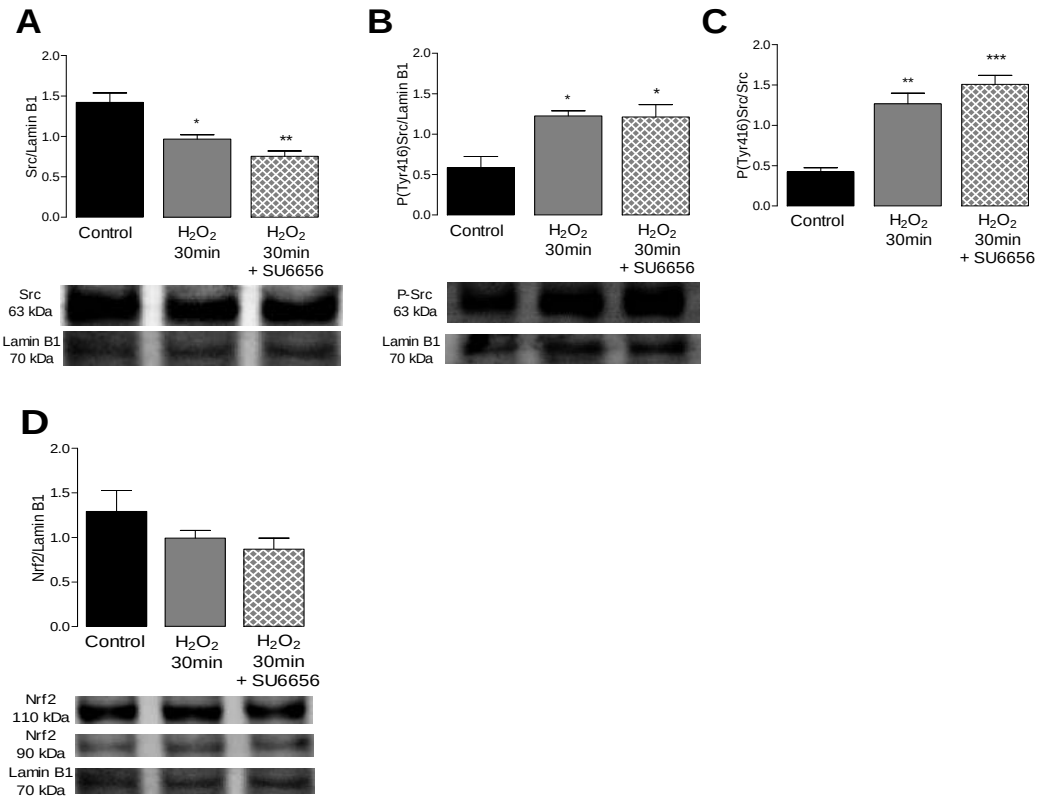

Fig. 23 | Src total and phosphorylated protein levels and Nrf2 total protein levels in nuclear fractions obtained from HT22 cells exposed to H_2O_2. Protein levels of Src/Lamin B1 (**A**), P(Tyr416)Src/Lamin B1 (**B**), P(Tyr416)Src/Src (**C**) and Nrf2/Lamin B1 (**D**) were assessed, by Western Blotting, in nuclear-enriched fractions from HT22 cells incubated for 30 min with H_2O_2 (1 mM) and SU6656 (5 μM). Data are expressed in arbitrary units relative to Lamin B1 as the mean ± SEM of n=3 independent experiments. Nrf2 total levels were considered both at 90 and 110 kDa. Statistical analysis: $^{*}p < 0.05$, $^{**}p < 0.01$, $^{***}p < 0.001$ *versus* Control (one-way ANOVA, followed by Bonferroni post-hoc test).

Subsequently, we also evaluated the same protein levels in the nuclear fractions of HT22 cells, expressing the constitutively active form of Src (Y527F-Src) and the negative one (K295R-Src) – preliminary data. Cells expressing the constitutive activated Src showed higher levels of phosphorylated Src in the nucleus (**Fig. 24B, C),** although no differences in Src total levels were verified (**Fig. 24A**). Again, no significant differences were observed in nuclear Nrf2 protein levels (**Fig. 24D**).

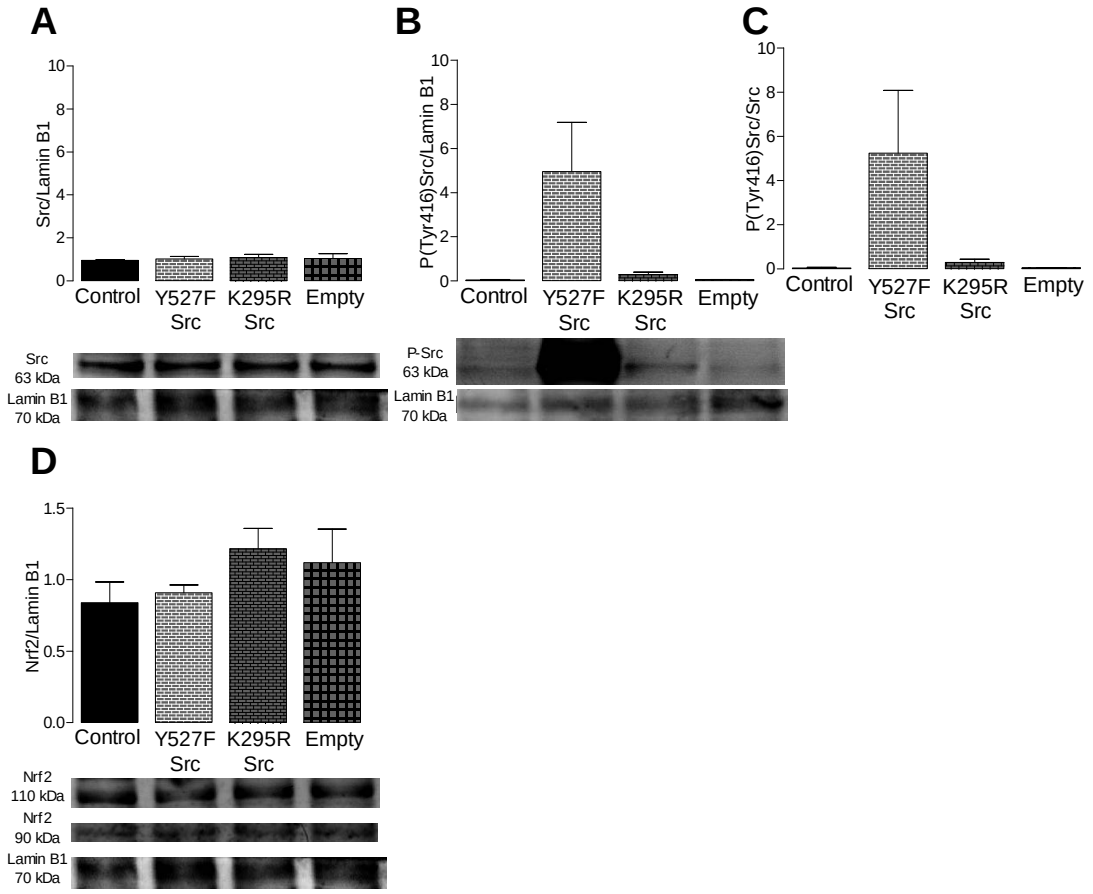

Fig. 24 | Src total and phosphorylated protein levels and Nrf2 total protein levels in nuclear fractions from HT22 cells transfected with constitutively active and inactive forms of Src. HT22 cells were transfected with plasmids constructs codifying for the constitutively active form of Src (Y527F-Src), the negative form (K295R-Src) and the empty vector (empty). Expression of plasmids was allowed for 48 hours and levels of Src/Lamin B1 (**A**), P(Tyr461)Sr/Lamin B1 (**B**) and P(Tyr461)Src/Src (**C**) and Nrf2/Lamin B1 (**D**), were assessed in nuclear-enriched fractions by Western Blotting. Data are expressed in arbitrary units relative to Lamin B1 as the mean ± SEM of n=2 experiments. Nrf2 total levels were considered both at 90 and 110 kDa.

In mature hippocampal neurons, sensitive to $A\beta_{1-42,}$ we evaluated the relationship between Nrf2 and Src. Preliminary results showed no differences in total Src or Nrf2 protein levels in nuclear fractions of neurons pre-exposed to $A\beta_{1-42}$ oligomers, for 30 min (**Fig. 25**).

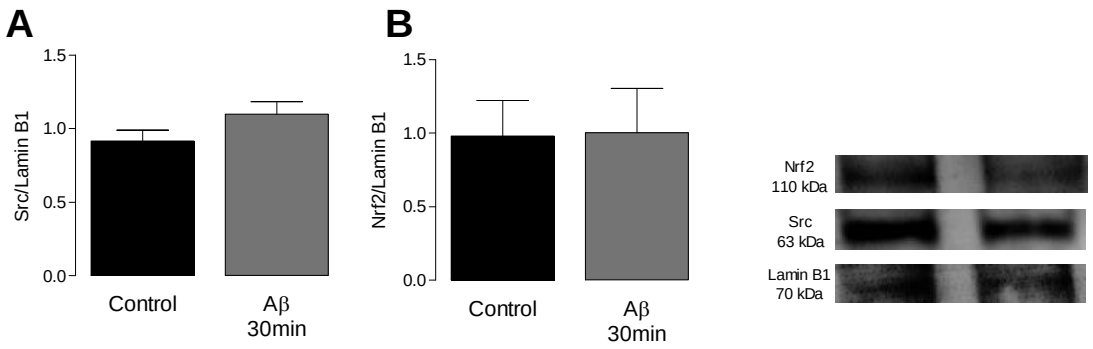

Fig. 25 | Src and Nrf2 protein levels in nuclear fractions isolated from mature hippocampal neurons exposed to $A\beta_{1-42}$. Protein levels of Src/Lamin B1 (**A**) and Nrf2/Lamin B1 (**B**) were assessed in nuclear-enriched fractions by Western Blotting in hippocampal mature cells incubated for 30 min with $A\beta_{1-42}$ (1 μM). Data are expressed in arbitrary units relative to Lamin B1 as the mean ± SEM of n=2 experiments. (Note that no band was detected at 90 kDa in these experiments).

All together, these results suggest that $A\beta_{1-42}$ oligomers induce $Ca^{2+}{}_i$ increase and mitochondrial H_2O_2 generation, this last appearing to be responsible for Src activation and phosphorylation of Nrf2 at Ser40. Interestingly, our findings support the hypothesis that Nrf2 phosphorylation at Ser40 occurs in a Src-dependent manner. Moreover, despite increased Nrf2 phosphorylation at Ser40 is commonly associated to is nuclear translocation, we did not observe higher levels of Nrf2 in the nucleus; this suggests either: (i) that the chosen time point for analysis of Nrf2 in nuclear fractions may not have been appropriate, (ii) a failure in Nrf2 nuclear translocation, and/or (iii) another cellular role related with Nrf2 phosphorylation at Ser40.

3.7 H_2O_2 exposure in HT22 cells induces Src and Nrf2 phosphorylation in mitochondrial fractions

Although Src activation was shown to mediate Nrf2 phosphorylation at Ser40 in cytosol, no changes were observed in Nrf2 levels in the nucleus. Thus, we decided to evaluate other subcellular compartment, namely mitochondria, where the presence of both Src and Nrf2 was previously described.

Previous data showed that Src protein can be detected in rat mitochondria (Salvi et al., 2002), further interacting and phosphorylating different proteins in this organelle, namely, complexes III and IV (Miyazaki et al., 2006). Moreover, previous studies showed the presence of Nrf2 in mitochondria, associated to the MOM of mice myocardium cells (Strom et al., 2016). Therefore, in this study we were also interested in exploring a possible role of Src in mitochondria and its possible relationship with Nrf2. First we validated the presence of Src in mitochondria from HT22 cells by immunocytochemistry. Fluorescence images in **Fig. 26** showed the co-labeling of Src with nucleus and the mitochondrial protein Hsp60.

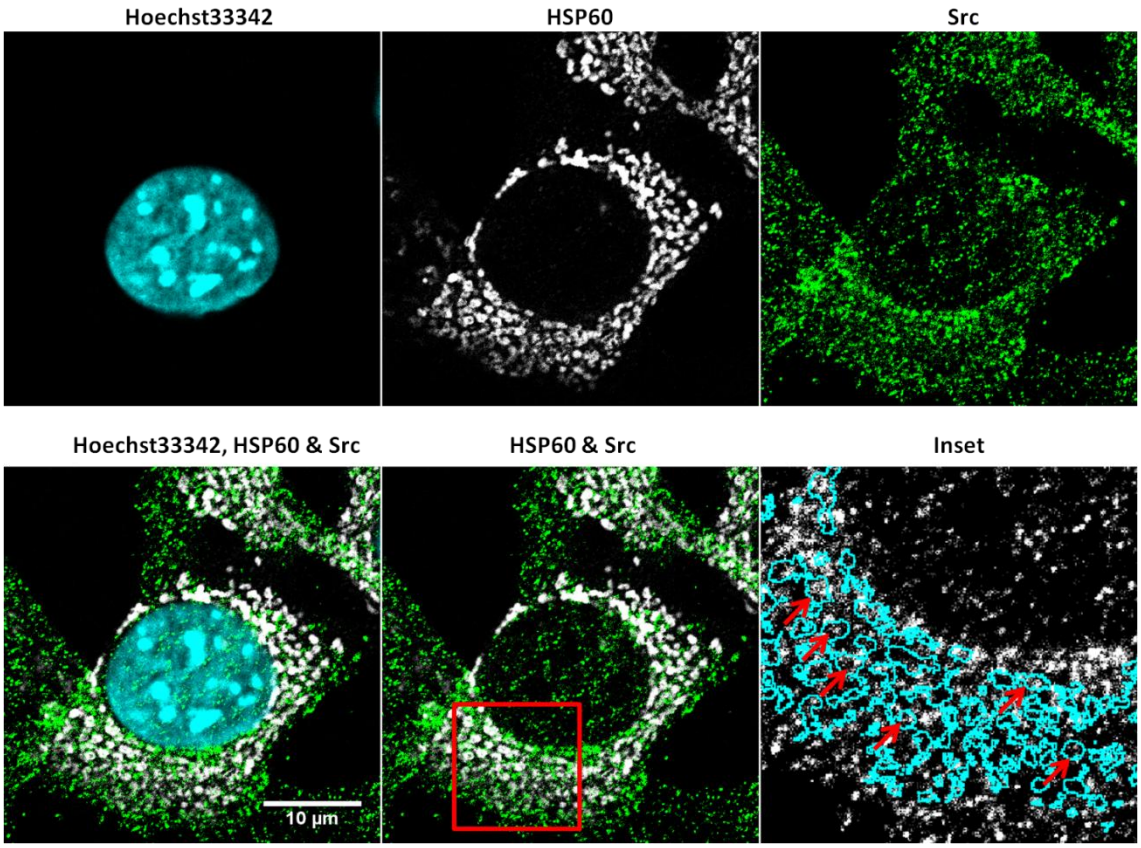

Fig. 26 | Src protein in HT22 cells mitochondria. Nucleus was visualized by Hoechst staining (blue), mitochondria were labeled with an antibody against HSP60 (white) and Src was immunostained with a specific antibody (green). Images were treated using Fiji program. In inset image, the perimeters delimited by blue selections are mitochondria and white labeling represents Src. Confocal images obtained with a 63x objective, NA=1.4 on a Zeiss LSM 710 inverted microscope. Scale bar: 10 µm

We further evaluated Src protein phosphorylation levels in mitochondrial extracts of HT22 cells following 30 min or 4h exposure to H_2O_2, in the presence or absence of Src inhibitor, SU6656. Significantly higher phosphorylation levels of Src protein at Tyr416 were observed in HT22 cells mitochondria (**Fig. 27B and C**), which was prevented by SU6656, whereas no differences in total protein levels were observed (**Fig. 27A**), suggesting a H_2O_2-mediated activation of Src associated to mitochondria. Considering the possible relationship of Src and Nrf2 phosphorylation, we further determined Nrf2 proteins levels and its phosphorylation at Ser40 in mitochondrial fractions derived from HT22 cells. We observed a significant increase in mitochondrial Nrf2 phosphorylation at Ser40 after 30 min or 4h of H_2O_2 treatment (**Fig. 27E and F**) with unchanged total levels (**Fig. 27D**). Interestingly, phosphorylation levels of Nrf2

exhibited a tendency for decrease in the presence of Src inhibitor, SU6656, especially after 4h of H_2O_2 exposure (**Fig. 27E and F**); these data are in accordance with our previous results regarding the dependence on Src for Nrf2 phosphorylation at Ser40, which also seems to occur at the level of mitochondria.

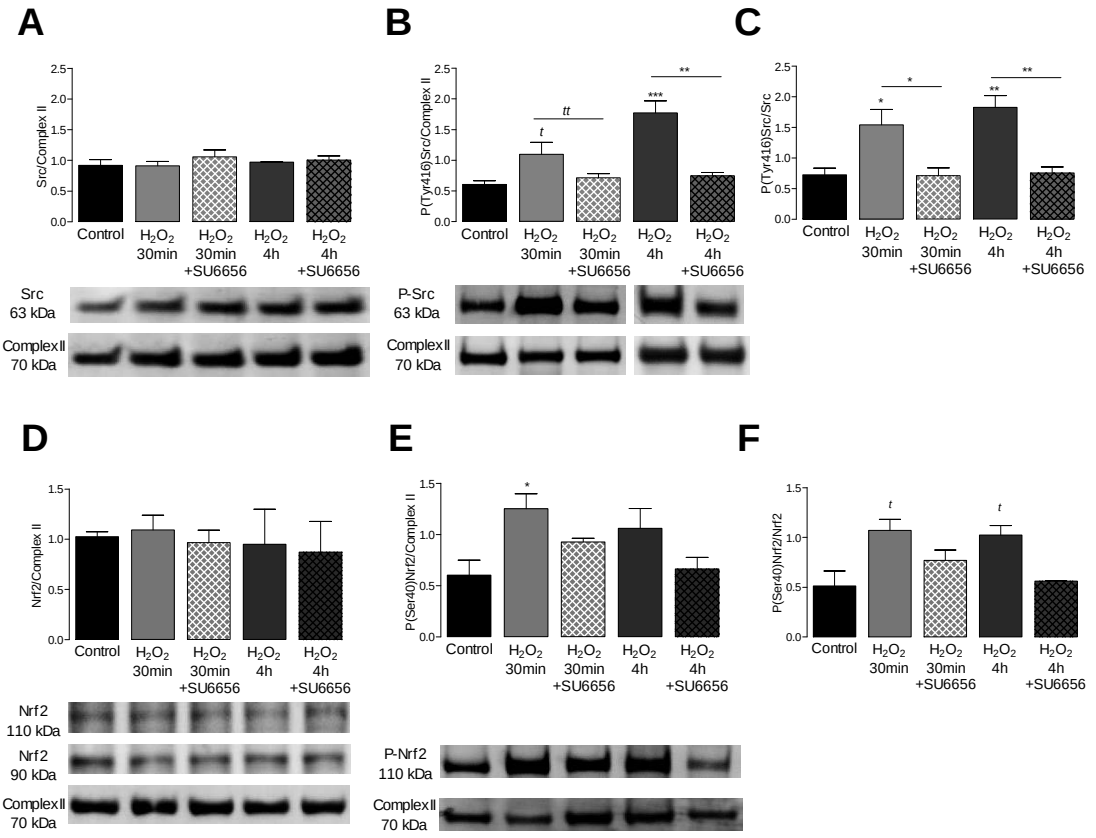

Fig. 27 | Src and Nrf2 protein levels and phosphorylation in mitochondrial fractions of HT22 cells. HT22 cells were incubated for 30 min or 4 h with H_2O_2 (1 mM) in the absence or presence of the Src inhibitor SU6656 (5 μM). Src/Complex II (**A**), P(Tyr461)Src/Complex II (**B**), P(Tyr461)Src/Src (**C**); Nrf2/Complex II (**D**), P(Ser40)Nrf2/Complex II (**E**) and P(Ser40)Nrf2/Nrf2 (**F**) levels were assessed in mitochondrial-enriched fractions by Western Blotting. Data are expressed in arbitrary units relatively to ComplexII (70 kDa subunit) as the mean ± SEM of n=3 to 7 experiments (A, B and C) and 2 to 6 independent experiments (D, E and F). Statistical analysis: $^{***}p < 0.001$, $^{**}p < 0.01$ and $^{*}p < 0.05$ (one-way ANOVA, followed by Bonferroni post-hoc test); $^{t}p < 0.05$ and $^{tt}p < 0.01$ (Student's *t-test*)

In order to further evaluate the relationship between Src and Nrf2 in mitochondria, we analyzed the changes in these proteins in mitochondria from transfected HT22 cells expressing the constitutively active form of Src (Y527F-Src), negative form (K295R-Src) and empty vector (empty). Although these are preliminary results, we observed higher levels of Src phosphorylation at Tyr416 in mitochondria of cells transfected with constitutively active form (**Fig. 28B and C**), while no differences in Src total levels were verified (**Fig. 28A**). Surprisingly, no significant differences were observed in Nrf2 protein levels, total or phosphorylated (**Fig. 28D-F**), suggesting that overactivation of Src only may not be sufficient to influence Nrf2 activation in mitochondria.

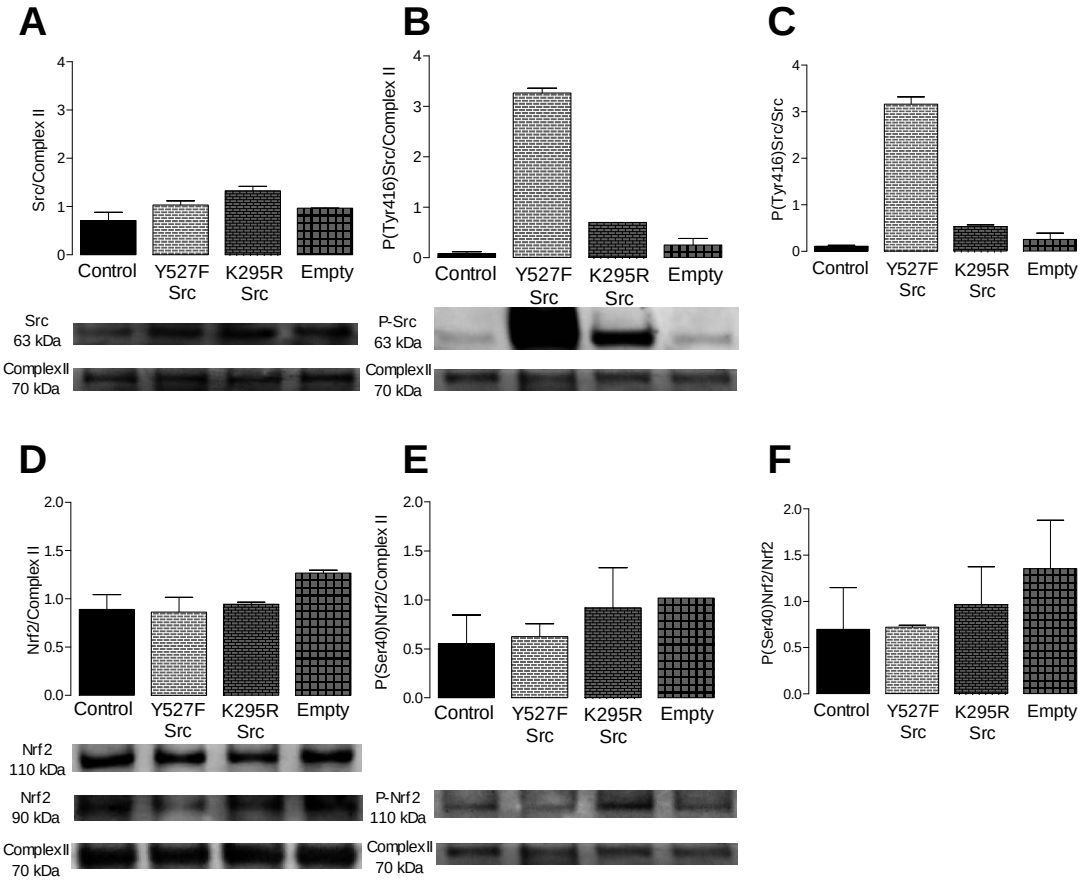

Fig. 28 | Src and Nrf2 total and phosphorylated protein levels in mitochondrial fractions from HT22 cells transfected with constitutively active or inactive forms of Src protein. HT22 cells were transfected with plasmid constructs codifying for the constitutively active form of Src (Y527F-Src), the negative form (K295R-Src) and the empty vector (empty). Expression of plasmids was allowed for 48 hours and levels of Src/Complex II (**A**), P(Tyr461)Src/Complex II (**B**) and P(Tyr461)Src/Src (**C**); Nrf2/Complex II (**D**), P(Ser40)Nrf2/Complex II (**E**) and P(Ser40)Nrf2/Nrf2 (**F**) were assessed in mitochondrial-enriched fractions by Western Blotting. Data are expressed in arbitrary units relative to ComplexII (70 kDa subunit) as the mean ± SEM of n=2 experiments.

3.8 H_2O_2 induces modified levels of HSP60 and Drp1 proteins in mitochondrial fractions of HT22 cells: influence of Src

Src has been suggested to be essential for regulating the oxidative phosphorylation system and consequently for maintaining cell viability (Ogura et al., 2012, 2014). Moreover, mitochondria are dynamic structures continuously subjected to cycles of fission and fusion, contributing for cell survival. Since we verified the presence of Src in HT22 cells mitochondria, we further investigated the possible role of Src in this organelle, more particularly in the regulation of levels of proteins related with mitochondrial dynamics, namely fusion and fission.

HT22 cell mitochondria exposed to 1 mM H_2O_2 revealed a significant increase in P(Tyr416)Src/Src ratio, indicating an increased phosphorylation of the protein related with protein activation (**Fig. 27A-C**). Under the same experimental conditions (30 min exposure to H_2O_2), we analyzed the levels of different mitochondrial proteins, in the presence or absence of the Src inhibitor, SU6656, in mitochondrial subfractions obtained from HT22 cells. Our results showed a strong tendency for a decrease in mitochondrial Drp1 levels after 30 min of H_2O_2 exposure that was prevented by SU6656 (**Fig. 29B**). Data suggest that H_2O_2 may decrease mitochondrial fission, at least after a short time exposure, and that Src protein may be involved in this process. No differences were verified in mitochondrial fusion proteins, namely, Mitofusin2 and Opa1 (**Fig. 29C, F**).

In addition, protein levels of Tom20, a central component of the TOM (translocase of outer membrane) receptor complex responsible for the recognition and translocation of cytosolic-synthesized mitochondrial proteins, and HSP60, a protein implicated in mitochondrial protein import that is required for folding, translocation and assembly of native proteins, were also measured. We observed a significant increase in HSP60 protein levels following inhibition of Src by SU6656 (**Fig. 29E**). No significant changes were observed in Tom20 protein levels (**Fig. 29D**). Lastly, Tfam levels, known as the major transcriptional regulator of mtDNA, showed no significant differences under the same experimental conditions (**Fig. 29A**).

Results obtained in HT22 cell line suggest that both Src and Nrf2 can be phosphorylated in mitochondria after H_2O_2 treatment, especially for long time exposure (4h). Moreover, we observed a possible involvement of Src on mitochondrial fission under oxidative stress conditions. Considering the preliminary nature of these data, future experiments will be required to characterize the role of Src in mitochondria.

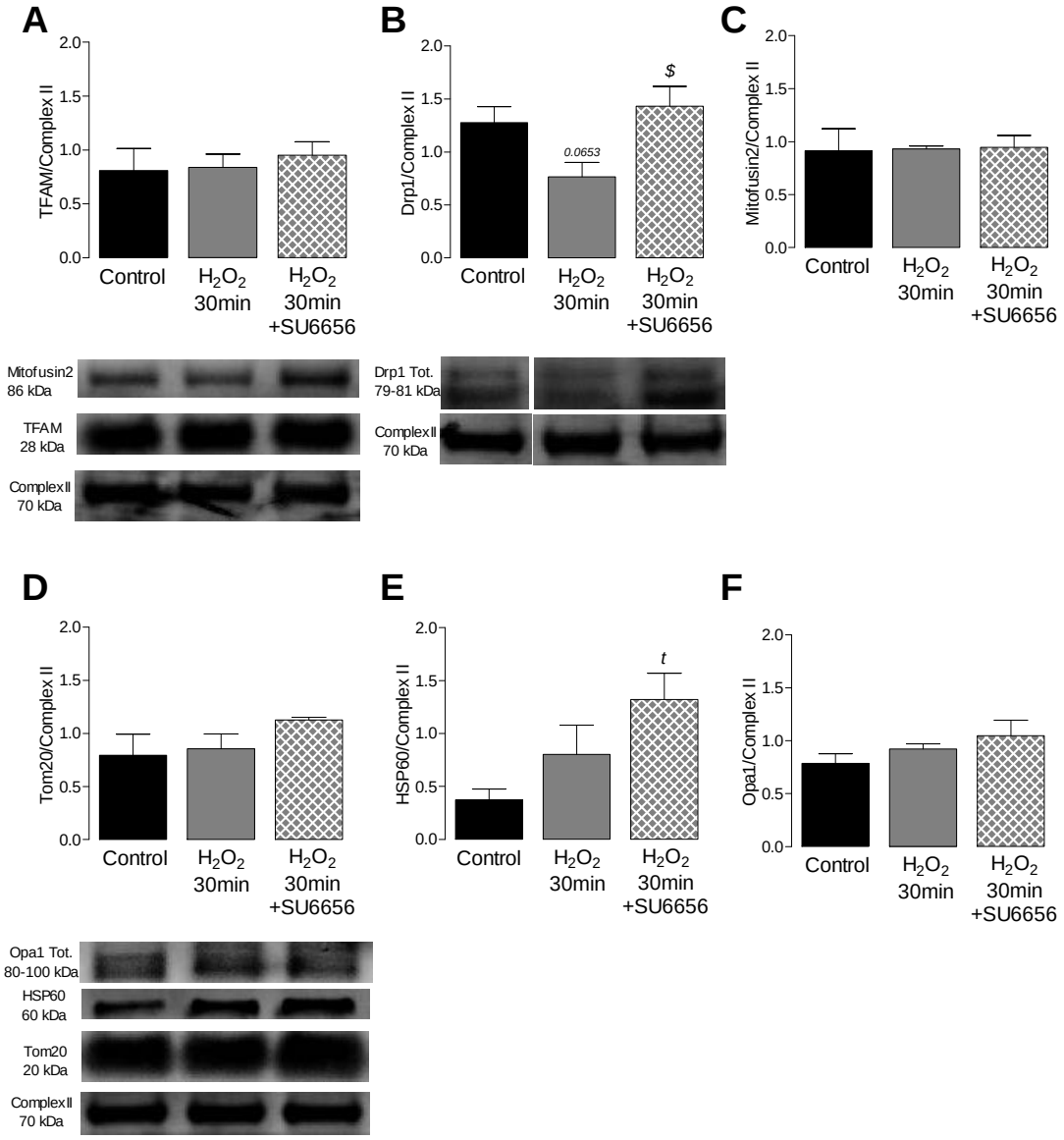

Fig. 29 | Mitochondrial protein levels in mitochondrial fractions obtained from HT22 cells after exposure to H_2O_2. HT22 cells were incubated for 30 min with H_2O_2 (1 mM) in the absence or presence of Src inhibitor, SU6656 (5 µM). Levels of TFAM (**A**), Drp1 (**B**), Mitofusin2 (**C**), Tom20 (**D**), HSP60 (**E**) and Opa1 (**F**) were assessed in mitochondrial-enriched fractions by Western Blotting. Data are expressed in arbitrary units relative to ComplexII (70 kDa subunit) as the mean ± SEM of n=2 to 3 experiments. Statistical analysis: (B) $^{t}p < 0.05$ and p=0.0653 *versus* Control; $^{\$}p < 0.05$ *versus* H_2O_2 30min (Student's *t-test*);

CHAPTER IV – DISCUSSION AND CONCLUSIONS

4.1 DISCUSSION

Accumulation of Aβ in AD has been described to stimulate numerous signaling pathways leading to synaptic degeneration, neuronal loss and decline of cognitive functions (Goedert and Spillantini, 2006; Walsh and Selkoe, 2007; Yankner and Lu, 2009; Zhao and Zhao, 2013). In early studies, $A\beta_{25-35}$ was shown to increase hydrogen peroxide and lipid peroxides levels in PC12 cells and rat cortical neurons (Behl, 1994). Also, increased H_2O_2 and nitric oxide production were observed in various AD transgenic mouse models, linking Aβ peptide accumulation to oxidative stress (Matsuoka et al., 2001; Mohmmad Abdul et al., 2006; Smith et al., 1998). Concordantly, in the present study we demonstrate $A\beta_{1-42}$ oligomers-mediated H_2O_2 production in mature hippocampal neurons. Furthermore, this production seems to occur mainly in mitochondria, although the existence of two different pools of ROS production cannot be discarded. The preventive effect of MK-801, an antagonist of NMDARs, evidenced the involvement of NMDARs in Aβ-induced H_2O_2 levels. These results are similar to those obtained by De Felice and colleagues regarding the role of NMDARs in the induction of ROS production by soluble Aβ oligomers in hippocampal neuronal cells (De Felice et al., 2007). Interestingly, the effect of Aβ was also prevented by SU6656, an inhibitor of the Src tyrosine kinase, previously recognized to be a regulator of NMDARs (Yu et al., 1997). In contrast, in HT22 cell line, oligomers of $A\beta_{1-42}$ did not show any effect on H_2O_2 production, which may be explained by the absence of functional NMDARs in these cells (Zhao et al., 2012), as $A\beta_{1-42}$ forms were previously shown to interact with extracellular motifs of GluN1 and GluN2B subunits (Costa et al., 2012).

Neurodegeneration observed in AD has been associated to abnormal homeostasis of intracellular Ca^{2+} (reviewed by Mota et al., 2014; Supnet and Bezprozvanny, 2010). Importantly, studies evidenced that the intracellular Ca^{2+} rise induced by Aβ occur through NMDARs. Indeed, we previously demonstrated an immediate increase in cytosolic Ca^{2+}, involving GluN2B-composed NMDARs in hippocampal and cortical neurons after $A\beta_{1-42}$ oligomeric stimulus, further resulting in impaired ER and

mitochondrial Ca^{2+} homeostasis (Costa et al., 2012; Ferreira et al., 2012, 2015). Concordantly, our present data show an increase in intracellular Ca^{2+} after $A\beta_{1-42}$ oligomers acute treatment, which was prevented by MK-801. Moreover, our results showed a preventive effect of SU6656, pointing out the importance of the relationship between Src protein and NMDARs. Indeed, phosphorylation of GluN2B at Tyr1472 residue through Src or Fyn was associated with enrichment of synaptic NMDARs and enhanced NMDARs activity (Goebel-Goody et al., 2009). In this context, inhibition of Src with SU6656 may lead to decreased levels of NMDARs at the membrane surface and a lower probability of NMDARs activation by Aβ. Interestingly, increased cytosolic Ca^{2+} was not reverted by antioxidants, strongly suggesting that Aβ-induced Ca^{2+} entry through NMDARs probably precede the increase in mitochondrial H_2O_2 production.

There are growing evidences of the involvement of Src kinase protein in AD pathogenesis. Zou and colleagues demonstrated that, in HEK293 cells and in mouse hippocampus, BACE activity and Aβ production could be inhibited by Src family kinase inhibitors and by depletion of endogenous Src with RNAi (Zou et al., 2007). Moreover, we previously showed reduced Src phosphorylation, which could be related with decreased GluN2B Tyr1472 phosphorylation in the hippocampus and cortex of 3 month-old 3xTg-AD male mice (Mota et al., 2014). Src kinase is redox-sensitive and can be activated by H_2O_2 (Akhand et al., 1999). At the same time, tyrosine-phosphatase proteins, which reduce Src phosphorylation, are also sensitive to H_2O_2, favoring Src activation (Hebert-Chatelain, 2013). In our models, namely mature hippocampal neurons and HT22 cell line, we verified a positive effect of H_2O_2 on Src regulation. We further observed, in mature hippocampal neurons, a significant increase in P(Tyr416)Src/Src ratio after $A\beta_{1-42}$ oligomers treatment, which was prevented by antioxidants, suggesting that increased H_2O_2 production induced by Aβ further leads to Src activation. Interestingly, Src activation induced by $A\beta_{1-42}$ was prevented by MK801, indicating the involvement of NMDARs, at least in part, in Src activation pathway.

Activation of the transcription factor Nrf2 can be induced by oxidative stress, leading to its phosphorylation at Ser40 and translocation to the nucleus, which result in ARE-dependent gene expression (Niture et al., 2009). In postmortem AD human brains,

nuclear Nrf2 levels were decreased (Ramsey et al., 2007), suggesting a lower activation. In contrast, other studies showed increased gene expression of Nrf2 targets in AD patients (Raina et al., 1999; Schipper et al., 1995; SantaCruz et al., 2004). We previously reported PBMCs from MCI individuals and 3 month-old male 3xTg-AD mice, increased Nrf2 phosphorylation at Ser40, and increased nuclear Nrf2 levels in brain cortex (Mota et al., 2015). In contrast, SOD1 protein levels, a target of Nrf2, were decreased in human MCI PBMCs, and in 3xTg-AD mice brain cortex we observed SOD1 protein and mRNA decrease as well as for HO-1 and Prdx-1 mRNA levels, suggesting a failure of the Nrf2 pathway function (Mota et al., 2015). In this study, our results in hippocampal neurons showed a significant Aβ-induced Nrf2 phosphorylation increase that was prevented by antioxidants. Interestingly, $A\beta_{1-42}$ oligomers-induced Nrf2 phosphorylation was also prevented by SU6656, suggesting to be Src-dependent. MK-801 was able to decrease Nrf2, however data are not significant, which may implicate a partial and/or indirect role of NMDARs on Nrf2 regulation in the presence of $A\beta_{1-42}$ oligomers. As referred above, HT22 cells appear to be non-sensitive to Aβ. However, we verified increased phosphorylation of Nrf2 under H_2O_2 exposure, which was prevented by the Src inhibitor SU6656, suggesting that phosphorylation of Nrf2 at Ser40 occurs in a Src-dependent manner, although indirectly considering that Src is a Tyr kinase. Accordingly, we also observed a significant increase in Nrf2 phosphorylation levels in HT22 cells transfected with the active form (Y527-Src).

Different studies have reported the presence of Src family members in nucleus (Jain and Jaiswal, 2006; Niture et al., 2011). Moreover, Niture and colleagues demonstrated that, in Hepa-1 cells, Src silencing by siRNA enhances Nrf2 nuclear accumulation and Nrf2 downstream gene expression; otherwise Src overexpression decreased nuclear Nrf2 and ARE-mediated expression in a dose-dependent manner. The same authors showed that nuclear Src kinase family members levels were minimal during the early phase of Nrf2 nuclear activation and import, but increased with longer exposure to stress, reaching the highest nuclear levels during a late phase that promotes Nrf2 nuclear phosphorylation of Tyr568 and its export from the organelle (Niture et al., 2011). Concordantly, in HT22 cells, we evidenced a significant decrease in total Src levels in the nucleus after short period of H_2O_2 stimulus, although this was not

accompanied by changes in nuclear Nrf2 levels. At the same time, we observed an increase in phosphorylated Tyr 416 Src levels, suggesting another role of Src in the nucleus apart from the previously described regulation of Nrf2 export. Surprisingly, inhibition of Src caused no effect on Src phosphorylation in the nucleus. This result could be explained by the fact that SU6656 may not cross the nuclear membrane, but further studies should be performed. Additionally, we observed higher levels of P(Tyr416)Src/Src ratio in nucleus of HT22 cells expressing the constitutively active form of Src (Y527F-Src), without changes in nuclear Nrf2 protein levels; suggesting that nuclear Src activation is not related with nuclear Nrf2 accumulation. This last result may be also due to the fact that the influence of Src on Nrf2 nuclear regulation can occur earlier and that 48h of plasmid expression may not be appropriate to evaluate this parameter.

In mature hippocampal neurons, preliminary data suggest that the increase in Nrf2 phosphorylation after Aβ treatment, normally associated with its nuclear translocation, was not accompanied by increased nuclear levels of Nrf2. This appears contradictory with our previous reports where we showed increased nuclear Nrf2 levels in 3xTg-AD mice brain cortex (Mota et al., 2015). The time of incubation of the present study may be a limitation; in fact, 30 min of treatment may not be enough to observe translocation of the transcription factor. On the other hand, Src nuclear levels were not altered in hippocampal neurons after Aβ stimulus, and thus further studies will be required.

There are evidences for the presence of Src kinase and Nrf2 within the mitochondria. Salvi and colleagues showed that Src is mainly located in the intermembrane space of rat brain mitochondria (Salvi et al., 2002). Src was also described in MIM of osteoclasts (Miyazaki et al., 2006). Here, we were able to demonstrate the presence of Src in mitochondria of HT22 cells. Importantly, relevant regulators of Src kinase activity, namely SHP-2 and PTP1B, have been found in rat brain mitochondria, suggesting that Src activity can be regulated directly in mitochondria (Salvi et al., 2004). Interestingly, we observed higher phosphorylated Src levels in HT22 cell mitochondria after short or longer (4h) H_2O_2 exposure, while no differences in total protein levels were observed.

On the other hand, in HEK-293T and HeLa cells, Keap-1, a major negative regulator of Nrf2, was previously reported to locate at the MOM. Apparently, its location is secured through an interaction with a phosphoglycerate mutase family member, PGAM5, which can form a ternary complex of Nrf2-Keap-1–PGAM5 and migrate to mitochondria (Lo and Hannink, 2008). Moreover, Strom and colleagues, recently showed increased susceptibility to mitochondrial swelling in Nrf2 knock-out rat cardiomyocytes; furthermore, they demonstrated the presence of Nrf2 protein in MOM isolated from rat hearts (Strom et al., 2016). We detected the presence of Nrf2 in HT22 cells mitochondria. Moreover, we evidenced a significant increase in phosphorylated Nrf2 at Ser40 levels after short and long time exposure to H_2O_2 stimulus in HT22 mitochondria, suggesting a role for Nrf2 in the mitochondria, as a sensor to further possibly regulate gene expression in response to changes in mitochondrial redox status. In fact, the Nrf2–Keap1 interaction appears to be maintained on the mitochondria since Keap1 is also present in mitochondrial fractions, specifically at MOM (Strom et al., 2016). Additionally, expressing the constitutively active form of Src (Y527F-Src), we observed higher levels of P(Tyr416)Src/Src ratio in mitochondria of HT22 cells, with no changes in mitochondrial Nrf2 protein levels; suggesting that overactivation of Src is not enough, *per se*, to influence Nrf2 activation in mitochondria.

H_2O_2 leads to abnormal mitochondrial morphology in rat cardiomyocytes (Strom et al., 2016). Recently, Gan and colleagues demonstrated that H_2O_2 treatment leads to mitochondrial fission, increasing total and phosphorylated levels of Drp1, which later resulted in mitochondrial dysfunction in osteoblasts; furthermore, they showed that Drp1 inhibition attenuates oxidative stress-induced osteoblast dysfunction (Gan et al., 2015). Moreover, Src can interact with various mitochondrial proteins namely, complexes I, III, IV and V (Hébert Chatelain et al., 2011). Taking into account the presence of Src in HT22 mitochondria and the fact that we observed mitochondrial Src activation under short time of H_2O_2 treatment, we finally addressed the possibility of mitochondrial Src activation to be involved in the regulation of mitochondrial dynamics, namely fission and fusion. Surprisingly, in short time H_2O_2 treated HT22 cells, we observed a decrease in mitochondrial Drp1 levels, which were reverted after

Src inhibition. These data suggest that under short oxidative stimuli Src inhibits the recruitment of Drp1 to the mitochondria. Additionally, HSP60 is a major mitochondrial chaperone that plays a crucial role in the folding and assembly of newly imported proteins (Cheng et al., 1990). Sarangi and colleagues showed that treatments with rotenone in BC-8 and IMR-32 cells, which induces H_2O_2 production, combined with cycloheximide caused HSP60 mitochondrial accumulation; furthermore, they demonstrated that overexpression of HSP60 with rotenone also resulted in HSP60 mitochondrial accumulation (Sarangi et al., 2013). In the present study, we did not observe an effect of H_2O_2, *per se,* on mitochondrial HSP60 levels; however, inhibition of Src under H_2O_2 stimulus induced significant HSP60 accumulation within mitochondria, suggesting that Src may have a role in mitochondrial HSP60 regulation, or may be the result of cellular stress.

4.2 CONCLUSIONS

Aβ has been largely described to increase ROS levels in the context of AD, which is associated with mitochondrial dysfunction. Cytosolic Ca^{2+} has been also described to be deregulated in various AD models, as a result of NMDARs activation. Furthermore, mild redox modifications can modify different pathways in neurons and interact with proteins such as Src and Nrf2. Herein, we explored the effect of $A\beta_{1-42}$ oligomers and H_2O_2 on Src and Nrf2 phosphorylation and their involvement in different pathways in mature hippocampal neurons and HT22 cells.

In hippocampal neurons, $A\beta_{1-42}$ oligomers induced intracellular Ca^{2+} increase through NMDARs in a ROS-independent manner. Moreover, H_2O_2 production associated with Aβ treatment, mainly occurs in mitochondria. Aβ effect was prevented by the use of SU6656, a Src inhibitor, suggesting the involvement of Src in Aβ-mediated effects. We hypothesized that inhibition of Src results in decreased levels of NMDARs at the membrane surface decreasing their activation by Aβ and consequently decreasing intracellular downstream pathways. Our results also showed that Aβ-mediated H_2O_2 results in Src and Nrf2 activation, which could be prevented by SU6656 and MK801, revealing that (i) Nrf2 phosphorylation occurs in a Src-dependent manner and (ii) NMDARs are involved in this process, most probably upstream of Src activation.

In HT22 cells, we observed that H_2O_2 causes decreased Src protein levels in the nucleus, while levels of phosphorylated Src were increased, suggesting a possible novel role for Src in the nucleus, independently of nuclear Nrf2. However, this result can be discussed taking into account the short time of exposure to H_2O_2, which may not be enough to allow Nrf2 import to the nucleus. Additionally, we were able to demonstrate the presence of Src and Nrf2 in mitochondria from HT22 cells. In this regard, we evaluated the effect of H_2O_2 in these mitochondrial proteins levels. Results showed apparently unrelated increased P(Tyr416)Src/Src and P(Ser40)Nrf2/Nrf2 ratios.

Interestingly, H_2O_2-mediated mitochondrial Src activation seemed to have a preventive effect in mitochondrial fission.

Overall, data evidence NMDARs- and ROS-dependent Src and Nrf2 activation, in hippocampal neurons exposed to $A\beta_{1-42}$ oligomers, providing new insights to the characterization of changes that may occur in AD pathogenesis. Our findings allow the elaboration of a temporal hypothesis. In this way we may propose that $A\beta_{1-42}$ interaction with NMDARs causes intracellular Ca^{2+} rise and (mitochondrial) ROS production, which mediates phosphorylation/activation of Src and Nrf2; on the other hand, Src may influence ROS production (probably through modulation of NMDARs) and indirectly regulates Nrf2 phosphorylation. Thus, Src dependent-AD pathogenesis seems to act as a loop. These results also suggest novel Src and Nrf2 roles in mitochondria and nucleus, highlighting the importance of these proteins in cell regulation. Thus, the understanding of these mechanisms in AD context will be very important for the development of new strategies aiming to restore cell homeostasis and consequently avoid the effect caused by Aβ oligomeric species.

REFERENCES

Abramov, A.Y., Canevari, L., and Duchen, M.R. (2003). Changes in intracellular calcium and glutathione in astrocytes as the primary mechanism of amyloid neurotoxicity. J. Neurosci. *23*, 5088–5095.

Aizenman, E., Hartnett, K.A., and Reynoldst, I.J. (1990). Oxygen free radicals regulate NMDA receptor function via a redox modulatory site. Neuron *5*, 841–846.

Akhand, A.A., Pu, M., Senga, T., Kato, M., Suzuki, H., Miyata, T., Hamaguchi, M., and Nakashima, I. (1999). Nitric oxide controls Src kinase activity through a sulfhydryl group modification-mediated Tyr-527-independent and Tyr-416-linked mechanism. J. Biol. Chem. *274*, 25821–25826.

Ali, D.W., and Salter, M.W. (2001). NMDA receptor regulation by Src kinase signalling in excitatory synaptic transmission and plasticity. Curr. Opin. Neurobiol. *11*, 336–342.

Almeida, A., Moncada, S., and Bolaños, J.P. (2004). Nitric oxide switches on glycolysis through the AMP protein kinase and 6-phosphofructo-2-kinase pathway. Nat. Cell Biol. *6*, 45–51.

Ambrósio, A.F., Silva, A.P., Malva, J.O., Mesquita, J.F., Carvalho, A.P., and Carvalho, C.M. (2000). Role of desensitization of AMPA receptors on the neuronal viability and an the [Ca2+](i) changes in cultured rat hippocampal neurons. Eur. J. Neurosci. *12*, 2021–2031.

Apelt, J., Bigl, M., Wunderlich, P., and Schliebs, R. (2004). Aging-related increase in oxidative stress correlates with developmental pattern of beta-secretase activity and beta-amyloid plaque formation in transgenic Tg2576 mice with Alzheimer-like pathology. In International Journal of Developmental Neuroscience, pp. 475–484.

Apopa, P.L., He, X., and Ma, Q. (2008). Phosphorylation of Nrf2 in the transcription activation domain by casein kinase 2 (CK2) is critical for the nuclear translocation and transcription activation function of Nrf2 in IMR-32 neuroblastoma cells. J. Biochem. Mol. Toxicol. *22*, 63–76.

Arachiche, A., Augereau, O., Decossas, M., Pertuiset, C., Gontier, E., Letellier, T., and Dachary-Prigent, J. (2008). Localization of PTP-1B, SHP-2, and Src exclusively in rat brain mitochondria and functional consequences. J. Biol. Chem. *283*, 24406–24411.

Arora, A., and Bhagat, N. (2016). Insight into the Molecular Imaging of Alzheimer's Disease. Int. J. Biomed. Imaging *2016*.

Augereau, O., Claverol, S., Boudes, N., Basurko, M.J., Bonneu, M., Rossignol, R., Mazat, J.P., Letellier, T., and Dachary-Prigent, J. (2005). Identification of tyrosine-phosphorylated proteins of the mitochondrial oxidative phosphorylation machinery. Cell. Mol. Life Sci. *62*, 1478–1488.

Baldeiras, I., Santana, I., Proença, M.T., Garrucho, M.H., Pascoal, R., Rodrigues, A., Duro, D., and Oliveira, C.R. (2008). Peripheral oxidative damage in mild cognitive impairment and mild Alzheimer's disease. J. Alzheimers. Dis. *15*, 117–128.

Barage, S.H., and Sonawane, K.D. (2015). Amyloid cascade hypothesis: Pathogenesis and therapeutic strategies in Alzheimer's disease. Neuropeptides *52*, 1–18.

Behl, C. (1994). Hydrogen peroxide mediates amyloid β protein toxicity. Cell *77*, 817–827.

Benilova, I., Karran, E., and De Strooper, B. (2012). The toxic Aβ oligomer and Alzheimer's disease: an emperor in need of clothes. Nat. Neurosci. *15*, 349–357.

Berridge, M.J. (2013). Dysregulation of neural calcium signaling in Alzheimer disease, bipolar disorder and schizophrenia. Prion *7*, 2–13.

Bhat, A.H., Dar, K.B., Anees, S., Zargar, M.A., Masood, A., Sofi, M.A., and Ganie, S.A. (2015). Oxidative stress, mitochondrial dysfunction and neurodegenerative diseases; a mechanistic insight. Biomed. Pharmacother. = Biomédecine Pharmacothérapie *74*, 101–110.

Bloudek, L.M., Spackman, D.E., Blankenburg, M., and Sullivan, S.D. (2011). Review and meta-analysis of biomarkers and diagnostic imaging in Alzheimer's disease. J. Alzheimer's Dis. *26*, 627–645.

Boerner, J.L., Demory, M.L., Silva, C., and Parsons, S.J. (2004). Phosphorylation of Y845 on the epidermal growth factor receptor mediates binding to the mitochondrial protein cytochrome c oxidase subunit II. Mol. Cell. Biol. *24*, 7059–7071.

Bolaños, J.P., Moro, M.A., Lizasoain, I., and Almeida, A. (2009). Mitochondria and reactive oxygen and nitrogen species in neurological disorders and stroke: Therapeutic implications☆. Adv. Drug Deliv. Rev. *61*, 1299–1315.

Brigman, J.L., Wright, T., Talani, G., Prasad-Mulcare, S., Jinde, S., Seabold, G.K., Mathur, P., Davis, M.I., Bock, R., Gustin, R.M., et al. (2010). Loss of GluN2B-containing NMDA receptors in CA1 hippocampus and cortex impairs long-term depression, reduces dendritic spine density, and disrupts learning. J. Neurosci. *30*, 4590–4600.

Brown, M.T., and Cooper, J.A. (1996). Regulation, substrates and functions of src. Biochim. Biophys. Acta - Rev. Cancer *1287*, 121–149.

Butterfield, D.A. (2002). Amyloid beta-peptide (1-42)-induced oxidative stress and neurotoxicity: implications for neurodegeneration in Alzheimer's disease brain. A review. Free Radic. Res. *36*, 1307–1313.

Butterfield, D. a, Castegna, a, Lauderback, C.M., and Drake, J. (2002). Evidence that amyloid b-peptide-induced lipid peroxidation and its sequelae in Alzheimer's disease brain contribute to neuronal death. Neurobiol Aging *23*, 655–664.

Cacace, R., Sleegers, K., and Van Broeckhoven, C. (2016). Molecular genetics of early-

onset Alzheimer disease revisited. Alzheimer's Dement.

Cao, X., Cui, Z., Feng, R., Tang, Y.P., Qin, Z., Mei, B., and Tsien, J.Z. (2007a). Maintenance of superior learning and memory function in NR2B transgenic mice during ageing. Eur. J. Neurosci. *25*, 1815–1822.

Cao, Z., George, J., Baden, D.G., and Murray, T.F. (2007b). Brevetoxin-induced phosphorylation of Pyk2 and Src in murine neocortical neurons involves distinct signaling pathways. Brain Res. *1184*, 17–27.

Carr, D.B., Goate, A., Phil, D., and Morris, J.C. (1997). Current concepts in the pathogenesis of Alzheimer's disease. Am J Med *103*, 3S – 10S.

Caspersen, C. (2005). Mitochondrial A : a potential focal point for neuronal metabolic dysfunction in Alzheimer's disease. FASEB J. *19*, 2040–2041.

Cataldi, M., Taglialatela, M., Guerriero, S., Amoroso, S., Lombardi, G., Di Renzo, G., and Annunziato, L. (1996). Protein-tyrosine kinases activate while protein-tyrosine phosphatases inhibit L-type calcium channel activity in pituitary GH3 cells. J. Biol. Chem. *271*, 9441–9446.

Chakrabarty, P., Jansen-West, K., Beccard, A., Ceballos-Diaz, C., Levites, Y., Verbeeck, C., Zubair, A.C., Dickson, D., Golde, T.E., and Das, P. (2010). Massive gliosis induced by interleukin-6 suppresses Abeta deposition in vivo: evidence against inflammation as a driving force for amyloid deposition. FASEB J. *24*, 548–559.

Chaufty, J., Sullivan, S.E., and Ho, a. (2012). Intracellular Amyloid Precursor Protein Sorting and Amyloid- Secretion Are Regulated by Src-Mediated Phosphorylation of Mint2. J. Neurosci. *32*, 9613–9625.

Cheng, M.Y., Hartl, F.U., and Horwich, a L. (1990). The mitochondrial chaperonin hsp60 is required for its own assembly. Nature *348*, 455–458.

Chojnacka, K., and Mruk, D.D. (2015). The Src non-receptor tyrosine kinase paradigm: New insights into mammalian Sertoli cell biology. Mol. Cell. Endocrinol. *415*, 133–142.

Chui, D.H., Tanahashi, H., Ozawa, K., Ikeda, S., Checler, F., Ueda, O., Suzuki, H., Araki, W., Inoue, H., Shirotani, K., et al. (1999). Transgenic mice with Alzheimer presenilin 1 mutations show accelerated neurodegeneration without amyloid plaque formation. Nat. Med. *5*, 560–564.

Corder, E.H., Saunders, A.M., Strittmatter, W.J., Schmechel, D.E., Gaskell, P.C., Small, G.W., Roses, A.D., Haines, J.L., and Pericakvance, M.A. (1993). Gene Dose of Apolipoprotein-E Type-4 Allele and the Risk of Alzheimers-Disease in Late-Onset Families. Science (80-.). *261*, 921–923.

Costa, R.O., Lacor, P.N., Ferreira, I.L., Resende, R., Auberson, Y.P., Klein, W.L., Oliveira, C.R., Rego, A.C., and Pereira, C.M.F. (2012). Endoplasmic reticulum stress occurs downstream of GluN2B subunit of N -methyl-D-aspartate receptor in mature

hippocampal cultures treated with amyloid-β oligomers. Aging Cell *11*, 823–833.

Cull-Candy, S., Brickley, S., and Farrant, M. (2001). NMDA receptor subunits: diversity, development and disease. Curr Opin Neurobiol *11*, 327–335.

Cullinan, S.B., Zhang, D., Hannink, M., Arvisais, E., Kaufman, R.J., and Diehl, J.A. (2003). Nrf2 is a direct PERK substrate and effector of PERK-dependent cell survival. Mol. Cell. Biol. *23*, 7198–7209.

D'Andrea, M.R., Nagele, R.G., Wang, H.-Y., and Lee, D.H.S. (2002). Consistent immunohistochemical detection of intracellular beta-amyloid42 in pyramidal neurons of Alzheimer's disease entorhinal cortex. Neurosci. Lett. *333*, 163–166.

Danysz, W., and Parsons, C.G. (2003). The NMDA receptor antagonist memantine as a symptomatological and neuroprotective treatment for Alzheimer's disease: Preclinical evidence. Int. J. Geriatr. Psychiatry *18*.

Dasuri, K., Zhang, L., and Keller, J.N. (2013). Oxidative stress, neurodegeneration, and the balance of protein degradation and protein synthesis. Free Radic. Biol. Med. *62*, 170–185.

Dhawan, G., and Combs, C.K. (2012). Inhibition of Src kinase activity attenuates amyloid associated microgliosis in a murine model of Alzheimer's disease. J. Neuroinflammation *9*, 117.

Droge, W. (2002). Free Radicals in the Physiological Control of Cell Function. Physiol Rev *82*, 47–95.

Du, C.-P., Gao, J., Tai, J.-M., Liu, Y., Qi, J., Wang, W., and Hou, X.-Y. (2009). Increased tyrosine phosphorylation of PSD-95 by Src family kinases after brain ischaemia. Biochem. J. *417*, 277–285.

Du, C.-P., Tan, R., and Hou, X.-Y. (2012). Fyn kinases play a critical role in neuronal apoptosis induced by oxygen and glucose deprivation or amyloid-β peptide treatment. CNS Neurosci. Ther. *18*, 754–761.

Du, H., Guo, L., Yan, S., Sosunov, A.A., McKhann, G.M., and Yan, S.S. (2010). Early deficits in synaptic mitochondria in an Alzheimer's disease mouse model. Proc. Natl. Acad. Sci. U. S. A. *107*, 18670–18675.

Dubois, B., Hampel, H., Feldman, H.H., Scheltens, P., Aisen, P., Andrieu, S., Bakardjian, H., Benali, H., Bertram, L., Blennow, K., et al. (2016). Preclinical Alzheimer's disease: Definition, natural history, and diagnostic criteria. Alzheimer's Dement. *12*, 292–323.

Dumont, M., Stack, C., Elipenahli, C., Jainuddin, S., Gerges, M., Starkova, N.N., Yang, L., Starkov, A. a, and Beal, F. (2011). Behavioral deficit, oxidative stress, and mitochondrial dysfunction precede tau pathology in P301S transgenic mice. FASEB J. *25*, 4063–4072.

Fadool, D.A., Holmes, T.C., Berman, K., Dagan, D., and Levitan, I.B. (1997). Tyrosine phosphorylation modulates current amplitude and kinetics of a neuronal voltage-gated

potassium channel. J. Neurophysiol. *78*, 1563–1573.

De Felice, F.G., Velasco, P.T., Lambert, M.P., Viola, K., Fernandez, S.J., Ferreira, S.T., and Klein, W.L. (2007). Abeta Oligomers Induce Neuronal Oxidative Stress through an N-Methyl-D-aspartate Receptor-dependent Mechanism That Is Blocked by the Alzheimer Drug Memantine. J. Biol. Chem. *282*, 11590–11601.

Feng, J., Lucchinetti, E., Enkavi, G., Wang, Y., Gehrig, P., Roschitzki, B., Schaub, M.C., Tajkhorshid, E., Zaugg, K., and Zaugg, M. (2010). Tyrosine phosphorylation by Src within the cavity of the adenine nucleotide translocase 1 regulates ADP/ATP exchange in mitochondria. Am. J. Physiol. Cell Physiol. *298*, C740–C748.

Fernández-Morales, J.C., Arranz-Tagarro, J.A., Calvo-Gallardo, E., Maroto, M., Padín, J.F., and García, A.G. (2012). Stabilizers of neuronal and mitochondrial calcium cycling as a strategy for developing a medicine for Alzheimer's disease. ACS Chem. Neurosci. *3*, 873–883.

Ferreira, I.L., Bajouco, L.M., Mota, S.I., Auberson, Y.P., Oliveira, C.R., and Rego, A.C. (2012). Amyloid beta peptide 1-42 disturbs intracellular calcium homeostasis through activation of GluN2B-containing N-methyl-d-aspartate receptors in cortical cultures. Cell Calcium *51*, 95–106.

Ferreira, I.L., Ferreiro, E., Schmidt, J., Cardoso, J.M., Pereira, C.M.F., Carvalho, A.L., Oliveira, C.R., and Rego, A.C. (2015). Aβ and NMDAR activation cause mitochondrial dysfunction involving ER calcium release. Neurobiol. Aging *36*, 680–692.

Ferreiro, E., Resende, R., Costa, R., Oliveira, C.R., and Pereira, C.M.F. (2006). An endoplasmic-reticulum-specific apoptotic pathway is involved in prion and amyloid-beta peptides neurotoxicity. Neurobiol. Dis. *23*, 669–678.

Fukumoto, H., Asami-Odaka, A., Suzuki, N., Shimada, H., Ihara, Y., and Iwatsubo, T. (1996). Amyloid beta protein deposition in normal aging has the same characteristics as that in Alzheimer's disease. Predominance of A beta 42(43) and association of A beta 40 with cored plaques. Am. J. Pathol. *148*, 259–265.

Gan, X., Huang, S., Yu, Q., Yu, H., and Yan, S.S. (2015). Blockade of Drp1 rescues oxidative stress-induced osteoblast dysfunction. Biochem. Biophys. Res. Commun. *468*, 719–725.

Gandhi, S., and Abramov, A.Y. (2012). Mechanism of oxidative stress in neurodegeneration. Oxid. Med. Cell. Longev.

Ghezzi, D., and Zeviani, M. (2012). Assembly factors of human mitochondrial respiratory chain complexes: physiology and pathophysiology. Adv Exp Med Biol *748*, 65–106.

Gibson, G.E., and Shi, Q. (2010). A mitocentric view of Alzheimer's disease suggests multi-faceted treatments. J. Alzheimer's Dis. *20*.

Gilgun-Sherki, Y., Melamed, E., and Offen, D. (2001). Oxidative stress induced-neurodegenerative diseases: The need for antioxidants that penetrate the blood brain barrier. Neuropharmacology *40*, 959–975.

Giménez-Llort, L., Blázquez, G., Cañete, T., Johansson, B., Oddo, S., Tobeña, A., LaFerla, F.M., and Fernández-Teruel, A. (2007). Modeling behavioral and neuronal symptoms of Alzheimer's disease in mice: A role for intraneuronal amyloid. Neurosci. Biobehav. Rev. *31*, 125–147.

Gingrich, J.R., Pelkey, K.A., Fam, S.R., Huang, Y., Petralia, R.S., Wenthold, R.J., and Salter, M.W. (2004). Unique domain anchoring of Src to synaptic NMDA receptors via the mitochondrial protein NADH dehydrogenase subunit 2. Proc. Natl. Acad. Sci. *101*, 6237–6242.

Goebel-Goody, S.M., Davies, K.D., Alvestad Linger, R.M., Freund, R.K., and Browning, M.D. (2009). Phospho-regulation of synaptic and extrasynaptic N-methyl-d-aspartate receptors in adult hippocampal slices. Neuroscience *158*, 1446–1459.

Goedert, M., and Spillantini, M.G. (2006). A century of Alzheimer's disease. Science *314*, 777–781.

Gonatas NK, Anderson W, E.I. (1967). Summary for The contribution of altered synapses in the senile plaque: an electron microscopic study in Alzheimer's dementia. In J Neuropathol Exp Neurol., Intergovernmental Panel on Climate Change, ed. (Cambridge: Cambridge University Press), pp. 1–30.

Gouras, G.K., Tsai, J., Naslund, J., Vincent, B., Edgar, M., Checler, F., Greenfield, J.P., Haroutunian, V., Buxbaum, J.D., Xu, H., et al. (2000). Intraneuronal Abeta42 accumulation in human brain. Am. J. Pathol. *156*, 15–20.

Gouras, G.K., Tampellini, D., Takahashi, R.H., and Capetillo-Zarate, E. (2010). Intraneuronal beta-amyloid accumulation and synapse pathology in Alzheimer's disease. Acta Neuropathol. *119*, 523–541.

Griffith, O.W. (1982). Mechanism of action, metabolism, and toxicity of buthionine sulfoximine and its higher homologs, potent inhibitors of glutathione synthesis. J. Biol. Chem. *257*, 13704–13712.

Gruart, A., Muñoz, M.D., and Delgado-García, J.M. (2006). Involvement of the CA3-CA1 synapse in the acquisition of associative learning in behaving mice. J. Neurosci. *26*, 1077–1087.

Guerreiro, R.J., Gustafson, D.R., and Hardy, J. (2012). The genetic architecture of Alzheimer's disease: Beyond APP, PSENS and APOE. Neurobiol. Aging *33*, 437–456.

Haass, C., and Selkoe, D.J. (2007). Soluble protein oligomers in neurodegeneration: lessons from the Alzheimer's amyloid beta-peptide. Nat. Rev. Mol. Cell Biol. *8*, 101–112.

Hansson Petersen, C.A., Alikhani, N., Behbahani, H., Wiehager, B., Pavlov, P.F., Alafuzoff, I., Leinonen, V., Ito, A., Winblad, B., Glaser, E., et al. (2008). The amyloid beta-peptide is imported into mitochondria via the TOM import machinery and localized to mitochondrial cristae. Proc. Natl. Acad. Sci. U. S. A. *105*, 13145–13150.

Harlan, J.M., Levine, J.D., Callahan, K.S., Schwartz, B.R., and Harker, L.A. (1984). Glutathione redox cycle protects cultured endothelial cells against lysis by extracellularly generated hydrogen peroxide. J. Clin. Invest. *73*, 706–713.

Hartley, D.M., Walsh, D.M., Ye, C.P., Diehl, T., Vasquez, S., Vassilev, P.M., Teplow, D.B., and Selkoe, D.J. (1999). Protofibrillar intermediates of amyloid beta-protein induce acute electrophysiological changes and progressive neurotoxicity in cortical neurons. J. Neurosci. *19*, 8876–8884.

Hébert Chatelain, E., Dupuy, J.-W., Letellier, T., and Dachary-Prigent, J. (2011). Functional impact of PTP1B-mediated Src regulation on oxidative phosphorylation in rat brain mitochondria. Cell. Mol. Life Sci. *68*, 2603–2613.

Hebert-Chatelain, E. (2013). Src kinases are important regulators of mitochondrial functions. Int. J. Biochem. Cell Biol. *45*, 90–98.

Hedskog, L., Pinho, C.M., Filadi, R., Rönnbäck, A., Hertwig, L., Wiehager, B., Larssen, P., Gellhaar, S., Sandebring, A., Westerlund, M., et al. (2013). Modulation of the endoplasmic reticulum-mitochondria interface in Alzheimer's disease and related models. Proc. Natl. Acad. Sci. U. S. A. *110*, 7916–7921.

Hirotsu, Y., Katsuoka, F., Funayama, R., Nagashima, T., Nishida, Y., Nakayama, K., Douglas Engel, J., and Yamamoto, M. (2012). Nrf2-MafG heterodimers contribute globally to antioxidant and metabolic networks. Nucleic Acids Res. *40*, 10228–10239.

Hoppins, S., Lackner, L., and Nunnari, J. (2007). The Machines that Divide and Fuse Mitochondria. Annu. Rev. Biochem. *76*, 751–780.

Hu, N.-W., Klyubin, I., Anwyl, R., and Rowan, M.J. (2009). GluN2B subunit-containing NMDA receptor antagonists prevent Abeta-mediated synaptic plasticity disruption in vivo. Proc. Natl. Acad. Sci. U. S. A. *106*, 20504–20509.

Huang, Y., and Mucke, L. (2012). Alzheimer mechanisms and therapeutic strategies. Cell *148*, 1204–1222.

Huang, H.C., Nguyen, T., and Pickett, C.B. (2002). Phosphorylation of Nrf2 at Ser-40 by protein kinase C regulates antioxidant response element-mediated transcription. J. Biol. Chem. *277*, 42769–42774.

Itoh, S., Lemay, S., Osawa, M., Che, W., Duan, Y., Tompkins, A., Brookes, P.S., Sheu, S.S., and Abe, J. (2005). Mitochondrial Dok-4 recruits Src kinase and regulates NF-kappaB activation in endothelial cells. J. Biol. Chem. *280*, 26383–26396.

Jain, A.K., and Jaiswal, A.K. (2006). Phosphorylation of tyrosine 568 controls nuclear

export of Nrf2. J. Biol. Chem. *281*, 12132–12142.

Jan, A., Adolfsson, O., Allaman, I., Buccarello, A.-L., Magistretti, P.J., Pfeifer, A., Muhs, A., and Lashuel, H.A. (2011). Abeta42 neurotoxicity is mediated by ongoing nucleated polymerization process rather than by discrete Abeta42 species. J. Biol. Chem. *286*, 8585–8596.

Jensen, L.E., Bultynck, G., Luyten, T., Amijee, H., Bootman, M.D., and Roderick, H.L. (2013). Alzheimer's disease-associated peptide Aβ42 mobilizes ER Ca(2+) via InsP3R-dependent and -independent mechanisms. Front. Mol. Neurosci. *6*, 36.

Kanninen, K., Malm, T.M., Jyrkkänen, H.-K., Goldsteins, G., Keksa-Goldsteine, V., Tanila, H., Yamamoto, M., Ylä-Herttuala, S., Levonen, A.-L., and Koistinaho, J. (2008). Nuclear factor erythroid 2-related factor 2 protects against beta amyloid. Mol. Cell. Neurosci. *39*, 302–313.

Kansanen, E., Kuosmanen, S.M., Leinonen, H., and Levonenn, A.L. (2013). The Keap1-Nrf2 pathway: Mechanisms of activation and dysregulation in cancer. Redox Biol. *1*, 45–49.

Kärkkäinen, V., Pomeshchik, Y., Savchenko, E., Dhungana, H., Kurronen, A., Lehtonen, S., Naumenko, N., Tavi, P., Levonen, A.-L., Yamamoto, M., et al. (2014). Nrf2 Regulates Neurogenesis and Protects Neural Progenitor Cells Against Aβ Toxicity. Stem Cells *32*, 1904–1916.

Kawai, Y., Garduno, L., Theodore, M., Yang, J., and Arinze, I.J. (2011). Acetylation-Deacetylation of the Transcription Factor Nrf2 (Nuclear Factor Erythroid 2-related Factor 2) Regulates Its Transcriptional Activity and Nucleocytoplasmic Localization. J. Biol. Chem. *286*, 7629–7640.

Kim, G.H., Kim, J.E., Rhie, S.J., and Yoon, S. (2015). The Role of Oxidative Stress in Neurodegenerative Diseases. Exp. Neurobiol. *24*, 325.

Kim, H.J., Chae, S.C., Lee, D.K., Chromy, B., Lee, S.C., Park, Y.C., Klein, W.L., Krafft, G.A., and Hong, S.T. (2003). Selective neuronal degeneration induced by soluble oligomeric amyloid beta protein. FASEB J. *17*, 118–120.

Kim, J., Keum, Y.-S., Kim, J., and Keum, Y.-S. (2016). NRF2, a Key Regulator of Antioxidants with Two Faces towards Cancer. Oxid. Med. Cell. Longev. *2016*, 1–7.

Köhr, G., and Seeburg, P.H. (1996). Subtype-specific regulation of recombinant NMDA receptor-channels by protein tyrosine kinases of the src family. J. Physiol. *492 (Pt 2*, 445–452.

Komatsu, M., Kurokawa, H., Waguri, S., Taguchi, K., Kobayashi, A., Ichimura, Y., Sou, Y.-S., Ueno, I., Sakamoto, A., Tong, K.I., et al. (2010). The selective autophagy substrate p62 activates the stress responsive transcription factor Nrf2 through inactivation of Keap1. Nat. Cell Biol. *12*, 213–223.

LaFerla, F.M., and Oddo, S. (2005). Alzheimer's disease: Abeta, tau and synaptic dysfunction. Trends Mol. Med. *11*, 170–176.

Lambert, J.C., and Amouyel, P. (2011). Genetics of Alzheimer's disease: New evidences for an old hypothesis? Curr. Opin. Genet. Dev. *21*, 295–301.

Lambert, J.C., Heath, S., Even, G., Campion, D., Sleegers, K., Hiltunen, M., Combarros, O., Zelenika, D., Bullido, M.J., Tavernier, B., et al. (2009). Genome-wide association study identifies variants at CLU and CR1 associated with Alzheimer's disease. Nat Genet *41*, 1094–1099.

Lau, L.F., and Huganir, R.L. (1995). Differential tyrosine phosphorylation of N-methyl-D-aspartate receptor subunits. J Biol Chem *270*, 20036–20041.

Lau, A., Wang, X.-J., Zhao, F., Villeneuve, N.F., Wu, T., Jiang, T., Sun, Z., White, E., and Zhang, D.D. (2010). A noncanonical mechanism of Nrf2 activation by autophagy deficiency: direct interaction between Keap1 and p62. Mol. Cell. Biol. *30*, 3275–3285.

Laws, S.M., Hone, E., Gandy, S., and Martins, R.N. (2003). Expanding the association between the APOE gene and the risk of Alzheimer's disease: Possible roles for APOE promoter polymorphisms and alterations in APOE transcription. J. Neurochem. *84*, 1215–1236.

Levinson, W.E., Varmus, H.E., Garapin, A.C., and Bishop, J.M. (1972). DNA of Rous sarcoma virus: its nature and significance. Science. *175(4017)*, 76–78.

Li, F., Calingasan, N.Y., Yu, F., Mauck, W.M., Toidze, M., Almeida, C.G., Takahashi, R.H., Carlson, G.A., Beal, M.F., Lin, M.T., et al. (2004). Increased plaque burden in brains of APP mutant MnSOD heterozygous knockout mice. J. Neurochem. *89*, 1308–1312.

Li, Y., Sun, H., Chen, Z., Xu, H., Bu, G., and Zheng, H. (2016). Implications of GABAergic neurotransmission in Alzheimer's disease. Front. Aging Neurosci. *8*.

Lipton, S.A., Choi, Y.B., Takahashi, H., Zhang, D., Li, W., Godzik, A., and Bankston, L.A. (2002). Cysteine regulation of protein function - As exemplified by NMDA-receptor modulation. Trends Neurosci. *25*, 474–480.

Liu, H., Wu, Y., Zhu, S., Liang, W., Wang, Z., Wang, Y., Lv, T., Yao, Y., Yuan, D., and Song, Y. (2015). PTP1B promotes cell proliferation and metastasis through activating src and ERK1/2 in non-small cell lung cancer. Cancer Lett. *359*, 218–225.

Livigni, A., Scorziello, A., Agnese, S., Adornetto, A., Carlucci, A., Garbi, C., Castaldo, I., Annunziato, L., Avvedimento, E. V, and Feliciello, A. (2006). Mitochondrial AKAP121 links cAMP and src signaling to oxidative metabolism. Mol Biol Cell *17*, 263–271.

Lluis, J.M., Buricchi, F., Chiarugi, P., Morales, A., and Fernandez-Checa, J.C. (2007). Dual role of mitochondrial reactive oxygen species in hypoxia signaling: activation of nuclear factor-{kappa}B via c-SRC and oxidant-dependent cell death. Cancer Res. *67*, 7368–7377.

Lo, S.C., and Hannink, M. (2008). PGAM5 tethers a ternary complex containing Keap1 and Nrf2 to mitochondria. Exp. Cell Res. *314*, 1789–1803.

Loboda, A., Damulewicz, M., Pyza, E., Jozkowicz, A., and Dulak, J. (2016). Role of Nrf2/HO-1 system in development, oxidative stress response and diseases: an evolutionarily conserved mechanism. Cell. Mol. Life Sci. *73*, 1–27.

Lu, W.Y., Xiong, Z.G., Lei, S., Orser, B. a, Dudek, E., Browning, M.D., and MacDonald, J.F. (1999). G-protein-coupled receptors act via protein kinase C and Src to regulate NMDA receptors. Nat. Neurosci. *2*, 331–338.

MacDermott, A.B., Mayer, M.L., Westbrook, G.L., Smith, S.J., and Barker, J.L. (1986). NMDA-receptor activation increases cytoplasmic calcium concentration in cultured spinal cord neurones. Nature *321*, 519–522.

Magi, S., Castaldo, P., Macrì, M.L., Maiolino, M., Matteucci, A., Bastioli, G., Gratteri, S., Amoroso, S., and Lariccia, V. (2016). Intracellular Calcium Dysregulation: Implications for Alzheimer's Disease. Biomed Res. Int. *2016*, 1–14.

Malenka, R.C., and Bear, M.F. (2004). LTP and LTD: An embarrassment of riches. Neuron *44*, 5–21.

Malenka, R.C., and Nicoll, R.A. (1999). Long-term potentiation -- A decade of progress ? Science (80-.). *285*, 1870–1874.

Manczak, M., Anekonda, T.S., Henson, E., Park, B.S., Quinn, J., and Reddy, P.H. (2006). Mitochondria are a direct site of A beta accumulation in Alzheimer's disease neurons: implications for free radical generation and oxidative damage in disease progression. Hum. Mol. Genet. *15*, 1437–1449.

Manczak, M., Calkins, M.J., and Reddy, P.H. (2011). Impaired mitochondrial dynamics and abnormal interaction of amyloid beta with mitochondrial protein Drp1 in neurons from patients with Alzheimer's disease: Implications for neuronal damage. Hum. Mol. Genet. *20*, 2495–2509.

Masliah, E., Terry, R.D., DeTeresa, R.M., and Hansen, L.A. (1989). Immunohistochemical quantification of the synapse-related protein synaptophysin in Alzheimer disease. Neurosci. Lett. *103*, 234–239.

Masliah E, T.R. (1993). The role of synaptic proteins in the pathogenesis of disorders of the central nervous system. Brain Pathol *3*, 77–85.

Masters, C.L., Simms, G., Weinman, N. a, Multhaup, G., McDonald, B.L., and Beyreuther, K. (1985). Amyloid plaque core protein in Alzheimer disease and Down syndrome. Proc Natl Acad Sci U S A *82*, 4245–4249.

Matarin, M., Salih, D.A., Yasvoina, M., Cummings, D.M., Guelfi, S., Liu, W., NahabooSolim, M.A., Moens, T.G., Paublete, R.M., Ali, S.S., et al. (2015). A Genome-wide gene-expression analysis and database in transgenic mice during development of

amyloid or tau pathology. Cell Rep. *10*, 633–645.

Matsuoka, Y., Picciano, M., La Francois, J., and Duff, K. (2001). Fibrillar beta-amyloid evokes oxidative damage in a transgenic mouse model of Alzheimer's disease. Neuroscience *104*, 609–613.

Mattson, M.P., Gleichmann, M., and Cheng, A. (2008). Mitochondria in Neuroplasticity and Neurological Disorders. Neuron *60*, 748–766.

McKhann, G.M., Knopman, D.S., Chertkow, H., Hyman, B.T., Jack, C.R., Kawas, C.H., Klunk, W.E., Koroshetz, W.J., Manly, J.J., Mayeux, R., et al. (2011). The diagnosis of dementia due to Alzheimer's disease: Recommendations from the National Institute on Aging-Alzheimer's Association workgroups on diagnostic guidelines for Alzheimer's disease. Alzheimer's Dement. *7*, 263–269.

Miyazaki, T., Tanaka, S., Sanjay, A., and Baron, R. (2006). The role of c-Src kinase in the regulation of osteoclast function. Mod. Rheumatol. *16*, 68–74.

Moghekar, A., Li, S., Lu, Y., Li, M., Wang, M.C., Albert, M., and O'Brien, R. (2013). CSF biomarker changes precede symptom onset of mild cognitive impairment. Neurology *81*, 1753–1758.

Mohmmad Abdul, H., Sultana, R., Keller, J.N., St. Clair, D.K., Markesbery, W.R., and Butterfield, D.A. (2006). Mutations in amyloid precursor protein and presenilin-1 genes increase the basal oxidative stress in murine neuronal cells and lead to increased sensitivity to oxidative stress mediated by amyloid β-peptide (1-42), H2O2 and kainic acid: implications for A. J. Neurochem. *96*, 1322–1335.

Moolman, D.L., Vitolo, O. V., Vonsattel, J.P.G., and Shelanski, M.L. (2004). Dendrite and dendritic spine alterations in Alzheimer models. J. Neurocytol. *33*, 377–387.

Moreira, P.I., Santos, M.S., Moreno, A., and Oliveira, C. (2001). Amyloid beta-peptide promotes permeability transition pore in brain mitochondria. Biosci. Rep. *21*, 789–800.

Morimoto, B.H., and Koshland, D.E. (1990). Induction and expression of long- and short-term neurosecretory potentiation in a neural cell line. Neuron *5*, 875–880.

Moss, S.J., Gorrie, G.H., Amato, a, and Smart, T.G. (1995). Modulation of GABAA receptors by tyrosine phosphorylation. Nature *377*, 344–348.

Mota, S.I., Ferreira, I.L., Pereira, C., Oliveira, C.R., and Rego, A.C. (2012). Amyloid-beta peptide 1-42 causes microtubule deregulation through N-methyl-D-aspartate receptors in mature hippocampal cultures. Curr. Alzheimer Res. *9*, 844–856.

Mota, S.I., Ferreira, I.L., and Rego, A.C. (2014a). Dysfunctional synapse in Alzheimer's disease - A focus on NMDA receptors. Neuropharmacology *76*, 16–26.

Mota, S.I., Ferreira, I.L., Valero, J., Ferreiro, E., Carvalho, A.L., Oliveira, C.R., and Rego, A.C. (2014b). Impaired Src signaling and post-synaptic actin polymerization in Alzheimer's disease mice hippocampus - Linking NMDA receptors and the reelin

pathway. Exp. Neurol. *261*, 698–709.

Mota, S.I., Costa, R.O., Ferreira, I.L., Santana, I., Caldeira, G.L., Padovano, C., Fonseca, A.C., Baldeiras, I., Cunha, C., Letra, L., et al. (2015). Oxidative stress involving changes in Nrf2 and ER stress in early stages of Alzheimer's disease. Biochim. Biophys. Acta - Mol. Basis Dis. *1852*, 1428–1441.

Motta, M., Imbesi, R., Di Rosa, M., Stivala, F., and Malaguarnera, L. (2007). Altered plasma cytokine levels in Alzheimer's disease: Correlation with the disease progression. Immunol. Lett. *114*, 46–51.

Muller, U.C., and Zheng, H. (2012). Physiological Functions of APP Family Proteins. Cold Spring Harb. Perspect. Med. *2*, a006288–a006288.

Nagele, R.G., D'Andrea, M.R., Anderson, W.J., and Wang, H.-Y. (2002). Intracellular accumulation of beta-amyloid(1-42) in neurons is facilitated by the alpha 7 nicotinic acetylcholine receptor in Alzheimer's disease. Neuroscience *110*, 199–211.

Naia, L., Luísa, I., Ferreiro, E., and Rego, A.C. (2016). Biochemical and Biophysical Research Communications Mitochondrial Ca2+ handling in Huntington ' s and Alzheimer ' s diseases e Role of ER-mitochondria crosstalk. Biochem. Biophys. Res. Commun. 1–9.

Nava-Mesa, M.O., Jiménez-Díaz, L., Yajeya, J., and Navarro-Lopez, J.D. (2014). GABAergic neurotransmission and new strategies of neuromodulation to compensate synaptic dysfunction in early stages of Alzheimer's disease. Front. Cell. Neurosci. *8*, 167.

Newpher, T.M., and Ehlers, M.D. (2009). Spine microdomains for postsynaptic signaling and plasticity. Trends Cell Biol. *19*, 218–227.

Nguyen, T., Sherratt, P.J., Huang, H.C., Yang, C.S., and Pickett, C.B. (2003). Increased protein stability as a mechanism that enhances Nrf2-mediated transcriptional activation of the antioxidant response element: Degradation of Nrf2 by the 26 S proteasome. J. Biol. Chem. *278*, 4536–4541.

Nimmrich, V., and Ebert, U. (2009). Is Alzheimer's disease a result of presynaptic failure? Synaptic dysfunctions induced by oligomeric beta-amyloid. Rev. Neurosci. *20*, 1–12.

Niture, S.K., Jain, A.K., and Jaiswal, A.K. (2009). Antioxidant-induced modification of INrf2 cysteine 151 and PKC-delta-mediated phosphorylation of Nrf2 serine 40 are both required for stabilization and nuclear translocation of Nrf2 and increased drug resistance. J. Cell Sci. *122*, 4452–4464.

Niture, S.K., Jain, A.K., Shelton, P.M., and Jaiswal, A.K. (2011). Src subfamily kinases regulate nuclear export and degradation of transcription factor Nrf2 to switch off Nrf2-mediated antioxidant activation of cytoprotective gene expression. J. Biol. Chem. *286*, 28821–28832.

Obuobi, S., Karatayev, S., Chai, C.L.L., Ee, P.L.R., and Mátyus, P. (2016). The role of modulation of antioxidant enzyme systems in the treatment of neurodegenerative diseases. J. Enzyme Inhib. Med. Chem. *6366*, 1–11.

Oddo, S., Caccamo, A., Kitazawa, M., Tseng, B.P., and LaFerla, F.M. (2003). Amyloid deposition precedes tangle formation in a triple transgenic model of Alzheimer's disease. In Neurobiology of Aging, pp. 1063–1070.

Ogura, M., Yamaki, J., Homma, M.K., and Homma, Y. (2012). Mitochondrial c-Src regulates cell survival through phosphorylation of respiratory chain components. Biochem. J. *447*, 281–289.

Ogura, M., Yamaki, J., Homma, M.K., and Homma, Y. (2014). Phosphorylation of flotillin-1 by mitochondrial c-Src is required to prevent the production of reactive oxygen species. FEBS Lett. *588*, 2837–2843.

Oliet, H.R., and Papouin, T. (2014). Organization , control and function of extrasynaptic NMDA receptors. Philos. Trans. R. Soc. 18–21.

Palotas, A., Kalman, J., Laskay, G., Juhasz, A., Janka, Z., and Penke, B. (2002). [Change of fibroblast calcium levels caused by beta-amyloid peptide in Alzheimer disease]. Ideggyogy Sz *55*, 164–167.

Papouin, T., Ladépêche, L., Ruel, J., Sacchi, S., Labasque, M., Hanini, M., Groc, L., Pollegioni, L., Mothet, J.P., and Oliet, S.H.R. (2012). Synaptic and extrasynaptic NMDA receptors are gated by different endogenous coagonists. Cell *150*, 633–646.

Patten, D.A., Germain, M., Kelly, M.A., and Slack, R.S. (2010). Reactive oxygen species: Stuck in the middle of neurodegeneration. J. Alzheimer's Dis. *20*.

Pennanen, C., Kivipelto, M., Tuomainen, S., Hartikainen, P., Hänninen, T., Laakso, M.P., Hallikainen, M., Vanhanen, M., Nissinen, A., Helkala, E.-L., et al. (2004). Hippocampus and entorhinal cortex in mild cognitive impairment and early AD. Neurobiol. Aging *25*, 303–310.

Petralia, R.S. (2012). Distribution of extrasynaptic NMDA receptors on neurons. ScientificWorldJournal. *2012*, 267120.

Pigino, G., Morfini, G., Atagi, Y., Deshpande, a, Yu, C., Jungbauer, L., LaDu, M., Busciglio, J., and Brady, S. (2009). Disruption of fast axonal transport is a pathogenic mechanism for intraneuronal amyloid beta. Proc. Natl. Acad. Sci. U. S. A. *106*, 5907–5912.

Pinho, C.M., Teixeira, P.F., and Glaser, E. (2014). Mitochondrial import and degradation of amyloid-β peptide. Biochim. Biophys. Acta - Bioenerg. *1837*, 1069–1074.

Potapenko, E.S., Biancardi, V.C., Zhou, Y., and Stern, J.E. (2013). Astrocytes modulate a postsynaptic NMDA-GABAA-receptor crosstalk in hypothalamic neurosecretory neurons. J. Neurosci. *33*, 631–640.

Prestia, A., Caroli, A., Van Der Flier, W.M., Ossenkoppele, R., Van Berckel, B., Barkhof, F., Teunissen, C.E., Wall, A.E., Carter, S.F., Schöll, M., et al. (2013). Prediction of dementia in MCI patients based on core diagnostic markers for Alzheimer disease. Neurology *80*, 1048–1056.

Raina, a K., Templeton, D.J., Deak, J.C., Perry, G., and Smith, M. a (1999). Quinone reductase (NQO1), a sensitive redox indicator, is increased in Alzheimer's disease. Redox Rep. *4*, 23–27.

Ramsey, C.P., Glass, C.A., Montgomery, M.B., Lindl, K.A., Ritson, G.P., Chia, L.A., Hamilton, R.L., Chu, C.T., and Jordan-Sciutto, K.L. (2007). Expression of Nrf2 in neurodegenerative diseases. J. Neuropathol. Exp. Neurol. *66*, 75–85.

Resende, R., Ferreiro, E., Pereira, C., and Resende de Oliveira, C. (2008a). Neurotoxic effect of oligomeric and fibrillar species of amyloid-beta peptide 1-42: Involvement of endoplasmic reticulum calcium release in oligomer-induced cell death. Neuroscience *155*, 725–737.

Resende, R., Moreira, P.I., Proença, T., Deshpande, A., Busciglio, J., Pereira, C., and Oliveira, C.R. (2008b). Brain oxidative stress in a triple-transgenic mouse model of Alzheimer disease. Free Radic. Biol. Med. *44*, 2051–2057.

Rojo, A.I., Medina-Campos, O.N., Rada, P., Zúñiga-Toalá, A., López-Gazcón, A., Espada, S., Pedraza-Chaverri, J., and Cuadrado, A. (2012). Signaling pathways activated by the phytochemical nordihydroguaiaretic acid contribute to a Keap1-independent regulation of Nrf2 stability: Role of glycogen synthase kinase-3. Free Radic. Biol. Med. *52*, 473–487.

Roskoski, R. (2004). Src protein-tyrosine kinase structure and regulation. Biochem. Biophys. Res. Commun. *324*, 1155–1164.

Roskoski, R. (2015). Src protein-tyrosine kinase structure, mechanism, and small molecule inhibitors. Pharmacol. Res. *94*, 9–25.

Rui, Y., Tiwari, P., Xie, Z., and Zheng, J.Q. (2006). Acute impairment of mitochondrial trafficking by beta-amyloid peptides in hippocampal neurons. J. Neurosci. *26*, 10480–10487.

Rui, Y., Gu, J., Yu, K., Hartzell, H.C., and Zheng, J.Q. (2010). Inhibition of AMPA receptor trafficking at hippocampal synapses by beta-amyloid oligomers: the mitochondrial contribution. Mol. Brain *3*, 10.

Sachse, C., Xu, C., Wieligmann, K., Diekmann, S., Grigorieff, N., and Fändrich, M. (2006). Quaternary structure of a mature amyloid fibril from Alzheimer's Abeta(1-40) peptide. J. Mol. Biol. *362*, 347–354.

Sagare, A.P., Bell, R.D., and Zlokovic, B. V. (2012). Neurovascular Dysfunction and Faulty Amyloid -Peptide Clearance in Alzheimer Disease. Cold Spring Harb. Perspect. Med. *2*, a011452–a011452.

Salter, M.W., and Kalia, L. V (2004). Src kinases: a hub for NMDA receptor regulation. Nat. Rev. Neurosci. *5*, 317–328.

Salvi, M., Brunati, A.M., Bordin, L., La Rocca, N., Clari, G., and Toninello, A. (2002). Characterization and location of Src-dependent tyrosine phosphorylation in rat brain mitochondria. Biochim. Biophys. Acta *1589*, 181–195.

Salvi, M., Stringaro, A., Brunati, A.M., Agostinelli, E., Arancia, G., Clari, G., and Toninello, A. (2004). Tyrosine phosphatase activity in mitochondria: Presence of Shp-2 phosphatase in mitochondria. Cell. Mol. Life Sci. *61*, 2393–2404.

Sandilands, E., and Frame, M.C. (2008). Endosomal trafficking of Src tyrosine kinase. Trends Cell Biol. *18*, 322–329.

SantaCruz, K.S., Yazlovitskaya, E., Collins, J., Johnson, J., and DeCarli, C. (2004). Regional NAD(P)H:quinone oxidoreductase activity in Alzheimer's disease. Neurobiol. Aging *25*, 63–69.

Sarangi, U., Singh, M.K., Abhijnya, K.V.V., Prasanna Anjaneya Reddy, L., Siva Prasad, A., Pitke, V.V., Paithankar, K., and Subbarao Sreedhar, A. (2013). Hsp60 chaperonin acts as barrier to pharmacologically induced oxidative stress mediated apoptosis in tumor cells with differential stress response. Drug Target Insights *2013*, 35–51.

Sasaki, N., Toki, S., Chowei, H., Saito, T., Nakano, N., Hayashi, Y., Takeuchi, M., and Makita, Z. (2001). Immunohistochemical distribution of the receptor for advanced glycation end products in neurons and astrocytes in Alzheimer's disease. Brain Res. *888*, 256–262.

Sato, H., Sato, M., Kanai, H., Uchiyama, T., Iso, T., Ohyama, Y., Sakamoto, H., Tamura, J., Nagai, R., and Kurabayashi, M. (2005). Mitochondrial reactive oxygen species and c-Src play a critical role in hypoxic response in vascular smooth muscle cells. Cardiovasc Res *67*, 714–722.

Scheff, S.W., and Price, D.A. (1993). Synapse loss in the temporal lobe in Alzheimer's disease. Ann. Neurol. *33*, 190–199.

Scheuner, D., Eckman, C., Jensen, M., Song, X., Citron, M., Suzuki, N., Bird, T.D., Hardy, J., Hutton, M., Kukull, W., et al. (1996). Secreted amyloid beta-protein similar to that in the senile plaques of Alzheimer's disease is increased in vivo by the presenilin 1 and 2 and APP mutations linked to familial Alzheimer's disease. Nat. Med. *2*, 864–870.

Schipper, H.M., Cissé, S., and Stopa, E.G. (1995). Expression of heme oxygenase-1 in the senescent and alzheimer-diseased brain. Ann. Neurol. *37*, 758–768.

Schmidt, M., Sachse, C., Richter, W., Xu, C., Fändrich, M., and Grigorieff, N. (2009). Comparison of Alzheimer Aβ(1–40) and Aβ(1–42) amyloid fibrils reveals similar protofilament structures. Proc. Natl. Acad. Sci. *106* , 19813–19818.

Scorziello, A., Meucci, O., Calvani, M., and Schettini, G. (1997). Acetyl-L-carnitine

arginine amide prevents beta 25-35-induced neurotoxicity in cerebellar granule cells. Neurochem. Res. *22*, 257–265.

Selkoe, D.J. (1996). Amyloid beta-protein and the genetics of Alzheimer's Disease. J. Biol. Chem. *271*, 18295–18298.

Selkoe, D.J. (2008). Soluble oligomers of the amyloid β-protein impair synaptic plasticity and behavior. Behav. Brain Res. *192*, 106–113.

Selkoe, D.J., and Hardy, J. (2016). The amyloid hypothesis of Alzheimer's disease at 25 years. EMBO Mol. Med. 1–14.

Selkoe, D.J., and Schenk, D. (2003). Alzheimer's disease: molecular understanding predicts amyloid-based therapeutics. Annu. Rev. Pharmacol. Toxicol. *43*, 545–584.

Shankar, G.M., Li, S., Mehta, T.H., Garcia-Munoz, A., Shepardson, N.E., Smith, I., Brett, F.M., Farrell, M.A., Rowan, M.J., Lemere, C.A., et al. (2008). Amyloid-beta protein dimers isolated directly from Alzheimer's brains impair synaptic plasticity and memory. Nat. Med. *14*, 837–842.

Shen, J., and Kelleher, R.J. (2007). The presenilin hypothesis of Alzheimer's disease: evidence for a loss-of-function pathogenic mechanism. Proc. Natl. Acad. Sci. U. S. A. *104*, 403–409.

Sheng, M., Sabatini, B.L., and Südhof, T.C. (2012). Synapses and Alzheimer's disease. Cold Spring Harb. Perspect. Biol. *4*, 10.

Sisodia, S.S., Koo, E.H., Hoffman, P.N., Perry, G., and Price, D.L. (1993). Identification and transport of full-length amyloid precursor proteins in rat peripheral nervous system. J Neurosci *13*, 3136–3142.

Smith, M. a, Hirai, K., Hsiao, K., Pappolla, M. a, Harris, P.L., Siedlak, S.L., Tabaton, M., and Perry, G. (1998). Amyloid-beta deposition in Alzheimer transgenic mice is associated with oxidative stress. J. Neurochem. *70*, 2212–2215.

Snyder, E.M., Nong, Y., Almeida, C.G., Paul, S., Moran, T., Choi, E.Y., Nairn, A.C., Salter, M.W., Lombroso, P.J., Gouras, G.K., et al. (2005). Regulation of NMDA receptor trafficking by amyloid-beta. Nat. Neurosci. *8*, 1051–1058.

Sokolova, A., Hill, M.D., Rahimi, F., Warden, L. a, Halliday, G.M., and Shepherd, C.E. (2009). Monocyte chemoattractant protein-1 plays a dominant role in the chronic inflammation observed in Alzheimer's disease. Brain Pathol. *19*, 392–398.

Stępkowski, T.M., and Kruszewski, M.K. (2011). Molecular cross-talk between the NRF2/KEAP1 signaling pathway, autophagy, and apoptosis. Free Radic. Biol. Med. *50*, 1186–1195.

Stix, B., and Reiser, G. (1998). β-Amyloid peptide 25–35 regulates basal and hormone-stimulated Ca2+ levels in cultured rat astrocytes. Neurosci. Lett. *243*, 121–124.

Strom, J., Xu, B., Tian, X., and Chen, Q.M. (2016). Nrf2 protects mitochondrial decay by oxidative stress. FASEB J. *30*, 66–80.

Sunderland, T., Linker, G., Mirza, N., Putnam, K.T., Friedman, D.L., Kimmel, L.H., Bergeson, J., Manetti, G.J., Zimmermann, M., Tang, B., et al. (2003). Decreased beta-amyloid1-42 and increased tau levels in cerebrospinal fluid of patients with Alzheimer disease. JAMA *289*, 2094–2103.

Supnet, C., and Bezprozvanny, I. (2010). Neuronal calcium signaling, mitochondrial dysfunction, and Alzheimer's disease. J. Alzheimers. Dis. *20 Suppl 2*, S487–S498.

Taguchi, K., Motohashi, H., and Yamamoto, M. (2011). Molecular mechanisms of the Keap1-Nrf2 pathway in stress response and cancer evolution. Genes to Cells *16*, 123–140.

Thal, D.R., Walter, J., Saido, T.C., and Fändrich, M. (2015). Neuropathology and biochemistry of Aβ and its aggregates in Alzheimer's disease. Acta Neuropathol. *129*, 167–182.

Thathiah, a, and De Strooper, B. (2011). The role of G protein-coupled receptors in the pathology of Alzheimer's disease. Nat. Rev. Neurosci. *12*, 73–87.

Thibault, O., Gant, J.C., and Landfield, P.W. (2007). Expansion of the calcium hypothesis of brain aging and Alzheimer's disease: Minding the store. Aging Cell *6*, 307–317.

Torres-Lista, V., Parrado-Fernández, C., Alvarez-Montón, I., Frontiñán-Rubio, J., Durán-Prado, M., Peinado, J.R., Johansson, B., Alcaín, F.J., and Giménez-Llort, L. (2014). Neophobia, NQO1 and SIRT1 as premorbid and prodromal indicators of AD in 3xTg-AD mice. Behav. Brain Res. *271*, 140–146.

Vardy, E.R.L.C., Catto, A.J., and Hooper, N.M. (2005). Proteolytic mechanisms in amyloid-beta metabolism: therapeutic implications for Alzheimer's disease. Trends Mol. Med. *11*, 464–472.

Walsh, D.M., and Selkoe, D.J. (2007). A? Oligomers ? a decade of discovery. J. Neurochem. *101*, 1172–1184.

Walsh, D.M., Klyubin, I., Fadeeva, J. V, Cullen, W.K., Anwyl, R., Wolfe, M.S., Rowan, M.J., and Selkoe, D.J. (2002). Naturally secreted oligomers of amyloid beta protein potently inhibit hippocampal long-term potentiation in vivo. Nature *416*, 535–539.

Wang, Y.T., and Salter, M.W. (1994). Regulation of NMDA receptors by tyrosine kinases and phosphatases. Nature *369*, 233–235.

Wang, K., Hackett, J.T., Cox, M.E., Hoek, M. Van, Lindstrom, J.M., Parsons, S.J., and Van Hoek, M. (2004). Regulation of the neuronal nicotinic acetylcholine receptor by SRC family tyrosine kinases. J. Biol. Chem. *279*, 8779–8786.

Wang, X., Su, B., Siedlak, S.L., Moreira, P.I., Fujioka, H., Wang, Y., Casadesus, G., and Zhu, X. (2008). Amyloid-beta overproduction causes abnormal mitochondrial dynamics

via differential modulation of mitochondrial fission/fusion proteins. Proc. Natl. Acad. Sci. U. S. A. *105*, 19318–19323.

Weidemann, A., König, G., Bunke, D., Fischer, P., Salbaum, J.M., Masters, C.L., and Beyreuther, K. (1989). Identification, biogenesis, and localization of precursors of Alzheimer's disease A4 amyloid protein. Cell *57*, 115–126.

Weidemann, A., Eggert, S., Reinhard, F.B.M., Vogel, M., Paliga, K., Baier, G., Masters, C.L., Beyreuther, K., and Evin, G. (2002). A novel epsilon-cleavage within the transmembrane domain of the Alzheimer amyloid precursor protein demonstrates homology with Notch processing. Biochemistry *41*, 2825–2835.

Whitlock, J.R., Heynen, A.J., Shuler, M.G., and Bear, M.F. (2006). Learning induces long-term potentiation in the hippocampus. Science *313*, 1093–1097.

Wirths, O., Multhaup, G., Czech, C., Blanchard, V., Moussaoui, S., Tremp, G., Pradier, L., Beyreuther, K., and Bayer, T.A. (2001). Intraneuronal Aβ accumulation precedes plaque formation in β-amyloid precursor protein and presenilin-1 double-transgenic mice. Neurosci. Lett. *306*, 116–120.

Wolfe, M.S. (2008). Inhibition and modulation of gamma-secretase for Alzheimer's disease. Neurotherapeutics *5*, 391–398.

Wu, G.-M., and Hou, X.-Y. (2010). Oligomerized Aβ25–35 induces increased tyrosine phosphorylation of NMDA receptor subunit 2A in rat hippocampal CA1 subfield. Brain Res. *1343*, 186–193.

Yan, R., Fan, Q., Zhou, J., and Vassar, R. (2016). Inhibiting BACE1 to reverse synaptic dysfunctions in Alzheimer's disease. Neurosci. Biobehav. Rev. *65*, 326–340.

Yankner, B.A., and Lu, T. (2009). Amyloid beta-protein toxicity and the pathogenesis of Alzheimer disease. J. Biol. Chem. *284*, 4755–4759.

Yu, X.M., Askalan, R., Keil, G.J., and Salter, M.W. (1997). NMDA channel regulation by channel-associated protein tyrosine kinase Src. Science *275*, 674–678.

Yuan Xiang, P., Janc, O., Grochowska, K.M., Kreutz, M.R., and Reymann, K.G. (2016). Dopamine agonists rescue Aβ-induced LTP impairment by Src-family tyrosine kinases. Neurobiol. Aging *40*, 98–102.

Zhang, Y., Li, P., Feng, J., and Wu, M. (2016). Dysfunction of NMDA receptors in Alzheimer's disease. Neurol. Sci. 1–9.

Zhao, Y., and Zhao, B. (2013). Oxidative stress and the pathogenesis of Alzheimer's disease. Oxid Med Cell Longev *2013*, 316523.

Zhao, Z., Lu, R., Zhang, B., Shen, J., Yang, L., Xiao, S., Liu, J., and Suo, W.Z. (2012). Differentiation of HT22 neurons induces expression of NMDA receptor that mediates homocysteine cytotoxicity. Neurol. Res. *34*, 38–43.

Zou, L., Wang, Z., Shen, L., Bao, G.B., Wang, T., Kang, J.H., and Pei, G. (2007). Receptor tyrosine kinases positively regulate BACE activity and Amyloid-beta production through enhancing BACE internalization. Cell Res. *17*, 389–401.

ATTACHMENTS

SUPPLEMENTARY DATA

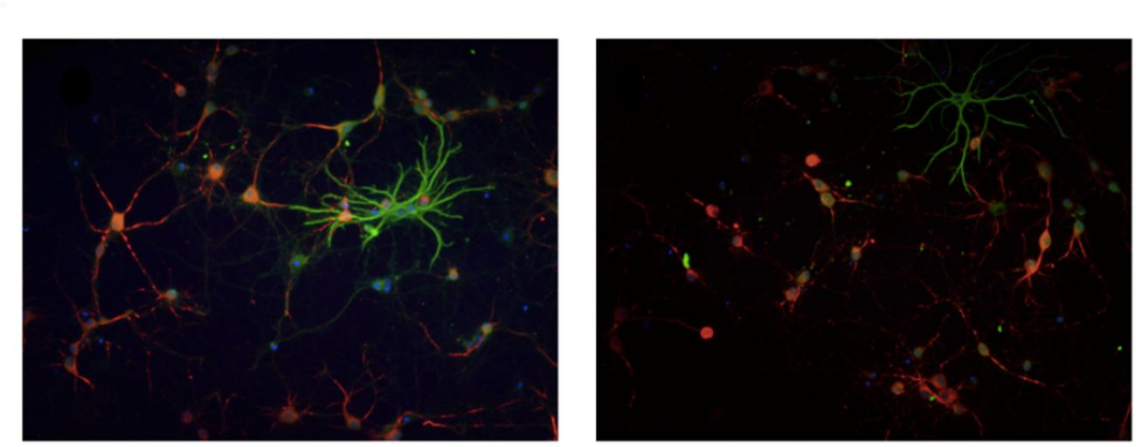

Fig. S1 | Characterization of rat hippocampal neuronal culture. Nucleus was visualized by Hoechst 33342 staining (blue), neurons were labeled with an antibody against MAP-2 (red) and astrocytes were against GFAP (green). Confocal images were obtained using an Axioscope 2 Plus upright microscope (Zeiss, Jena, Germany).

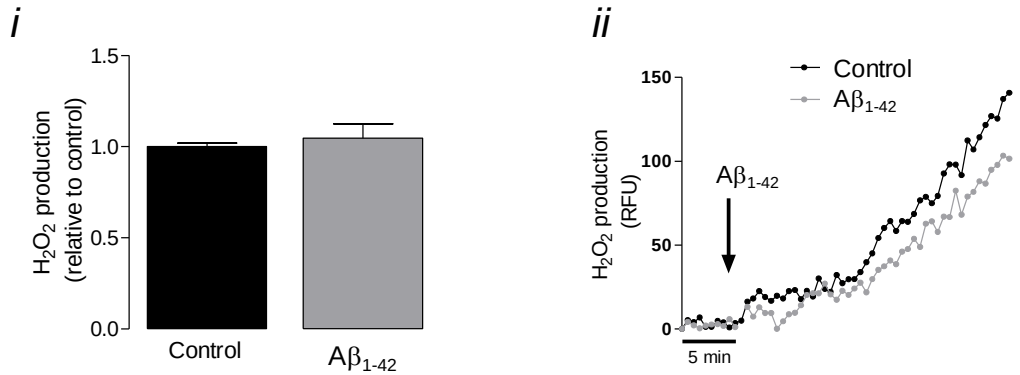

Fig. S2 | Aβ has no effect on H_2O_2 production in HT22 Cells. H_2O_2 production was evaluated by monitoring the fluorescence of resorufin using a microplate reader Spectrofluorometer Gemini EM (excitation 550 nm; emission 580 nm). Basal fluorescence levels were recorded for 3 min and the effect of $A\beta_{1-42}$ oligomers (1 µM) was recorded for 30 min. (i) Results were plotted as the difference between the last value achieved and the basal value before Aβ addition. Graphics (ii) are the representative line charts. Data are expressed as the mean ± SEM of 3 independent experiments performed in quadruplicates.

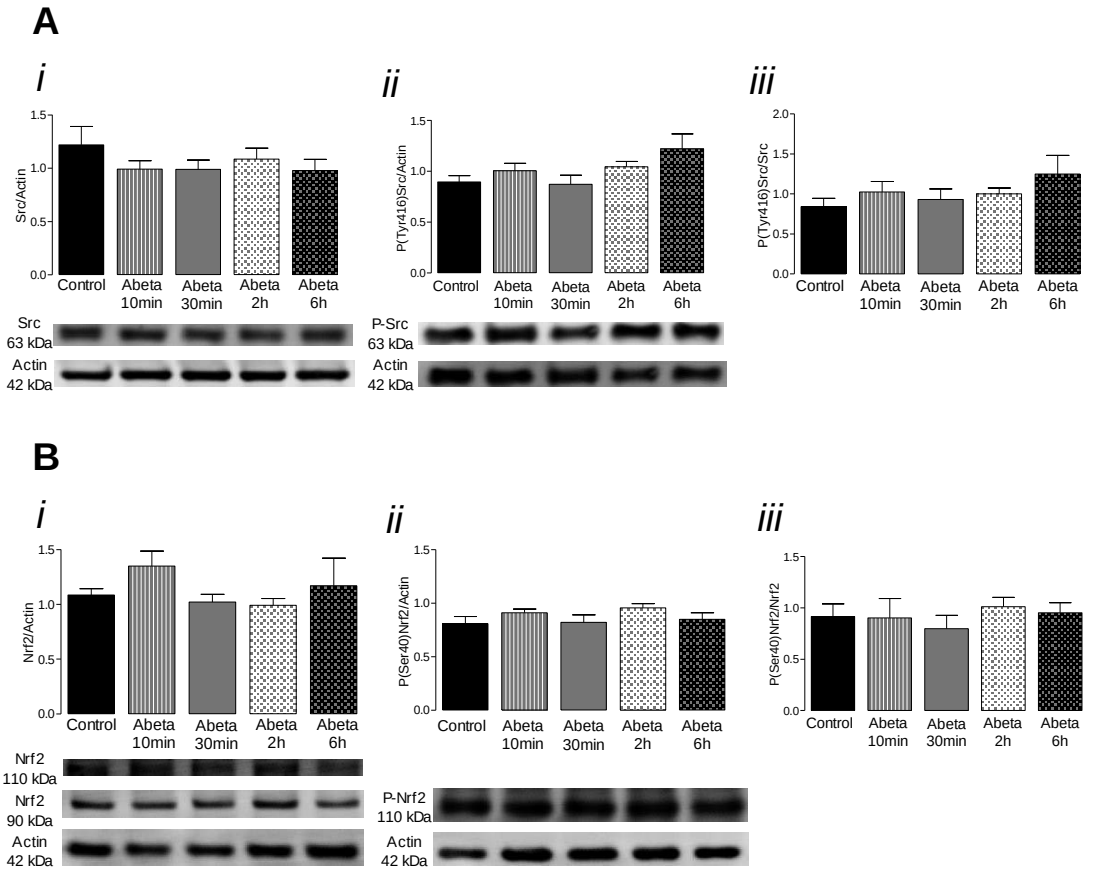

Fig. S3 | $A\beta_{1-42}$ does not induce Src activation or Nrf2 phosphorylation in HT22 cell line. HT22 cells were incubated for 10 min, 30 min, 2 h or 6 h with $A\beta_{1-42}$ (1 µM). In (**A**) levels of Src/actin (i), P(Tyr461)Src/actin (ii) and P(Tyr461)Src/Src (iii); and (**B**) Nrf2/actin (i), P(Ser40)Nrf2/actin (ii) and P(Ser40)Nrf2/Nrf2 (iii) were analyzed by Western blotting. Data are expressed in arbitrary units relative to actin as the mean ± SEM of n=4 to 8 experiments. Nrf2 total levels were considered both at 90 and 110 kDa.